Faculty of Science and Engineering

Chlorine Dioxide Oxidation in Water Treatment: Impact on Natural Organic Matter Characteristics, Disinfection Byproducts and Comparison with Other Oxidants

Valentin Roland Rougé

This thesis is present for the Degree of

Doctor of Philosophy

of

Curtin University

December 2018

Declaration

To the best of my knowledge and belief this thesis contains no material previously published by any other person except where due acknowledgment has been made.

This thesis contains no material which has been accepted for the award of any other degree or diploma in any university.

Signature: 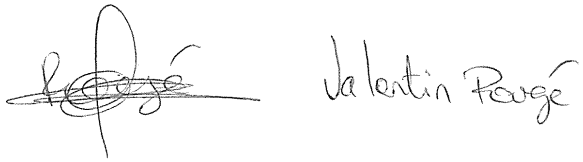

Date: 30/11/18

Acknowledgments

First of all, my sincere gratitude to Dr Sébastien Allard for his patience, guidance and thoughtful supervision across these years. My thanks also go to Professor Jean-Philippe Croué for his essential help, especially in the application process which allowed me to undergo this journey, and to Curtin University for their financial support through the Curtin International Postgraduate Research Scholarship.

I am grateful to Professor Urs von Gunten for his valuable collaboration and feedback on the different projects, to the opportunity he gave me to work in Eawag laboratories, which has been a major stepping-stone in my PhD, and to Elisabeth Salhi for her assistance in the laboratory.

I would also like to thank the people who has been helping and teaching me a great deal, always with patience and consideration: Deborah Liew, Peter Hopper, Jace Tan and Peter Chapman. I also am grateful to Mariette Lafont de Sentenac for her enthusiastic and valuable help in the laboratory during her internship.

These years would have been very different without the people who made the laboratory a cheerful place: Rhys Carter, Ina Kristiana, Maolida Nihemaiti, Jaime Cesar, Bettina Schaefer, Suona Zhang, Luis Restrepo Vieira, Ionut Caraene, Wei Hu, Viktor Kresners.

Finally, my parents, to whom I dedicate this Thesis, who always stood behind me no matter my choices.

Abstract

The use of disinfection has revolutionized the treatment of drinking water, ensuring pathogen-free supply and consequently preventing waterborne diseases. The ease of use and affordability of chlorine (also designated as free available chlorine, or FAC, in this Thesis) has made it the most common disinfectant in the world. However, in the 1970s, chlorine was found to produce unwanted compounds, called disinfection byproducts (DBPs). DBPs arise from reactions between the water matrix and chlorine. Notably, natural organic matter (NOM) is a major sink for chlorine. Early on, two classes of DBPs, trihalomethanes (THMs) and haloacetic acids (HAAs), were linked to negative health effects and proposed to be carcinogenic based on animal studies. As a result, these DBPs have drawn major attention in the last decades, and are now often regulated in drinking waters worldwide. The use of alternative disinfectants became of interest, as they usually produce lower quantities of these regulated DBPs, however, they can lead to other problems since they form their own set of unregulated DBPs which might be more potent. For example, the use of monochloramine as a disinfectant has been found to form the highly genotoxic and carcinogenic *N*-nitrosamines, and to promote the formation of iodinated DBPs whenever iodide is present in water, which are generally more toxic than their chlorinated counterparts. Despite the unfavorable effects linked to its usage, chlorine remains the most widely used disinfectant.

The two major challenges in the DBP research area have been (i) the identification and the toxicological evaluation of a large panel of DBPs, and (ii) their mitigation. Numerous emerging DBPs such as, halonitromethanes, haloacetamides, haloacetonitriles or the abovementioned *N*-nitrosamines have been identified. While their concentrations are usually significantly lower than those of regulated THMs or HAAs, many of these newly identified compounds are much more potent. Furthermore, the presence of bromide and/or iodide in waters can lead to the formation of brominated and/or iodinated DBPs, in addition to chlorinated DBPs, as well as mixed analogues, for which the toxicity generally

increases with bromine and iodine substitution; that is (in order of increasing toxicity) chlorinated DBPs < brominated DBPs < iodinated DBPs.

Currently the main strategy for the mitigation of DBPs is the removal of NOM prior to disinfection, hence minimizing the chlorine consumption and the formation of DBPs. While, conventional treatments, such as coagulation and sand filtration, are efficient in removing part of the NOM, they have limited effect in removing the lower molecular weight fraction of NOM. More advanced treatments, such as activated carbon or nanofiltration, can enhance the removal efficiency of NOM, however, these advanced treatments often see a significant increase in cost.

Pre-oxidizing the NOM is an alternative method to minimize its reaction with chlorine. Chlorine dioxide (ClO_2), ozone (O_3), ferrate (Fe(VI)) and permanganate (Mn(VII)) are oxidants that do not directly result in halogenated DBPs. Among them, O_3 has long been used for enhancing the efficiency of NOM removal, controlling taste and odor, eliminating micropollutants. One major drawback to the use of O_3 has been the resulting bromate formation for waters containing bromide, as bromate is genotoxic and carcinogenic in nature. The application of O_3 as a sole disinfectant is also limited, as O_3 doesn't result in a residual in finished waters. Ferrate has attracted attention in recent years as a "green" multi-purpose oxidant, i.e. disinfectant, coagulant aid and oxidant for micropollutant degradation. Permanganate is commonly applied for the oxidation of iron and manganese, the control of taste and odor compounds, as well as the removal of algae. Additionally to the abovementioned uses, these oxidants react with NOM and can reduce its reactivity during subsequent chlorination, leading to a lower formation of DBPs. ClO_2 has been efficiently used for purposes similar to these other oxidants, i.e. for disinfection, micropollutant degradation, taste and odor control, as well as iron and manganese removal. Despite being a very promising alternative to chlorine, the application of ClO_2 as a disinfectant has been limited, mainly due to the associated formation of chlorite (ClO_2^-), believed to induce blood cell oxidative stress and therefore often regulated. Instead, the dosage of smaller quantities of ClO_2 as a pre-treatment or in combination with another disinfectant (typically chlorine) is gaining interest.

During water treatment, NOM characteristics are affected. While, physicochemical characteristics such as the dissolved organic carbon (DOC), the UV absorbance at 254 nm (UVA_{254}) or humic- and protein-like fluorophores are well established parameters, electrochemical characteristics have been gaining attention. Specifically, methods for the measurement of electron donating capacity (EDC) for application to water treatment have recently been developed, which provide information complementary to physicochemical characteristics.

Although ClO_2, O_3, Fe(VI) and Mn(VII) have been used for a number of different purposes in water treatment, there still remain significant knowledge gaps regarding their impact on NOM characteristics and their implications on DBP formation.

Firstly, the aforementioned pre-oxidants react through very distinctive mechanisms with organic compounds. ClO_2 is known to react via a 1-electron transfer to form ClO_2^-, although the present Thesis provides evidence of additional reaction pathways. O_3, Mn(VII) and Fe(VI) are known to react via electrophilic attack or electron transfer. Furthermore, the degradation products of these oxidants can further react with NOM. When O_3 is used, the released OH radicals exhibit very high reactivity toward a wide range of NOM moieties, through addition or hydrogen abstraction. The degradation products associated with the use of Mn(VII) and Fe(VI), i.e., Mn(VI), Mn(V), Fe(V) and Fe(IV) are also highly reactive. It is therefore difficult to truly compare the effectiveness of these oxidants on DBP mitigation based on oxidant doses alone. Instead, the efficiency of these oxidants could be assessed based on their impact on NOM's properties and correlated to the formation of DBPs.

Secondly, while studies have provided valuable information surrounding the chemistry behind ClO_2 oxidation, its reaction mechanisms in water remain unclear and further investigations are required. Specifically, the molar recovery of dosed ClO_2 is often incomplete. Only a fraction of the dosed ClO_2 is accounted for when considering its byproducts, ClO_2^- and chlorate (ClO_3^-). Furthermore, the formation of low levels of halogenated DBPs during ClO_2 treatment remains unexplained.

Thirdly, when ClO_2 is applied as a pre-oxidant, the fate of ClO_2^- during subsequent chlorination has not been investigated. Although the FAC/ClO_2^- reaction has been extensively studied in concentrated solutions, the reaction under conditions relevant to drinking water treatment remains largely unexplored.

Lastly, while the impact of each oxidant on DBP formation has been studied separately, there is limited literature available that compares the efficiency of these oxidants on DBP mitigation. It is difficult to compare the different oxidants since the formation of DBPs is sensitive to experimental parameters: the dose and type of oxidant, the water characteristics, the class of DBPs targeted, and the potential use of complementary treatments (e.g. coagulation or activated carbon). With conflicting outcomes existing in the literature, and with very few studies providing a direct comparison of the impact of different pre-oxidants on the formation of DBPs, the impact of pre-oxidation on DBP mitigation is not fully understood.

This Thesis aims to investigate the current knowledge gaps associated with the use of ClO_2 in water treatment, and to compare its efficiency as pre-oxidant to O_3, Fe(VI) and Mn(VII), in terms of DBP mitigation..

Chapter 1 gives an overview of the research conducted in this Thesis.

Chapter 2 presents the validation of a size-exclusion chromatography system for the measurement of UVA_{254} and EDC throughout the studies conducted for this Thesis.

Chapter 3 used two surrogates, the UVA_{254} and the EDC, to provide an understanding of the impact of ClO_2, O_3, Fe(VI) and Mn(VII) on NOM characteristics during pre-oxidation and the implications in terms of formation of adsorbable organic halogens (AOX), THMs and haloacetonitriles (HANs) during subsequent chlorination. Applying increasing doses of those oxidants showed that the efficiency of oxidants on EDC abatement, based on molar concentrations, ranked in the order Mn(VII) > ClO_2 > Fe(VI)/O_3-tBuOH > O_3 while their efficiency on UVA_{254} abatement ranked in the order O_3-tBuOH/O_3/Mn(VII) > Fe(VI)/ClO_2. Two distinct phases were identified for ClO_2, Fe(VI) and Mn(VII). At low doses, increasing the oxidant dose led to limited decreases in UVA_{254} while the EDC was efficiently removed, suggesting the formation of quinone-type moieties which maintains

the UVA_{254} but not the EDC. At higher oxidant doses, a more efficient removal of UVA_{254} suggested reaction mechanisms leading to aromatic ring cleavage. By comparison, O_3 and O_3-tBuOH led to more efficient UVA_{254} reduction, due to a more efficient cleavage of aromatic rings. The distinctive impact of O_3-tBuOH on NOM compared to the other investigated pre-oxidants was confirmed by its impact on AOX. While equivalent EDC removals by ClO_2, Fe(VI) and Mn(VII) resulted in similar AOX mitigations, O_3-tBuOH led to lower AOX formation. The EDC was also demonstrated to be an oxidant-independent surrogate (same behavior for all oxidants) for chlorine demand and, interestingly, HAN formation. Comparatively, UVA_{254} was showed to be an oxidant-independent surrogate for AOX and THM formation. These results indicate that the combined use of EDC and UVA_{254} can be interesting for the monitoring of NOM reactivity and DBP control.

In Chapter 4, the mechanisms of ClO_2 reactions during water treatment were investigated. It was demonstrated that ClO_2 reacts through a 1-electron transfer with phenol followed by an oxygen transfer to the resulting phenoxyl radical, leading to the release of one mole of ClO_2^- and one mole of FAC per two moles of consumed ClO_2. It was also observed that similar mechanisms occurred during the oxidation of NOM by ClO_2. Up to 25% of the applied ClO_2 could form FAC *in situ*. Furthermore, up to 27% of this *in situ* formed FAC was incorporated into organic matter forming AOX, which represented up to 7% of the initial ClO_2 dose. Low concentrations of regulated THMs were produced which is likely due to an efficient mitigation of their precursors by ClO_2 oxidation. Conversely, dichloroacetonitrile formation from ClO_2-induced generation of FAC was higher than from addition of FAC in absence of ClO_2. The proposed updated mechanism of ClO_2 reactions during water treatment provides a complete mass balance on Cl for inorganic ClO_2 byproducts (FAC + ClO_2^- +ClO_3^-), explains the formation of halogenated DBPs during ClO_2 treatment, and shows that ClO_2 oxidation capacity may be underestimated.

Chapter 5 discussed the interaction of ClO_2^-, formed after ClO_2 pre-oxidation, with FAC. The reaction was found to be highly dependent on pH, and to form ClO_2 and ClO_3^-. A model that allows to simulate conditions analogous to those commonly employed during disinfection of drinking water was developed and applied to predict the ClO_2^-, ClO_3^- and

HOCl concentrations. The final ClO_2^- concentration was found to be accurately predicted under various controlled conditions, however was overestimated in real waters. In comparison to synthetic waters, real waters may catalyze the FAC/ClO_2^- reaction, probably through acid catalysis with bicarbonate, though this has not been elucidated during the PhD tenure. Furthermore, only about 70% of the ClO_2^- was recovered as ClO_3^-. The remaining Cl species was believed to be FAC formed via the reaction of NOM with *in situ* regenerated ClO_2, as demonstrated in Chapter 3. Since the ClO_2^- concentration was reduced during chlorination, higher doses of ClO_2 were applied during the pre-oxidation step while still complying with regulatory limits, which improved the mitigation of DBP formation, especially the very potent chlorinated and brominated HANs. This work provides a better understanding of the FAC/ClO_2^- interactions in typical drinking water treatment conditions, which can be used to optimize the ClO_2 pre-oxidation dose and therefore better control the formation of DBPs.

Chapter 6 provides a comparative study of the efficiency of ClO_2 with three pre-oxidants, O_3, Fe(VI) and Mn(VII), for the mitigation of AOX, THMs and HANs during subsequent chlorination. The influence of pH and the presence of bromide on the formation of DBPs and its mitigation by pre-oxidation was evaluated. A theoretical toxicity evaluation was performed based on the formation of the specific DBPs (THMs, HANs). All oxidants were found to be efficient in mitigating the formation of DBPs, except Mn(VII) for THMs. O_3-tBuOH was generally more efficient than the other oxidants to reduce AOX and THM formation but all the pre-oxidants were readily mitigating the formation of HANs (> 45% reduction at high dose). Decreasing the pH enhanced the efficiency of O_3-tBuOH and Fe(VI) pre-oxidation on AOX reduction and, for O_3-tBuOH, on THM reduction while diminishing the efficiency of Mn(VII) pre-oxidation on the reduction of all DBPs. In presence of bromide, the pre-oxidation treatments had limited effects on brominated DBP formation. Furthermore, di- and tribrominated DBPs were often enhanced, especially when O_3-tBuOH was used as pre-treatment. The HANs were found at much lower concentration than the THMs. However, they were major contributors to the calculated toxicity, particularly the brominated HANs (bromochloroacetonitrile and dibromochloroacetonitrile), whenever bromide was present in solution. The increase in dibromochloroacetonitrile concentration, due to the pre-oxidation treatments, was a major

issue counteracting the benefit of mitigating other DBPs in terms of estimated toxicity. Generally, a better trade-off between chlorinated DBP mitigation and brominated DBP enhancement was obtained by using lower pre-oxidant doses, particularly for O_3-tBuOH. In comparison to the other oxidants, ClO_2 was consistently mitigating HANs and by extent the estimated toxicity in the different conditions tested.

Finally, Chapter 7 is a summary of the main outcomes and research perspectives highlighted in the previous Chapters.

Table of Contents

List of Tables

Chapters 3-6:

Appendix Chapters 2-6:

List of Figures

Chapters 2-6:

Appendix Chapters 2-6:

List of Abbreviations

AOX	Adsordable Organic Halogen
BCAN	Bromochloroacetonitrile
Br-DBP	Brominated Disinfection Byproduct
BSF	Bromine Substitution Factor
CAN	Chloroacetonitrile
Cl-DBP	Chlorinated Disinfection Byproduct
ClO_2	Chlorine Dioxide
DBCM	Dibromochloromethane
DBP	Disinfection Byproduct
DCAN	Dichloroacetonitrile
DCBM	Dichlorobromomethane
DOC	Dissolved Organic Carbon
EDC	Electron Donating Capacity
FAC	Free Available Chlorine
Fe(VI)	Ferrate
HAN	Haloacetonitrile
Mn(VII)	Permanganate
NLFA	Nordic Lake Fulvic Acid

NOM	Natural Organic Matter
O_3	Ozone
PLFA	Pony Lake Fulvic Acid
SRNOM	Suwannee River NOM extract
TBM	Tribromomethane
tBuOH	*tert*-butanol
TCAN	Trichloroacetonitrile
TCM	Trichloromethane
THM	Trihalomethane
UMRNOM	Upper Mississippi River NOM extract
UVA_{254}	UV Absorbance at 254 nm

List of Publications and Presentations Arising from this Thesis

Peer-reviewed journal articles

Rougé, V.; Allard, S.; Croué, J.-P.; von Gunten, U., In Situ Formation of Free Chlorine during ClO_2 Treatment: Implications on the Formation of Disinfection Byproducts. *Environmental Science & Technology* **2018,** *52*, (22), 13421-13429.

Rougé, V. et al., Electron Donating Capacity and UVA_{254} as Surrogates for Pre-oxidation Treatment Efficiency (to be submitted to *Environmental Science & Technology*)

Rougé, V. et al., Optimizing ClO_2 Pre-oxidation by Predicting Chlorite Oxidation during Chlorination (to be submitted to *Water Research*).

Rougé, V. et al., Impact of Pre-oxidation on Disinfection Byproduct Formation during Chlorination: Ozone vs Chlorine Dioxide vs Ferrate vs Permanganate (to be submitted to *Water Research*).

Oral presentations

Rougé, V.; Allard, S.; Von Gunten, U.; Croué, J. P. "Monitoring of Chemical Pre-oxidation Efficiency by Electron Donating Capacity for Mitigation of Disinfection By-products during Chlorination". IWA 10th Micropol & Ecohazard Conference, Sep 2017, Vienna, Austria.

Rougé, V.; Allard, S.; Von Gunten, U.; Croué, J. P. "Comparison of O_3, Ferrate, ClO_2, and Permanganate Pre-treatment on NOM's Characteristics and Formation of DBPs". IOA EA3G Conference, Sep 2018; Lausanne, Switzerland.

Allard, S.; Rougé, V.; Von Gunten, U.; Croué, J. P. "Impact of different pre-treatment processes on NOM's electrochemical properties and subsequent DBPs formation from chlorination". What is in Our Water Conference, Oct 2018; Canberra, Australia.

Chapter 1. Thesis overview

This Thesis contains 7 chapters. Chapter 1 presents an overview of the Thesis. Chapter 2 provides the validation of an analytical tool used throughout the Thesis. Chapters 3 to 6 discuss results of the various topics investigated, and Chapter 7 provides a general conclusion of the main outcomes of this dissertation as well as research perspectives.

Chapter 2 presents the validation of a size exclusion chromatography followed by UV detection at 254 nm and a post-column reaction to measure the electron donating capacity. This analytical system was used to simultaneously measure the UVA_{254} and EDC of water samples before and after treatment throughout the whole investigations carried out during this Thesis.

Chapter 3 presents the characterization of the impact of ClO_2, O_3, Fe(VI) and Mn(VII) on a Suwannee River NOM extract by two surrogates, UVA_{254} and EDC, using the analytical system developed in Chapter 2. Several mechanistic similarities and differences were demonstrated between the oxidants. The potential use of UVA_{254} and EDC as surrogates for chlorine demand, as well as the formation of AOX, THMs and HANs are investigated. Results of this work will be submitted soon to Environmental Science & Technology.

Chapter 4 demonstrates the formation of free available chlorine (FAC) during ClO_2 reactions. This investigation measured the formation of FAC during the reaction of ClO_2 with a model compound, phenol, and with Suwannee River and Upper Mississippi River NOM extracts. The AOX, THMs and HANs arising from the *in situ* formed FAC with model compounds and standard NOMs were compared to directly dosed FAC. Control experiments with glycine, to quench the FAC, were also conducted. Finally, the formation of ClO_2-induced DBP was investigated in real waters. This work has been published in Environmental Science & Technology: "Rougé, V.; Allard, S.; Croué, J.-P.; von Gunten, U., In Situ Formation of Free Chlorine During ClO2 Treatment: Implications on the Formation of Disinfection Byproducts. *Environmental Science & Technology* **2018,** *52*, (22), 13421-13429".

Chapter 5 focuses on the modelling of the reaction of ClO_2^- with FAC to optimize the ClO_2 pre-oxidation treatment. The FAC/ClO_2^- reaction was followed in ultrapure water buffered at different pHs (6.6-8.1) to develop a conceptual model using Kintecus software. The impact of NOM on the reaction was evaluated and the model was tested

to predict the abatement of ClO_2^- in both synthetic and real waters. The real waters were pre-oxidized with different doses of ClO_2 to investigate the benefit of increasing ClO_2 doses for the mitigation of DBP formation during subsequent chlorination, while keeping the formed ClO_2^- under regulatory limits. This work will make the basis of a manuscript that will be submitted to Water Research.

A comparative study of the efficiency of pre-oxidation by ClO_2, O_3, Fe(VI) or Mn(VII) for the mitigation of DBPs during subsequent chlorination is presented in Chapter 6. The impact of the pH and bromide concentration on DBP formation and speciation, as well as on the pre-oxidation efficiency was investigated. The mitigation of THM and HAN formation in real and synthetic waters was evaluated in terms of calculated cytotoxicity. These results will form the basis of a manuscript that will be submitted to the peer reviewed journal Water Research.

Chapter 2. Natural Organic Matter characterization by Electron Donating Capacity

The content of Chapter 2 and Appendix 2 is unable to be reproduced here as they are under embargo due to current consideration for publication in the journal *Environmental Science & Technology*, with the following contributing co-authors: Sébastien Allard, Jean-Philippe Croué and Urs von Gunten.

I, Valentin Rougé, as the primary author, conducted all the experimental work and data analysis, including creating figures and tables, and writing and editing the manuscript.

I, as a Co-Author, endorsed that this level of contribution by the candidate indicated above is appropriate.

Sébastien Allard

Jean-Philippe Croué

Urs von Gunten

2.1 Introduction

The UVA_{254}, a proxy for NOM aromaticity, is commonly used in water treatment for monitoring NOM reactivity.[1, 2] In order to observe an impact on NOM properties by UVA_{254} absorbance, aromatic moieties need to be either removed or cleaved. However, oxidative treatments can lead to the modification of aromatic moieties without cleavage, such as the oxidation of phenolic-type moieties to quinone-type moieties.[3] Alternatively, the electron donating capacity (EDC) is a parameter used to describe the antioxidant properties of NOM.[4, 5] A number of analytical tools have been recently developed to improve the measurement of the EDC such as a mediated electrochemical oxidation (MEO),[5] a size exclusion chromatography (SEC),[6] and a flow injection analysis system (FIA).[7] These recent developments improved the sensitivity of the EDC measurement, allowing measurement at lower DOC concentration, relevant to drinking water treatment. The three aforementioned methods are based on the monitoring of the reaction of NOM with the stable radical cation 2,2'-azino-bis(3-ethylbenzothiazoline-6-sulphonic acid) ($ABTS^{+\bullet}$), by amperometry for MEO and FIA, or spectrophotometry for SEC.

The different moieties composing NOM exhibit wide ranges of redox potentials and reaction kinetics with the $ABTS^{+\bullet}$. Therefore, the EDC is operatively defined by parameters such as the applied voltage, the pH or the contact time between NOM and $ABTS^{+\bullet}$.[7, 8] Nevertheless, comparable results between the different methods have been obtained. The EDC reduction after oxidative treatment was shown to be similar when using SEC, MEO or FIA.[6, 9, 10] Furthermore, the EDC measured by MEO and FIA was found to correlate with the phenolic content of NOM.[7, 8]

A SEC system similar to that developed by Chon et al.[6] was assembled. The aim of this chapter is to validate the use of this system for UVA_{254}/EDC measurement.

2.2 Material and methods

2.2.1 Chemicals and reagents

Blue dextran (0.10-0.12 mmol reactive blue per gram of dextran) was purchased from Sigma-Aldrich and trolox (≥ 98%) Toronto Research Chemicals. All other chemicals were of analytical grade quality (≥ 98%). Solutions were prepared with ultrapure water (Purelab Ultra, Elga, UK). NOM extracts were purchased from the International Humic Substances Society and are given in Table A-2-1.

2.2.2 System description

An Agilent 1100 series system was used to measure the UVA_{254} and EDC. 2.5 mL of 0.45 µm filtered samples were eluted by a borate buffer (50 mM, pH 7.8) at 0.2 mL min^{-1} through a Toyopearl HW-50S column (8 x 300 mm, 30 µm) followed by a first UV detector at 254 nm. The sample was then mixed through a mixing tee with the post-column reagent, added by a post-column delivery system pressurized by helium at 0.05 mL min^{-1}. The mixing tee was followed by a 750 µL reaction coil and a second UV detector at 405 nm. This second UV detector monitored the concentration of $ABTS^{+\bullet}$ which exhibits a high absorbance at this wavelength (Figure 2-1a).[11] In presence of NOM, $ABTS^{+\bullet}$ undergoes a 1-electron transfer and is reduced to ABTS which doesn't absorb at 405 nm (eq 2-1, Figure 2-1a).

$$ABTS^{+\bullet} + NOM \rightarrow ABTS + NOMox \qquad \text{eq 2-1}$$

The post-column reagent was prepared by mixing 6 mM of ABTS with 2 mM of sodium persulfate for 16 h to ensure a complete reduction of persulfate (eq 2-2). The resulting solution was then diluted 100-fold in 20 µM H_2SO_4 to obtain a final solution containing 40 µM $ABTS^{+\bullet}$ and 20 µM ABTS at pH 4 to optimize $ABTS^{+\bullet}$ stability.[7]

$$2ABTS + {S_2O_8}^{2-} \rightarrow 2ABTS^{+\bullet} + 2{SO_4}^{2-} \qquad \text{eq 2-2}$$

The $ABTS^{+\bullet}$ absorbance was measured at 405 nm. The absorbance of the fresh solutions were within a ± 5% range and remained stable for at least a week when stored either at 5 or 22°C (Figure 2-1b).

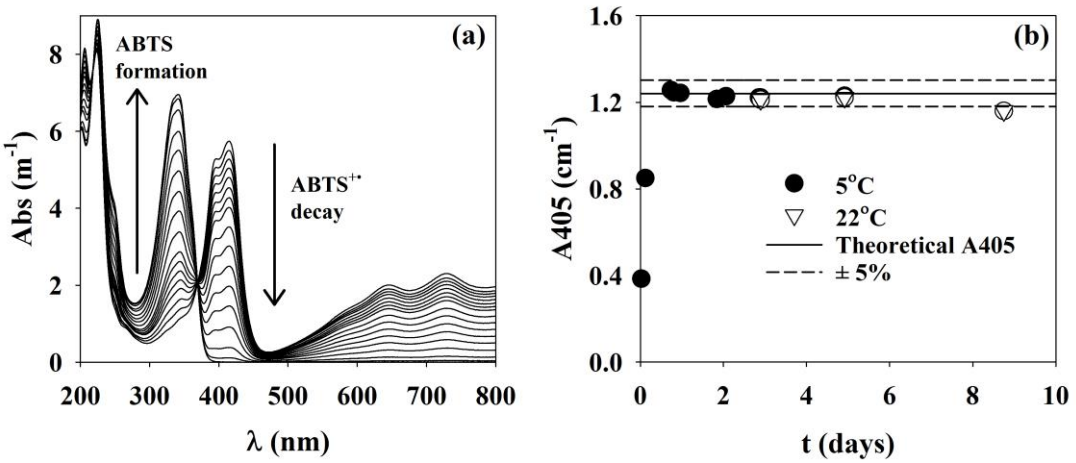

Figure 2-1. (a) ABTS/$ABTS^{+\bullet}$ spectra and (b) $ABTS^{+\bullet}$ formation and stability at 5 and 22°C.

2.3 Results and discussion

2.3.1 System calibration and validation

The column excluded and included volumes were determined by blue dextran and acetone, respectively. They corresponded to elution times of 30 min and 65 min, respectively. Therefore, all samples were expected to elute within these retention times.

2.3.1.1 Validation of the EDC measurement

Trolox is a widely used standard for the measurement of antioxidant capacity assay in food.[12, 13] It is known to rapidly exchange two electrons with $ABTS^{+\bullet}$ and was therefore used as a standard for the EDC. The injection of increasing concentrations of trolox gave defined peaks toward the latest retention times (65 min) (Figure A-2-1a). The spiked concentrations of trolox peaks were expressed in $\mu eqe^{-}\ L^{-1}$ (1 µM = 2 $\mu eqe^{-}\ L^{-1}$) and were very well correlated with the peak integrations (0.9996, Figure A-2-1b).

Different NOM isolates from the International Humic Substance Society, of which characteristics are given in Table A-2-1, were spiked at 1 mgC L^{-1}. The trolox calibration shown in Figure A-2-1b was used to calculate the NOM EDCs in $\mu eqe^{-}\ L^{-1}$, which was then compared to their EDCs found in literature (Figure 2-2).[7, 8] A good agreement was found between the EDC from the SEC (this study) and the EDC from MEO (literature), except for LHA which exhibited a much lower EDC when measured by SEC compared to MEO (3.1 versus 5.1 $\mu eqe^{-}\ L^{-1}$, respectively). The value of LHA

EDC measured by FIA was closer to the measurement by SEC (4.0 versus 3.1 µeqe$^-$ L^{-1}, respectively). Conversely, the EDC value of SRNOM I from SEC was closer to the EDC measured by MEO than by FIA (4.3 µeqe$^-$ L^{-1} by SEC versus 4.6 and 5.1 µeqe$^-$ L^{-1} by MEO and FIA, respectively). Comparatively to the other NOMs, LHA was the only terrestrial humic substance tested and therefore presented features very different from aquatic humic substances,[14] which may explain the differences in EDC observed between the different techniques (SEC, FIA and MEO).

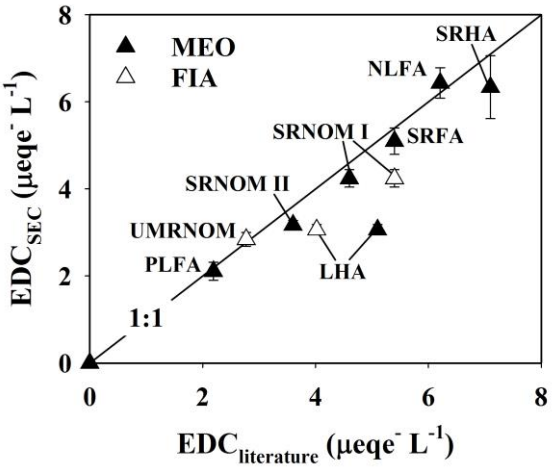

Figure 2-2. Measured EDC (EDC$_{SEC}$) compared to the EDC from the literature.[7, 8] The line represents a 1:1 ratio. The error bars represent duplicated analysis. [NOM] = 1 mgC L^{-1}.

2.3.1.2 SRNOM calibration

Figure 2-3a and b show the UVA$_{254}$ and EDC chromatograms of increasing concentrations of SRNOM (0.1–5 mgC L^{-1}). The large variety of molecular sizes in SRNOM led to peaks occupying almost all of the column capacity (30 to 65 min).[15] UVA$_{254}$ increased in presence of SRNOM due to the absorbance of aromatic moieties (Figure 2-3a). Conversely, a decrease in absorbance at 405 nm in presence of SRNOM was observed for the EDC (Figure 2-3b), resulting from the reduction of ABTS$^{+\bullet}$ back to ABTS (eq 2-1).

In comparison to UVA$_{254}$ peaks, the elution of EDC peaks were shifted by about 3 min due to the reaction time in the mixing tee. The integrations of UVA$_{254}$ and EDC peaks were well correlated with the SRNOM concentrations ranging from 0.1 to 4 mgC L^{-1} (r^2 = 0.9988 and 0.9978, Figure 2-3c and d). For the EDC of SRNOM concentrations of 5 mgC L^{-1} and above, a significant deviation from linearity was observed (Figure 2-3d), probably due to a significant decrease in the ABTS$^{+\bullet}$ (> 60% of the

$ABTS^{+\bullet}$ consumed) and a short contact time (~ 3 min). Therefore, the EDC signal of samples was kept < 2 AU min, corresponding to SRNOM concentrations < 5 mgC L^{-1}.

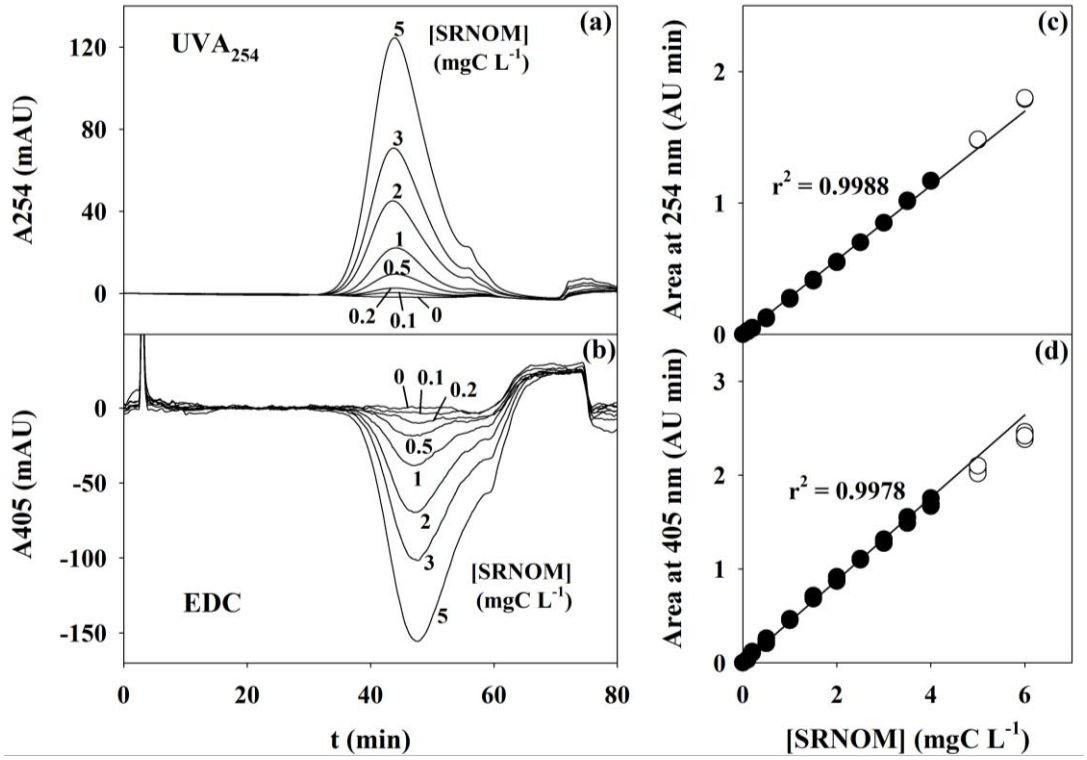

Figure 2-3. UVA_{254} (a) and EDC (b) spectra of SRNOM samples and corresponding UVA_{254} (c) and EDC (d) calibrations. Open circles are excluded from the regression. Each concentration was run in triplicate.

The limits of detection and quantification of the EDC and UVA_{254} were determined using the standard deviation of 6 consecutive injections of 0.1 mgC L^{-1} of SRNOM. The limit of detection was corresponding to 0.09 and 0.02 mgC L^{-1} of SRNOM for EDC and UVA_{254}, respectively. The limit of quantification was corresponding to 0.28 and 0.08 mgC L^{-1} of SRNOM for EDC and UVA_{254}, respectively. The relative standard deviations of the samples were 8–15% for SRNOM concentrations < 1 mgC L^{-1} for both UVA_{254} and EDC (Figure A-2-2). At SRNOM concentrations > 1 mgC L^{-1}, the sample relative standard deviations were 2–5% and 1–3% for EDC and UVA_{254}, respectively (Figure A-2-2).

2.3.3 Conclusion

The developed SEC system was found to be sensitive for EDC and UVA_{254} measurement, with limits of detection corresponding to 0.09 and 0.02 mgC L^{-1} of SRNOM, respectively and repeatability within ± 15% for SRNOM concentrations < 1 mgC L^{-1} and within ± 5% for SRNOM concentrations > 1 mgC L^{-1}. The calibration

of the EDC using trolox as an internal standard showed that the EDCs measured by the SEC system was similar to values reported in the literature with other methods.

Since the EDC is operatively defined and parameters such as the presence of buffer can affect the SEC profile (although the resulting integration remains within 10%), the EDC and UVA_{254} will usually be expressed relative to a blank (sample before oxidation for example) i.e., EDC/EDC_0 and UVA/UVA_0.

2.4 References

1. Weishaar, J. L.; Aiken, G. R.; Bergamaschi, B. A.; Fram, M. S.; Fujii, R.; Mopper, K., Evaluation of Specific Ultraviolet Absorbance as an Indicator of the Chemical Composition and Reactivity of Dissolved Organic Carbon. *Environmental Science & Technology* **2003,** *37*, (20), 4702-4708.
2. Croué, J.-P.; Violleau, D.; Labouyrie, L., Disinfection By-Product Formation Potentials of Hydrophobic and Hydrophilic Natural Organic Matter Fractions: A Comparison Between a Low- and a High-Humic Water. In *Natural Organic Matter and Disinfection By-Products*, American Chemical Society: 2000; Vol. 761, pp 139-153.
3. Tentscher, P. R.; Bourgin, M.; von Gunten, U., Ozonation of Para-Substituted Phenolic Compounds Yields p-Benzoquinones, Other Cyclic α,β-Unsaturated Ketones, and Substituted Catechols. *Environmental Science & Technology* **2018,** *52*, (8), 4763-4773.
4. Bauer, M.; Heitmann, T.; Macalady, D. L.; Blodau, C., Electron transfer capacities and reaction kinetics of peat dissolved organic matter. *Environmental Science and Technology* **2007,** *41*, (1), 139-145.
5. Aeschbacher, M.; Sander, M.; Schwarzenbach, R. P., Novel electrochemical approach to assess the redox properties of humic substances. *Environmental Science and Technology* **2010,** *44*, (1), 87-93.
6. Chon, K.; Salhi, E.; von Gunten, U., Combination of UV absorbance and electron donating capacity to assess degradation of micropollutants and formation of bromate during ozonation of wastewater effluents. *Water Res.* **2015,** *81*, 388-397.
7. Walpen, N.; Schroth, M. H.; Sander, M., Quantification of Phenolic Antioxidant Moieties in Dissolved Organic Matter by Flow-Injection Analysis with Electrochemical Detection. *Environmental Science & Technology* **2016,** *50*, (12), 6423-6432.
8. Aeschbacher, M.; Graf, C.; Schwarzenbach, R. P.; Sander, M., Antioxidant properties of humic substances. *Environmental Science and Technology* **2012,** *46*, (9), 4916-4925.
9. Wenk, J.; Aeschbacher, M.; Salhi, E.; Canonica, S.; Von Gunten, U.; Sander, M., Chemical oxidation of dissolved organic matter by chlorine dioxide, chlorine, and ozone: Effects on its optical and antioxidant properties. *Environmental Science and Technology* **2013,** *47*, (19), 11147-11156.
10. Önnby, L.; Walpen, N.; Salhi, E.; Sander, M.; von Gunten, U., Two analytical approaches quantifying the electron donating capacities of dissolved organic matter to monitor its oxidation during chlorination and ozonation. *Water Res.* **2018,** *144*, 677-689.
11. Pinkernell, U.; Nowack, B.; Gallard, H.; Von Gunten, U., Methods for the photometric determination of reactive bromine and chlorine species with ABTS. *Water Res.* **2000,** *34*, (18), 4343-4350.
12. van den Berg, R.; Haenen, G. R. M. M.; van den Berg, H.; Bast, A., Applicability of an improved Trolox equivalent antioxidant capacity (TEAC) assay for evaluation of antioxidant capacity measurements of mixtures. *Food Chemistry* **1999,** *66*, (4), 511-517.
13. Zheng, L.; Zhao, M.; Xiao, C.; Zhao, Q.; Su, G., Practical problems when using ABTS assay to assess the radical-scavenging activity of peptides: Importance of controlling reaction pH and time. *Food Chemistry* **2016,** *192*, 288-294.

14. Malcolm, R. L., The uniqueness of humic substances in each of soil, stream and marine environments. *Analytica Chimica Acta* **1990,** *232*, 19-30.
15. Leenheer, J. A.; Croué, J. P., Characterizing aquatic dissolved organic matter. *Environmental Science and Technology* **2003,** *37*, (1), 18A-26A.

Every reasonable effort has been made to acknowledge the owners of copyright material. I would be pleased to hear from any copyright owner who has been omitted or incorrectly acknowledged.

Chapter 3. Electron Donating Capacity and UVA_{254} as Surrogates for Pre-oxidation Treatment Efficiency

The content of Chapter 3 and Appendix 3 is unable to be reproduced here as they are under embargo due to current consideration for publication in the journal *Environmental Science & Technology*, with the following contributing co-authors: Sébastien Allard, Jean-Philippe Croué and Urs von Gunten.

I, Valentin Rougé, as the primary author, conducted all the experimental work and data analysis, including creating figures and tables, and writing and editing the manuscript.

I, as a Co-Author, endorsed that this level of contribution by the candidate indicated above is appropriate.

Sébastien Allard

Jean-Philippe Croué

Urs von Gunten

3.1 Abstract

In order to mitigate the formation of disinfection byproducts during chlorination, different oxidants can be used as a pre-treatment to decrease the reactivity of the water matrix. However, it is challenging to compare the efficiency of the different oxidants since they react through different mechanisms. This study provides an understanding of the impact of four oxidants, chlorine dioxide (ClO_2), ozone (with or without tert-butanol O_3-tBuOH/O_3), ferrate (Fe(VI)) and permanganate (Mn(VII)) on Natural Organic Matter (NOM) characteristics using the UV absorbance at 254 nm (UVA_{254}) and the electron donating capacity (EDC). The implications in terms of NOM reactivity and DBPs precursors is also assessed. The impact of pre-oxidants (based on molar concentration) on EDC ranked in the order (Mn(VII)) > (ClO_2) > (Fe(VI))/O_3-tBuOH > O_3, while the efficiency of pre-oxidation on UVA_{254} was following the order O_3/O_3-tBuOH/Mn(VII) > Fe(VI)/ClO_2. Two phases were observed. In phase I, at low oxidant doses corresponding to < 50% EDC abatement, ClO_2, Fe(VI) and Mn(VII) exhibited a limited decrease in UVA_{254} comparatively to the EDC (~ 1% UVA_{254} reduction per 10% EDC reduction). This suggests the formation of quinone-type moieties which absorbed some UVA_{254} while losing EDC. In phase II, at higher doses (> 50% EDC abatement), a more efficient removal of UVA_{254} (~ 5-8% UVA_{254} decrease per 10% EDC decrease), suggesting aromatic ring cleavage. By comparison to the other oxidants, O_3 (with or without tBuOH) was decreasing the UVA_{254} more effectively, due to a more efficient cleavage of aromatic rings. The distinctive impact of O_3-tBuOH on NOM compared to the other investigated pre-oxidants was confirmed by the lowest formation of adsorbable organic halogens (AOX). ClO_2, Fe(VI) and Mn(VII) led to similar mitigation of AOX formation for an equivalent EDC reduction, while O_3-tBuOH led to lower concentrations of AOX. The EDC was also demonstrated to be an oxidant-independent surrogate for chlorine demand and, interestingly, haloacetonitrile formation. Comparatively, UVA_{254} was found to be an oxidant-independent surrogate for AOX and trihalomethanes. These results emphasize the interest in combining the EDC and UVA_{254} measurement for monitoring NOM reactivity and controlling DBPs

3.2 Introduction

During water treatment, a major fraction of chlorine (Cl_2), the most commonly used disinfectant, reacts with natural organic matter (NOM), leading to the formation of disinfection byproducts (DBPs).[1, 2] Pre-oxidation is a promising alternative to reduce NOM reactivity prior to disinfection and to mitigate DBPs formation.[3-5] Depending on the type of oxidant, the water characteristics and the type of DBPs targeted, differences in DBP mitigation efficiency have been observed during pre-oxidation treatment.[5-8] In previous studies, the choice of oxidant dose has been based either on an equivalent mass concentration,[4, 9] molar concentration,[10] virus inactivation efficiency,[11] or on practical usage.[5, 12, 13] However, each oxidant reacts through its own set of mechanisms. Chlorine dioxide (ClO_2) is reacting through a 1-electron transfer to form chlorite (ClO_2^-), but recent studies (Chapter 4) have highlighted the importance of oxygen transfer mechanisms releasing hypochlorous acid (HOCl).[14, 15] Most of ozone (O_3) reactions lead to an oxygen or electron transfer associated with the possible release of OH radical ($^{\bullet}OH$) or hydrogen peroxide (H_2O_2).[16] O_3 is particularly reactive toward olefins, leading to the breakage of C=C bonds through Criegee mechanism.[17] Permanganate (Mn(VII)) and ferrate (Fe(VI)) can react through electrophilic attack on double bonds, or electron transfer, notably with phenolic compounds and amines.[18-20] Furthermore, the degradation products of these oxidants can also be reactive. The hydroxyl radicals ($^{\bullet}OH$) released by O_3 exhibit a very high reactivity toward a wide range of moieties through addition or hydrogen abstraction,[21] while the HOCl released by ClO_2 can react through 2-electron transfer or chlorine substitution.[22] Mn(VI), Mn(V), Fe(V) and Fe(IV) associated with the use of Mn(VII) and Fe(VI) are also highly reactive.[23-26]

Considering the large array of possible reaction mechanisms it is difficult to truly compare the impact of each pre-oxidation treatment on the mitigation of DBPs based on an equivalent oxidant dose. Alternatively, comparing the reactivity of oxidants based on their impact on NOM characteristics before final disinfection seems to be a better practical option. Historically, the absorbance at 254 nm (UVA_{254}), or the $SUVA_{254}$ (UV absorbance at 254 nm divided by dissolved organic carbon, DOC), have been used as a proxy for NOM aromaticity.[27, 28] These spectrophotometric indicators correlate with the trihalomethane (THM), trihaloacetic acid or adsordable organic halogen (AOX) formation potential.[28-32] A previous study linked the formation of *N*-

nitrosodimethylamine during chloramination to the $SUVA_{272}$ of the water after pre-oxidation with Mn(VII), H_2O_2, O_3 and Cl_2.[13] However, limitations have been reported.[27, 33] Recently, the measurement of the electron donating capacity (EDC) was developed as a proxy for activated aromatic,[34, 35] which are important precursors of halogenated DBPs. The use of EDC combined with UVA_{254} revealed insights on the reaction mechanisms of ClO_2, O_3 and Cl_2 with NOM.[36-38]

The aims of this study are (i) to compare ClO_2, O_3, Fe(VI) and Mn(VII) in terms of EDC and UVA_{254} abatement and (ii) to explore the possibility of using the EDC and UVA_{254} as complementary surrogates for predicting Cl_2 demand, as well as AOX, THMs and haloacetonitriles (HANs) formation during disinfection.

3.3 Materials and methods

3.3.1 Chemicals and reagents

Sodium chlorite (80%) and a sodium hypochlorite solution (10–15%) were purchased from Sigma-Aldrich. All other chemicals were of analytical grade quality (≥ 98%). Solutions were prepared with ultrapure water (Purelab Ultra, Elga, UK). Suwannee River NOM extract was purchased from the International Humic Substances Society (Cat. No. 2R101N).

3.3.2 Preparation of oxidant solutions

Chlorine stock solutions were prepared from a sodium hypochlorite solution standardized by direct UV measurement at 292 nm ($\varepsilon_{292} = 362\ M^{-1}\ cm^{-1}$).[39] ClO_2 was produced by mixing solutions of sodium persulfate (40 g L^{-1}) and sodium chlorite (80 g L^{-1}) under N_2 bubbling for about 1 h.[40, 41] The ClO_2 produced was retrieved in chilled ultrapure water and standardized by direct UV measurement at 359 nm ($\varepsilon_{359} = 1230\ M^{-1}\ cm^{-1}$).[39] The K_2FeO_4 was prepared by oxidation of ferric nitrate with potassium hypochlorite.[42] The final product was stable with a purity of 43%. The rest of the solid was potassium hydroxide. The Mn(VII) and Fe(VI) solutions were prepared by dissolution of $KMnO_4$ in ultrapure water for Mn(VII), or of K_2FeO_4 in a phosphate/borate buffer at pH 9.5 (5 mM / 1 mM) for Fe(VI). The stock solutions were then filtered through 0.22 µm (Polyethersulfone, Merck Millipore) and standardized by direct UV measurement at 525 nm ($\varepsilon_{525} = 2430\ M^{-1}\ cm^{-1}$)[43] for Mn(VII) or 510 nm ($\varepsilon_{510} = 1150\ M^{-1}\ cm^{-1}$)[44] for Fe(VI). O_3 stock solution was prepared by bubbling an ozone-oxygen mixture produced by an O_3 generator (American Ozone System Inc.) in ultrapure water cooled at < 5°C. The O_3 stock solution was standardized by direct UV measurement at 258 nm ($\varepsilon_{258} = 2900\ M^{-1}\ cm^{-1}$).[45]

3.3.3 Pre-oxidation and chlorination experiments

The synthetic waters were prepared with 3.0 mgC L^{-1} of a Suwannee River extract buffered at pH 8 (40 mM borate), with or without bromide (150 µg L^{-1}). For EDC and UVA_{254} experiments, samples of 40 mL were spiked with O_3 (with or without 5 mM of tert-butanol, tBuOH), ClO_2, Mn(VII) or Fe(VI) (1–150 µM), kept without headspace (< 10% of total volume) and protected from light until complete depletion of the oxidants. tBuOH was used as a $^{\bullet}OH$ scavenger to account for molecular O_3

reactions only.[46] The samples were then filtered through 0.22 µm (Polyethersulfone, Merck Millipore) and analyzed for EDC and UVA_{254}.

For chlorination experiments, a similar experimental procedure was used with 500 mL samples. After pre-oxidation, 200 mL of the filtered pre-oxidized sample was chlorinated with 85 µM of sodium hypochlorite (6.0 $mgCl_2\ L^{-1}$) for 3 days, without headspace (< 10% of total volume) and protected from light. Preliminary experiments were carried out to determine the chlorine dose needed to obtain an oxidant residual around 1.5 $mgCl_2\ L^{-1}$ after 3 days at pH 8 for a sample without bromide and without pre-treatment. The oxidant residual was quenched by sulfite (10% excess) for AOX measurements, or by a large excess of ascorbic acid for THM and HAN measurements.

3.3.4 Analytical methods

THMs and HANs were analyzed by headspace GC-MS with a method adapted from previously published methods, of which details are given in Text A-3-1.[47, 48] The AOX was measured by combustion and ion chromatography after adsorbing samples on activated carbon.[49] The Cl_2 residual was measured by ABTS (2,2'-azino-bis(3-ethylbenzothiazoline-6-sulfonic acid) diammonium salt).[50] The EDC, a proxy for antioxidant capacity of NOM,[34, 36] and the UVA_{254} were measured on an Agilent 1100 series system using a size-exclusion chromatography (SEC) (Text A-3-2, Chapter 2).[37, 51] The EDC and UVA_{254} results are presented as percentage of reduction compared to the untreated sample.

3.4 Results and discussion

The primary goal of the present study is to investigate the impact of oxidative treatments on electrochemical and physicochemical NOM properties, and the implications for DBP formation during chlorination. In practice, supplementary treatments such as coagulation/sedimentation or biofiltration may be applied between pre-oxidation and disinfection, which would also affect NOM properties. The filtration step performed between pre-oxidation and disinfection was added to remove MnO_2 particles hence preventing their interaction with Cl_2, and was not affecting the EDC or UVA_{254}.

3.4.1 Impact of oxidants on SRNOM properties

The EDC and UVA_{254} abatement, expressed in percentage reduction, were measured after treatment of 3 mgC L^{-1} of SRNOM at pH 8 with different doses of ClO_2, O_3 (with or without tBuOH), Fe(VI) or Mn(VII) (Figure 3-1a and b). Both the EDC and UVA_{254} were decreasing with increasing doses of oxidant and the decrease was dependent on the type of oxidant used.

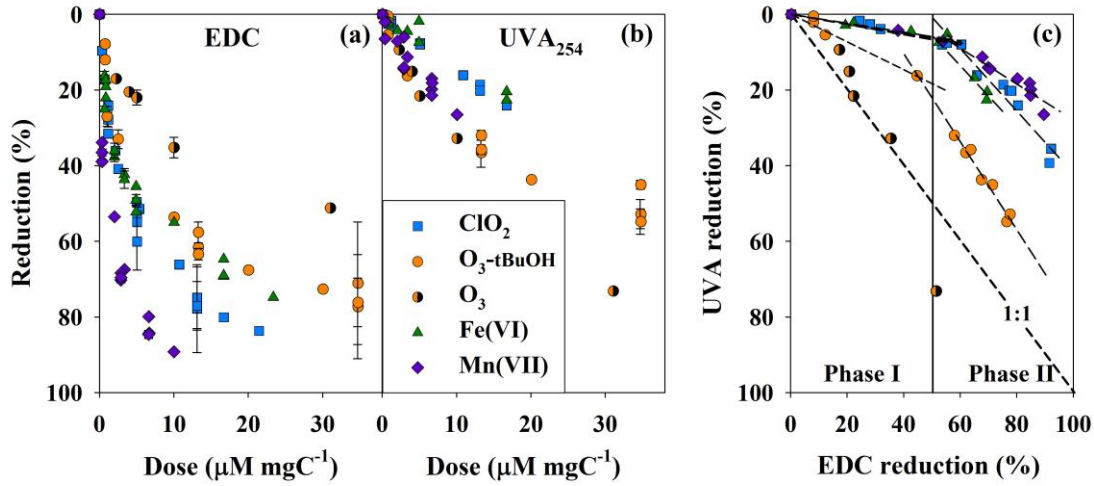

Figure 3-1. EDC (a) and UVA_{254} (b) abatement after ClO_2, O_3 (with or without tBuOH), Fe(VI) or Mn(VII) oxidation and relationship between EDC and UVA_{254} abatement of the different oxidants (c). [ClO_2] = 1–64.3 µM, [O_3-tBuOH] = 2.2–104.1 µM, [O_3] = 6.7–93 µM, [Fe(VI)] = 2–50 µM, [Mn(VII)] = 1–30 µM, [SRNOM] = 3 mgC L^{-1}, [Br^-] = 0 or 150 µg L^{-1}, pH 8 (40 mM borate). Error bars represent the range of analytical results from one experiment.

3.4.1.1 EDC

For a pre-oxidant dose of 4 µM mgC^{-1}, the EDC removal was highest for Mn(VII), with ~ 70–75% EDC abatement, equivalent for ClO_2, Fe(VI) and O_3-tBuOH, with ~ 40–44% EDC abatement, and lowest for O_3 with ~ 20% EDC abatement (Figure 3-1a). For doses > 4 µM mgC^{-1}, O_3-tBuOH and Fe(VI) became less efficient than ClO_2 in decreasing the EDC. At 10 µM mgC^{-1}, Mn(VII) and ClO_2 reduced the EDC by 90 and 65%, respectively, while O_3-tBuOH and Fe(VI) removed ~ 54% of the EDC.

As shown in Figure 3-1a the EDC reduction observed for Mn(VII) was the most important among the tested oxidants. This is in accordance with the theoretical ability of Mn(VII) to exchange more electrons than the other tested oxidants (between 3 (Mn(IV)) and 5 electrons (Mn(II)) depending on the final reduced form). It was verified that the higher EDC abatement by Mn(VII) was not due to the adsorption of NOM onto MnO_2 particles and subsequent filtration of MnO_2.[52] No dissolved organic carbon (DOC) was lost after filtration, and a difference ≤ 4% of EDC abatement was observed between the filtered and unfiltered samples. The reactivity of Mn(IV) is considered to be negligible at neutral pH and above,[53, 54] which was consistent with the precipitate observed in our experiments corresponding to the formation of MnO_2 particles.

Similarly to Mn(VII), Fe(VI) is theoretically able to exchange 3 (Fe(III)) or 4 electrons (Fe(II)). However, Fe(VI) reduced the EDC much less efficiently than Mn(VII) (Figure 3-1a). Fe(VI) and its degradation products are known to rapidly self-decay leading to a lower oxidant exposure and therefore a lower reduction in EDC. More details on kinetics and degradation pathways of Fe and Mn species are given in Text A-3-3.

Comparatively to Mn(VII), the lower EDC abatement by ClO_2 was consistent with the known 1-electron transfer producing ClO_2^- (Figure 3-1a).[55] However, ClO_2 is also capable of oxygen transfer with radical intermediates, corresponding to a 3-electron transfer releasing $HOCl/OCl^-$.[14, 56] The *in situ* formed $HOCl/OCl^-$ can further react, increasing the oxidation capacity of ClO_2 and the EDC abatement.

A lesser EDC abatement was observed for O_3-tBuOH and O_3, which is theoretically able to exchange 2 electrons, compared to ClO_2 (Figure 3-1a). O_3 is unstable in aqueous solution because it reacts with $^{\bullet}OH$.[57] The addition of tBuOH stabilizes the O_3 by scavenging the $^{\bullet}OH$ and the increased O_3 exposure in presence of tBuOH led to a more efficient EDC abatement compared to the experiment with O_3 alone.

3.4.1.2 Comparison with UVA_{254}

In contrast to the EDC, the reduction of UVA_{254} after O_3 (with and without tBuOH) was higher than after ClO_2 or Fe(VI) and similar to the UVA_{254} reduction after Mn(VII) (Figure 3-1b). For a pre-oxidant dose of 4 µM mgC^{-1}, equivalent UVA_{254} abatements were reached by Mn(VII) and O_3 (with and without tBuOH) with ~ 15% reduction, while ClO_2 and Fe(VI) decreased the UVA_{254} by only 4–5% (Figure 3-1b). The UVA_{254} and EDC abatements were similar for O_3 (~ 15% versus ~ 20% at 4 µM mgC^{-1}, respectively) while the UVA_{254} reduction was significantly lower than the EDC reduction for the other oxidants (< 20% versus > 30% at 4 µM mgC^{-1}, respectively).

To emphasize the differences between oxidants, the UVA_{254} abatement was plotted against the EDC abatement (Figure 3-1c). Figure 3-1c shows that O_3 depleted the EDC and the UVA_{254} to a similar extent while ClO_2, Fe(VI) and Mn(VII) exhibited much higher EDC removal compared to UVA_{254}. The O_3-tBuOH experiments exhibited an intermediate behavior. For ClO_2, O_3-tBuOH, Fe(VI) and Mn(VII), two distinct phases were observed. In phase I (< 50% EDC reduction), a limited UVA_{254} decrease was observed comparatively to the EDC, while in phase II (> 50% EDC reduction), the UVA_{254} decreased more efficiently (Figure 3-1c). Table 3-1 shows the ratios of UVA_{254} decrease on EDC decrease ($\Delta UVA_{254}/\Delta EDC$) during phase I and II for each oxidant. In the first phase, a reduction of 50% of the EDC led to ~ 6–7% of UVA_{254} reduction for ClO_2, Fe(VI) and Mn(VII) while ~ 19% of the UVA_{254} was abated by O_3-tBuOH (Table 3-1, Figure 3-1c). In phase II, the UVA_{254} decrease was equivalent to the EDC decrease for ClO_2, Fe(VI) and O_3-tBuOH with ~ 42–58% of the UVA_{254} abated for 50% EDC decrease (Table 3-1, Figure 3-1c). The UVA_{254} abatement was more limited for Mn(VII), with 24% of the UVA_{254} removed for 50% EDC abatement.

Comparatively to the other oxidants, O_3 could not reach an EDC reduction > 50% for the tested doses (up to 93 µM). However, the UVA_{254} seemed to decrease faster than

the EDC ($\Delta UVA_{254}/\Delta EDC \approx 1.7$) although limited data were available. This behavior has previously been observed and explained by the cleavage of nonphenolic aromatics such as methoxylated compounds which are not detected by EDC.[36]

Table 3-1. Ratio of UVA_{254} decrease on EDC decrease ($\Delta UVA_{254}/\Delta EDC$) calculated from the linear regression between UVA_{254} and EDC in phase I and II, for each oxidant (Figure 3-1c). The regression coefficients (r^2) are indicated in brackets.

Oxidant	Phase I	Phase II
ClO_2	0.14 (0.907)	0.83 (0.926)
O_3-tBuOH	0.37 (0.954)*	1.16 (0.985)
Fe(VI)	0.12 (0.877)	0.83 (0.868)
Mn(VII)	0.13 (0.986)*	0.47 (0.903)

* Limited data available

The EDC and UVA_{254} decrease obtained with ClO_2 and O_3 (with and without tBuOH) (Figure 3-1a,b) were consistent with previous studies conducted on SRFA at pH 7.[36, 38] The different patterns observed for the EDC and UVA_{254} were previously explained, for ClO_2, by the formation of benzoquinones from the oxidation of phenolic moieties, which mitigates the EDC but not the UVA_{254},[36] and for O_3 (with and without tBuOH), by ring cleavage which affects both EDC and UVA_{254}.[36, 38]

The EDC versus UVA_{254} decrease observed for Mn(VII) and Fe(VI) was similar to that of ClO_2 (Figure 3-1c), suggesting that analogous reaction mechanisms occur with Mn(VII) and Fe(VI), i.e. the formation of quinones. This is consistent with the 1-electron transfer pathways with phenol suggested for both Mn(VII) and Fe(VI), leading to quinone and dimeric structures.[18, 24, 58-60] In a previous study, ClO_2, O_3-tBuOH and chlorine were shown to impact the UV-VIS properties of NOM differently.[36] The differential UV spectra of chlorine were exhibiting a characteristic band around 270 nm while the ClO_2 oxidation led to a broad shoulder between 275 and 325 nm.[36] By comparison, the differential UV spectra after O_3 were not presenting any specific feature.[36] A shown in Figure A-3-1, the differential UV spectrum after Mn(VII) oxidation was exhibiting an inflexion around 280–320 nm similar to ClO_2 oxidation. This further supports that Mn(VII) and ClO_2 are reacting through similar

mechanisms. Differential UV spectra could not be obtained for Fe(VI) due to spectral interferences.

The presence of two phases, similar to a previous study,[37] can provide further insights on the impact of the different oxidants on SRNOM characteristics. It is suggested that in phase I (between 0 and 50% EDC reduction), ClO_2, Mn(VII) and Fe(VI) oxidized phenolic-type moieties to quinone-type moities, reducing the EDC but not the UVA_{254} (Figure 3-1c). This resulted in small $\Delta UVA_{254}/\Delta EDC$ reduction ratios (0.12–0.14, Table 3-1). In phase II (between 50 and 80% EDC reduction), NOM moieties were further oxidized and aromatic ring cleavage occurred, resulting in larger UVA_{254}/EDC reduction ratios (0.47–0.83, Table 3-1).[55, 61, 62] In the case of O_3-tBuOH, ring cleavage already occurred in phase I and intensified in phase II to a similar extent compared to ClO_2 and Fe(VI) (Figure 3-1c and Table 3-1).

3.4.2 Cl_2 demand and AOX formation

Preliminary experiments carried out with solutions containing 3 mgC L^{-1} of SRNOM at pH 8, with or without bromide (150 µg L^{-1}) and without pre-oxidation treatment showed that 58 ± 2 µM of Cl_2 were consumed and 16 ± 0.4 µM of AOX were produced after 72 h. The Cl_2 demand after 72 h was decreasing with increasing the pre-oxidant dose and the different oxidants exhibited different behaviors (Figure A-3-2a). For example, about 2, 5, 10 and 17 µM mgC^{-1} were needed to reduce the Cl_2 demand by ~ 20% (~ 45 µM) for Mn(VII), ClO_2, O_3-tBuOH and Fe(VI), respectively (Figure A-3-2a). The formation of AOX after 72 h chlorination was also exhibiting large differences between the oxidants. To achieve a ~ 20% reduction of AOX, 3–4 µM mgC^{-1} of O_3-tBuOH or Mn(VII) and 13 and 17 µM mgC^{-1} of ClO_2 and Fe(VI) were needed, respectively, (Figure A-3-2b).

Figure 3-2a shows the Cl_2 demand based on the relative UVA_{254} reduction for the different oxidants. Similarly to the oxidant dose, large differences were observed between oxidants when comparing the Cl_2 demand based on the UVA_{254} reduction. For example, to reduce the Cl_2 demand by ~ 20%, a UVA_{254} abatement of 8–9% for ClO_2 and Mn(VII), and 20–24% for Fe(VI) and O_3-tBuOH was needed (Figure 3-2a). These results suggest that UVA_{254} is not necessarily representative of Cl_2-consuming moieties. However, the AOX formation correlated well with the UVA_{254} ($r^2 = 0.911$, Figure 3-2b) although the correlation was driven by the O_3-tBuOH data exhibiting a

high UVA_{254} abatement ($r^2 = 0.790$ without the O_3-tBuOH data, Figure 3-2b). These results confirm that UVA_{254} is a useful indicator of AOX precursor,[30, 63] even when different pre-oxidant treatments are applied.

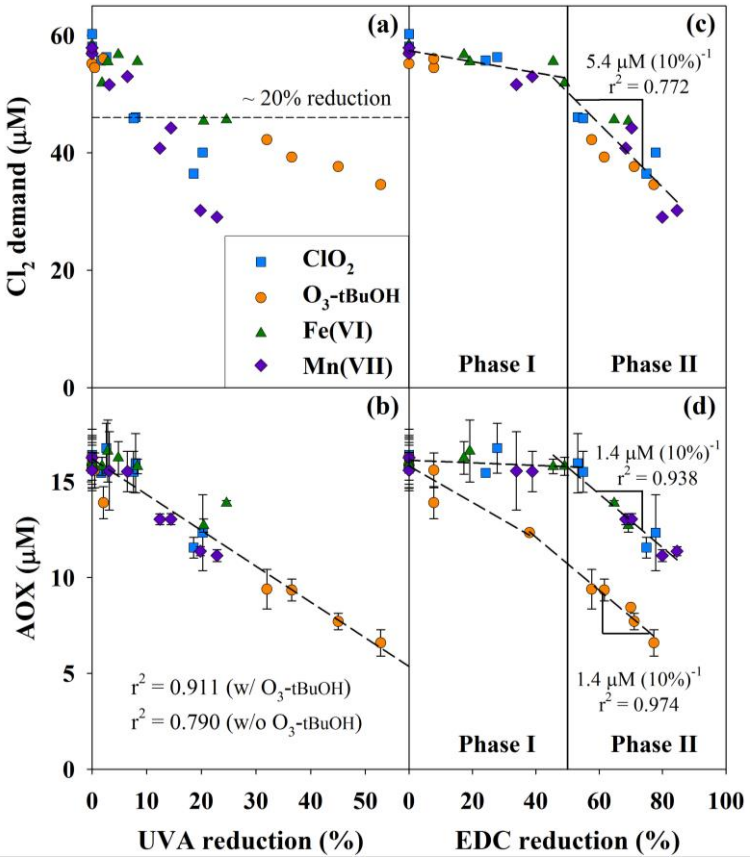

Figure 3-2. Cl_2 demand and AOX formation compared to the UVA_{254} (a–b) and to the EDC (c–d). [ClO_2] = 3.5–39 µM, [O_3-tBuOH] = 2.2–104 µM, [Fe(VI)] = 2.5–50 µM, [Mn(VII)] = 1–20 µM, [SRNOM] = 3 mgC L^{-1}, [Br^-] = 0 or 150 µg L^{-1}, 40 mM borate (pH 8). Error bars for AOX represent the range of analytical results for duplicated experiments (the two highest doses of Fe(VI) and Mn(VII) were not duplicated experiments). No duplicate was done for the Cl_2 demand.

Figure 3-2c and d show that a two-phase trend was observed for the Cl_2 demand and the AOX formation when plotted against the EDC abatement (Figure 3-1c). These results are explained based on the mechanisms previously described. In phase I, ClO_2, Mn(VII) and Fe(VI) mainly oxidized phenolic-type moieties to quinone-type moieties. These moieties have a lower EDC, but can still react with chlorine.[62, 64] Therefore, a limited reduction in Cl_2 demand was observed (< 10%) while a large EDC fraction was abated (up to 50%, Figure 3-2c). As a consequence, due to the limited reduction in Cl_2 demand, the AOX was not significantly reduced (< 10%, Figure 3-2d). In phase II, moieties were further oxidized and aromatic ring cleavage occurred, decreasing the reactivity with Cl_2.[65, 66] Therefore, a significant diminution of Cl_2 demand and

consequently of AOX formation was observed. Over the entire phase I, ≤ 5 µM and < 0.5 µM of reduction in Cl_2 demand and AOX formation, respectively, was observed for ClO_2, Mn(VII) and Fe(VI) (Figure 3-2c and Figure 3-2d). In phase II, 5.4 µM and 1.4 µM reduction in Cl_2 demand and AOX formation per 10% EDC reduction were observed for ClO_2, Mn(VII) and Fe(VI) (Figure 3-2c and Figure 3-2d).

In the case of O_3-tBuOH, it is suggested from Figure 3-1c that ring cleavage occurred in phase I, which led to a significant decrease in AOX formation for EDC reduction < 50% (Figure 3-2d), i.e. ~ 5 µM of reduction in AOX formation at 50% EDC reduction. In phase II, the AOX mitigation was similar to the other oxidants, with 1.4 µM of AOX abatement per 10% EDC reduction. Although the AOX formation was ~ 5 µM lower after O_3-tBuOH pre-oxidation than after the other oxidants in phase II, the Cl_2 demand was similar for all the oxidants (Figure 3-2c). This suggests that products from the reaction of O_3-tBuOH with SRNOM were consuming Cl_2 without forming AOX. H_2O_2 is a byproduct of the reaction of O_3-tBuOH with phenolic compounds, notably during ring cleavage.[67] It is hypothesized that the H_2O_2 produced during O_3 reaction consumed part of the chlorine.[68] Assuming a 28% halogenation yield (0.28 µM of AOX produced by µM of Cl_2), ~ 18 µM of the Cl_2 may have been quenched by H_2O_2.

3.4.3 THMs and HANs

The impact of pre-oxidation on THM and HAN formation was also evaluated. THMs are important regulated DBPs,[69] while HANs are unregulated but more toxic compounds.[70] Preliminary experiments carried out with solutions containing 3 mgC L^{-1} of SRNOM at pH 8, with or without bromide (150 µg L^{-1}) and without pre-oxidation treatment showed that 2.8 ± 0.1 µM of THMs and 48 ± 2 nM of HANs were formed after 72 h. As shown in Figure 3-3a, the formation of THMs was correlated to the reduction of UVA_{254} ($r^2 = 0.752$, Figure 3-3a), although the correlation was again driven by the O_3-tBuOH data ($r^2 = 0.574$ without the O_3-tBuOH data, Figure 3-3a). The correlation between THM formation and UVA_{254} has already been observed in several studies.[27, 31, 32] A similar correlation was observed with the oxidant dose ($r^2 = 0.708$, Figure A-3-2c), which was improved without the O_3-tBuOH data ($r^2 = 0.716$, Figure A-3-2c).

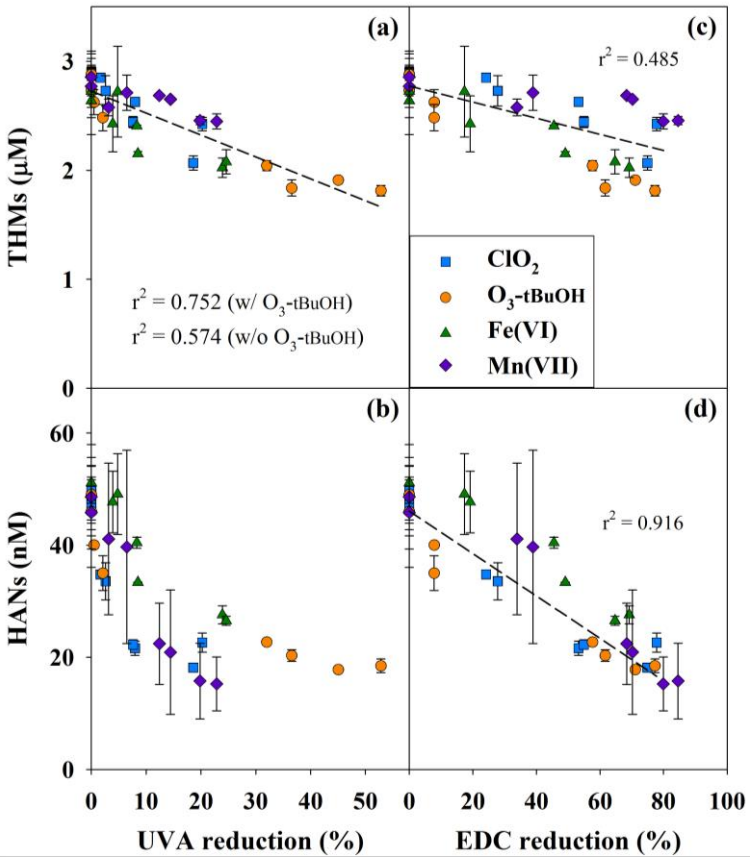

Figure 3-3. THM and HAN formation compared to the UVA_{254} (a-b) and to the EDC (d-e). [ClO_2] = 3.5–39 μM, [O_3-tBuOH] = 2.2–104 μM, [Fe(VI)] = 2.5–50 μM, [Mn(VII)] = 1–20 μM, [SRNOM] = 3 mgC L^{-1}, [Br^-] = 0 or 150 μg L^{-1}, 40 mM borate (pH 8). Error bars represent the range of analytical results for duplicated experiments (the two highest doses of Fe(VI) and Mn(VII) were not duplicated experiments).

As shown in Figure 3-3c, the EDC reduction was poorly correlated to the THM formation (r^2 = 0.485, Figure 3-3c), which contrasted with the correlation observed between EDC and AOX for ClO_2, Fe(VI) and Mn(VII) in Figure 3-2d. Within AOX precursors, THM precursors represent only a fraction, toward which ClO_2, Fe(VI) and Mn(VII) may present distinct reactivity. The results shown in Figure 3-2d and Figure 3-3c suggest that the EDC is not necessarily representative of these THM precursors while being representative of AOX precursors. For example, within the phenolic-type moieties, dihydroxybenzenes are significant THM precursors moieties, that may not account for a significant part of the EDC,[34] whereas the total of phenolic-type moieties, significant AOX precursors, correlated with the EDC.[34, 35]

The formation of HANs was not correlated to the UVA_{254} reduction (Figure 3-3b), consistent with a previous study,[63] or the dose of oxidant (Figure A-3-2d), but a good correlation was found with the EDC abatement (r^2 = 0.916, Figure 3-3d).

The HAN formation pathways have been extensively studied, and primary amines are referred as primary precursors.[66, 72] However, combined and free amino acids such as glycine, alanine or aspartic acid, which are commonly found in water and account for a significant fraction of the dissolved organic nitrogen,[73] are unreactive with $ABTS^{+\bullet}$ and will not account for the EDC.[74] Furthermore, although O_3-tBuOH and Fe(VI) exhibit some reactivity with aliphatic amino acids (10^2–10^3 M^{-1} s^{-1} and 10^1–10^2 M^{-1} s^{-1}, respectively),[75-77] Mn(VII) and ClO_2 are essentially unreactive with these compounds (10^{-2} M^{-1} s^{-1} and 10^{-5}–10^{-4} M^{-1} s^{-1}, respectively).[19, 78, 79] Therefore, since a similar HAN mitigation is observed for all the oxidants, other precursors are responsible of HAN formation (Figure 3-3e). Other aromatic amino acids such as tryptophan and tyrosine, commonly used to characterize DOM by fluorescence,[80, 81] yield to significant HAN concentrations from chlorination.[66, 82]

The correlation between HAN formation and EDC may be explained by the reactivity of oxidants with HAN precursors such as tryptophan. At pH 8, tryptophan and phenol are reacting within the same order of magnitude with O_3-tBuOH (7 and 18 x 10^6 M^{-1} s^{-1}, respectively),[75, 76] ClO_2 (1.2 and 5 x 10^5 M^{-1} s^{-1}, respectively)[78, 83] and Fe(VI) (12 and 9 x 10^1 M^{-1} s^{-1}, respectively).[84, 85] No data could be found for the reactivity of tryptophan with Mn(VII), but tyrosine, another HAN precursor, is reacting with Mn(VII).[86] Tryptophan-like and phenolic moieties would degrade to similar proportions with the different oxidants, and may explain the concomitant reduction of EDC (through the degradation of phenolic compounds) and HAN mitigation (through the degradation of precursors such as tryptophan). These results suggest that aliphatic amino acids may not be the primary HANs precursors.

3.4.4 Toxicity

The sum of DBPs (in µM) as well as their cumulative calculated toxicity were compared with the decrease of UVA_{254} and EDC for samples without bromide (Figure 3-4a and b). The cumulative toxicity was calculated as the sum of the ratios between the concentration of a specific DBP (C) and its cytotoxicity (C_{50}) (eq 3-1). The cytotoxicity was represented by the concentration of a specific DBP resulting in a 50% reduction of Chinese hamster ovary cells density.[87]

$$\text{Toxicity} = \sum \frac{C}{C_{50}} \qquad \text{eq 3-1}$$

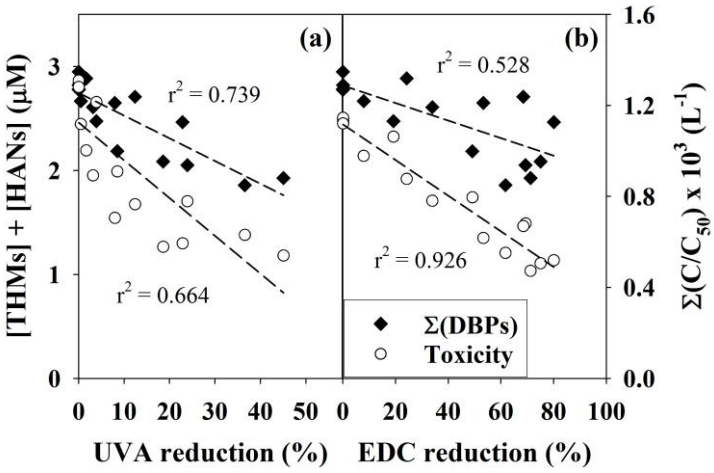

Figure 3-4. Sum of DBPs (dark diamonds) and cumulative estimated toxicity (open circles) compared to the UVA_{254} (a) and EDC (b). $[ClO_2]$ = 3.5–39 μM, $[O_3$-tBuOH] = 2.2–104 μM, [Fe(VI)] = 2.5–50 μM, [Mn(VII)] = 1–20 μM, [SRNOM] = 3 mgC L^{-1}, 40 mM borate (pH 8), no Br^-.

The sum of DBPs was decreased by a maximum of 33% by pre-oxidation treatment while a much higher abatement of toxicity of 58% was observed in our experimental conditions (~ 50% UVA_{254} reduction and ~ 80% EDC reduction, Figure 3-4a,b). Since the THM concentrations were about 50 times higher than the HAN concentrations, a better correlation was obtained with UVA_{254} (r^2 = 0.739, Figure 3-4a) than with EDC (r^2 = 0.528, Figure 3-4b) for the sum of DBPs. However, the cytotoxicity of the THMs is negligible compared to the HANs (C_{50} = 10^{-3}–10^{-2} and 10^{-6}–10^{-4} M for THMs and HANs, respectively),[87] and therefore a better correlation was observed between the estimated cumulative toxicity and the EDC (r^2 = 0.926, Figure 3-4b) compared to UVA_{254} (r^2 = 0.664, Figure 3-4a). In presence of bromide, the cumulative calculated toxicity was not well correlated with the EDC reduction since the very potent brominated HANs were not necessarily mitigated by pre-oxidation (c.f. Chapter 6).

3.4.5 Practical implications

The concomitant use of EDC and UVA_{254} revealed that the overall impact of ClO_2, Fe(VI) and Mn(VII) on NOM characteristics is similar, and confirmed that O_3 reacts through a different mechanism. EDC can be used as a surrogate for the chlorine demand after pre-oxidation with ClO_2, Fe(VI), Mn(VII) and O_3 while both UVA_{254} and EDC are useful indicators for AOX formation, even though O_3 exhibited a different EDC behavior. However, the EDC was poorly correlated to the formation of THMs. In this case, UVA_{254} was a better surrogate. Interestingly, the UVA_{254} was not representative of HAN formation whereas EDC showed a good correlation. The

emergence of potent DBPs such as HANs, haloacetamides or halonitromethanes needs to be considered since it might represent a major part of the DBP-induced toxicity. A more exhaustive DBP evaluation would be required to speculate about UVA_{254} and EDC correlation with toxicity. The EDC abatement usually exhibits much larger differences than the UVA_{254} abatement, especially at low oxidant doses, which allows to monitor the changes in NOM characteristics more accurately. The EDC measurement is also less affected by UV-interfering compounds such as nitrate, chlorite or metals.[27] Overall the concomitant use of EDC and UVA_{254}, or other spectral techniques such as the fluorescence, could give more detailed information about the change in NOM characteristics during water treatment, allowing a better control of the dose of disinfectant required and ultimately a reduction of the formation of toxic DBPs.

3.5 References

1. Sedlak, D. L.; von Gunten, U., The Chlorine Dilemma. *Science* **2011,** *331*, (6013), 42-43.
2. Richardson, S. D.; Plewa, M. J.; Wagner, E. D.; Schoeny, R.; DeMarini, D. M., Occurrence, genotoxicity, and carcinogenicity of regulated and emerging disinfection by-products in drinking water: A review and roadmap for research. *Mutat. Res-Rev. Mutat.* **2007,** *636*, (1–3), 178-242.
3. Gallard, H.; von Gunten, U., Chlorination of natural organic matter: kinetics of chlorination and of THM formation. *Water Res.* **2002,** *36*, (1), 65-74.
4. Jiang, Y.; Goodwill, J. E.; Tobiason, J. E.; Reckhow, D. A., Comparison of the Effects of Ferrate, Ozone, and Permanganate Pre-Oxidation on Disinfection Byproduct Formation from Chlorination. In *Ferrites and Ferrates: Chemistry and Applications in Sustainable Energy and Environmental Remediation*, American Chemical Society: 2016; Vol. 1238, pp 421-437.
5. Yang, X.; Guo, W.; Zhang, X.; Chen, F.; Ye, T.; Liu, W., Formation of disinfection by-products after pre-oxidation with chlorine dioxide or ferrate. *Water Res.* **2013,** *47*, (15), 5856-5864.
6. Gan, W.; Sharma, V. K.; Zhang, X.; Yang, L.; Yang, X., Investigation of disinfection byproducts formation in ferrate(VI) pre-oxidation of NOM and its model compounds followed by chlorination. *J. Hazard. Mater.* **2015,** *292*, 197-204.
7. Jiang, Y.; Goodwill, J. E.; Tobiason, J. E.; Reckhow, D. A., Impacts of ferrate oxidation on natural organic matter and disinfection byproduct precursors. *Water Res.* **2016,** *96*, 114-125.
8. Yang, X.; Guo, W.; Lee, W., Formation of disinfection byproducts upon chlorine dioxide preoxidation followed by chlorination or chloramination of natural organic matter. *Chemosphere* **2013,** *91*, (11), 1477-1485.
9. Xie, P.; Ma, J.; Fang, J.; Guan, Y.; Yue, S.; Li, X.; Chen, L., Comparison of Permanganate Preoxidation and Preozonation on Algae Containing Water: Cell Integrity, Characteristics, and Chlorinated Disinfection Byproduct Formation. *Environ. Sci. Technol.* **2013,** *47*, (24), 14051-14061.
10. Lee, C.; Schmidt, C.; Yoon, J.; Von Gunten, U., Oxidation of N-nitrosodimethylamine (NDMA) precursors with ozone and chlorine dioxide: Kinetics and effect on NDMA formation potential. *Environ. Sci. Technol.* **2007,** *41*, (6), 2056-2063.
11. Selbes, M.; Kim, D.; Karanfil, T., The effect of pre-oxidation on NDMA formation and the influence of pH. *Water Res.* **2014,** *66*, 169-179.
12. Jones, D. B.; Song, H.; Karanfil, T., The effects of selected preoxidation strategies on I-THM formation and speciation. *Water Res.* **2012,** *46*, (17), 5491-5498.
13. Chen, Z.; Valentine, R. L., The influence of the pre-oxidation of natural organic matter on the formation of N-nitrosodimethylamine (NDMA). *Environ. Sci. Technol.* **2008,** *42*, (14), 5062-5067.
14. Rougé, V.; Allard, S.; Croué, J.-P.; von Gunten, U., In Situ Formation of Free Chlorine During ClO_2 Treatment: Implications on the Formation of Disinfection Byproducts. *Environ. Sci. Technol.* **2018,** *52*, (22), 13421-13429.
15. Terhalle, J.; Kaiser, P.; Jütte, M.; Buss, J.; Yasar, S.; Marks, R.; Uhlmann, H.; Schmidt, T. C.; Lutze, H. V., Chlorine dioxide – Pollutant transformation and formation of hypochlorous acid as a secondary oxidant. *Environ. Sci. Technol.* **2018**.
16. von Gunten, U., Ozonation of drinking water: Part I. Oxidation kinetics and product formation. *Water Res.* **2003,** *37*, (7), 1443-1467.

17. Dowideit, P.; von Sonntag, C., Reaction of Ozone with Ethene and Its Methyl- and Chlorine-Substituted Derivatives in Aqueous Solution. *Environ. Sci. Technol.* **1998,** *32*, (8), 1112-1119.
18. Waldemer, R. H.; Tratnyek, P. G., Kinetics of contaminant degradation by permanganate. *Environ. Sci. Technol.* **2006,** *40*, (3), 1055-1061.
19. Perez-Benito, J. F., Autocatalytic Reaction Pathway on Manganese Dioxide Colloidal Particles in the Permanganate Oxidation of Glycine. *J. Phys. Chem. C* **2009,** *113*, (36), 15982-15991.
20. Shin, J.; Lee, Y., Elimination of Organic Contaminants during Oxidative Water Treatment with Ferrate(VI): Reaction Kinetics and Transformation Products. In *Ferrites and Ferrates: Chemistry and Applications in Sustainable Energy and Environmental Remediation*, American Chemical Society: 2016; Vol. 1238, pp 255-273.
21. von Sonntag, C., The basics of oxidants in water treatment. Part A: OH radical reactions. *Water Sci. Technol.* **2007,** *55*, (12), 19-23.
22. Criquet, J.; Rodriguez, E. M.; Allard, S.; Wellauer, S.; Salhi, E.; Joll, C. A.; von Gunten, U., Reaction of bromine and chlorine with phenolic compounds and natural organic matter extracts - Electrophilic aromatic substitution and oxidation. *Water Res.* **2015,** *85*, 476-486.
23. Rush, J. D.; Bielski, B. H. J., The Oxidation of Amino Acids By Ferrate(V). A Pre-Mix Pulse Radiolysis Study. *Free Radical Res.* **1995,** *22*, (6), 571-579.
24. Rush, J. D.; Cyr, J. E.; Zhao, Z.; Bielski, B. H. J., The Oxidation of Phenol by Ferrate(VI) and Ferrate(V). A Pulse Radiolysis and Stopped-Flow Study. *Free Radical Res.* **1995,** *22*, (4), 349-360.
25. Záhonyi-Budó, É.; Simándi, L., Oxidation of propane-1,2-diol by acidic manganese(V) and manganese(VI). *Inorg. Chim. Acta* **1996,** *248*, (1), 81-84.
26. Simándi, L.; Záhonyi-Budó, É., Relative reactivities of hydroxy compounds with short-lived manganese(V). *Inorg. Chim. Acta* **1998,** *281*, (2), 235-238.
27. Weishaar, J. L.; Aiken, G. R.; Bergamaschi, B. A.; Fram, M. S.; Fujii, R.; Mopper, K., Evaluation of Specific Ultraviolet Absorbance as an Indicator of the Chemical Composition and Reactivity of Dissolved Organic Carbon. *Environ. Sci. Technol.* **2003,** *37*, (20), 4702-4708.
28. Croué, J.-P.; Violleau, D.; Labouyrie, L., Disinfection By-Product Formation Potentials of Hydrophobic and Hydrophilic Natural Organic Matter Fractions: A Comparison Between a Low- and a High-Humic Water. In *Natural Organic Matter and Disinfection By-Products*, American Chemical Society: 2000; Vol. 761, pp 139-153.
29. Korshin, G. V.; Li, C.-W.; Benjamin, M. M., Use of UV Spectroscopy To Study Chlorination of Natural Organic Matter. In *Water Disinfection and Natural Organic Matter*, American Chemical Society: 1996; Vol. 649, pp 182-195.
30. Archer, A. D.; Singer, P. C., Effect of SUVA and enhanced coagulation on removal of TOX precursors. *J. Am. Water Works Ass.* **2006,** *98*, (8), 97-107.
31. Edzwald, J. K.; Becker, W. C.; Wattier, K. L., Surrogate Parameters for Monitoring Organic Matter and THM Precursors. *J. Am. Water Works Ass.* **1985,** *77*, (4), 122-132.
32. Amy, G. L.; Chadik, P. A.; Chowdhury, Z. K., Developing Models for Predicting Trihalomethane Formation Potential and Kinetics. *J. Am. Water Works Ass.* **1987,** *79*, (7), 89-97.

33. Ates, N.; Kitis, M.; Yetis, U., Formation of chlorination by-products in waters with low SUVA–correlations with SUVA and differential UV spectroscopy. *Water Res.* **2007,** *41*, (18), 4139-4148.
34. Aeschbacher, M.; Graf, C.; Schwarzenbach, R. P.; Sander, M., Antioxidant properties of humic substances. *Environ. Sci. Technol.* **2012,** *46*, (9), 4916-4925.
35. Walpen, N.; Schroth, M. H.; Sander, M., Quantification of Phenolic Antioxidant Moieties in Dissolved Organic Matter by Flow-Injection Analysis with Electrochemical Detection. *Environ. Sci. Technol.* **2016,** *50*, (12), 6423-6432.
36. Wenk, J.; Aeschbacher, M.; Salhi, E.; Canonica, S.; Von Gunten, U.; Sander, M., Chemical oxidation of dissolved organic matter by chlorine dioxide, chlorine, and ozone: Effects on its optical and antioxidant properties. *Environ. Sci. Technol.* **2013,** *47*, (19), 11147-11156.
37. Chon, K.; Salhi, E.; von Gunten, U., Combination of UV absorbance and electron donating capacity to assess degradation of micropollutants and formation of bromate during ozonation of wastewater effluents. *Water Res.* **2015,** *81*, 388-397.
38. Önnby, L.; Salhi, E.; McKay, G.; Rosario-Ortiz, F. L.; von Gunten, U., Ozone and chlorine reactions with dissolved organic matter - Assessment of oxidant-reactive moieties by optical measurements and the electron donating capacities. *Water Res.* **2018,** *144*, 64-75.
39. Furman, C. S.; Margerum, D. W., Mechanism of Chlorine Dioxide and Chlorate Ion Formation from the Reaction of Hypobromous Acid and Chlorite Ion. *Inorg. Chem.* **1998,** *37*, (17), 4321-4327.
40. Granstrom, M. L.; Lee, G. F., Generation and Use of Chlorine Dioxide in Water Treatment. *J. Am. Water Works Ass.* **1958,** *50*, (11), 1453-1466.
41. Gates, D. J., *The Chlorine Dioxide Handbook*. American Water Works Association: 1998.
42. Li, C.; Li, X. Z.; Graham, N., A study of the preparation and reactivity of potassium ferrate. *Chemosphere* **2005,** *61*, (4), 537-543.
43. Ramseier, M. K.; Peter, A.; Traber, J.; von Gunten, U., Formation of assimilable organic carbon during oxidation of natural waters with ozone, chlorine dioxide, chlorine, permanganate, and ferrate. *Water Res.* **2011,** *45*, (5), 2002-2010.
44. Lee, Y.; Yoon, J.; Von Gunten, U., Spectrophotometric determination of ferrate (Fe(VI)) in water by ABTS. *Water Res.* **2005,** *39*, (10), 1946-1953.
45. Hoigné, J.; Bader, H., The role of hydroxyl radical reactions in ozonation processes in aqueous solutions. *Water Res.* **1976,** *10*, (5), 377-386.
46. Staehelin, J.; Hoigne, J., Decomposition of ozone in water in the presence of organic solutes acting as promoters and inhibitors of radical chain reactions. *Environ. Sci. Technol.* **1985,** *19*, (12), 1206-1213.
47. Allard, S.; Charrois, J. W. A.; Joll, C. A.; Heitz, A., Simultaneous analysis of 10 trihalomethanes at nanogram per liter levels in water using solid-phase microextraction and gas chromatography mass-spectrometry. *J. Chromatogr. A* **2012,** *1238*, 15-21.
48. Kristiana, I.; Joll, C.; Heitz, A., Analysis of halonitriles in drinking water using solid-phase microextraction and gas chromatography–mass spectrometry. *J. Chromatogr. A* **2012,** *1225*, 45-54.
49. Langsa, M.; Allard, S.; Kristiana, I.; Heitz, A.; Joll, C. A., Halogen-specific total organic halogen analysis: Assessment by recovery of total bromine. *J. Environ. Sci.* **2017,** *58*, 340-348.

50. Pinkernell, U.; Nowack, B.; Gallard, H.; Von Gunten, U., Methods for the photometric determination of reactive bromine and chlorine species with ABTS. *Water Res.* **2000,** *34*, (18), 4343-4350.
51. Önnby, L.; Walpen, N.; Salhi, E.; Sander, M.; Von Gunten, U., Two analytical approached to quantify the oxidation of dissolved organic matter by chlorine and ozone. *Water Res.* **2018**.
52. Allard, S.; Gutierrez, L.; Fontaine, C.; Croué, J.-P.; Gallard, H., Organic matter interactions with natural manganese oxide and synthetic birnessite. *Sci. Total Environ.* **2017,** *583*, 487-495.
53. Jiang, J.; Gao, Y.; Pang, S.-Y.; Wang, Q.; Huangfu, X.; Liu, Y.; Ma, J., Oxidation of Bromophenols and Formation of Brominated Polymeric Products of Concern during Water Treatment with Potassium Permanganate. *Environ. Sci. Technol.* **2014,** *48*, (18), 10850-10858.
54. Song, Y.; Jiang, J.; Ma, J.; Pang, S.-Y.; Liu, Y.-z.; Yang, Y.; Luo, C.-w.; Zhang, J.-q.; Gu, J.; Qin, W., ABTS as an Electron Shuttle to Enhance the Oxidation Kinetics of Substituted Phenols by Aqueous Permanganate. *Environ. Sci. Technol.* **2015,** *49*, (19), 11764-11771.
55. Gordon, G.; Kieffer, R. G.; Rosenblatt, D. H., The Chemistry of Chlorine Dioxide. In *Progress in Inorg. Chem.*, Lippard, S. J., Ed. John Wiley & Sons, Inc.: New York, 1972; Vol. 15, pp 201-286.
56. Wajon, J. E.; Rosenblatt, D. H.; Burrows, E. P., Oxidation of phenol and hydroquinone by chlorine dioxide. *Environ. Sci. Technol.* **1982,** *16*, (7), 396-402.
57. von Sonntag, C.; von Gunten, U., *Chemistry of Ozone in Water and Wastewater Treatment*. International Water Association: 2012.
58. Lee, D. G.; Sebastian, C. F., The oxidation of phenol and chlorophenols by alkaline permanganate. *Can. J. Chem.* **1981,** *59*, 2776-2779.
59. Huang, H.; Sommerfeld, D.; Dunn, B. C.; Eyring, E. M.; Lloyd, C. R., Ferrate(VI) Oxidation of Aqueous Phenol: Kinetics and Mechanism. *J. Phys. Chem. A* **2001,** *105*, (14), 3536-3541.
60. Jiang, J.; Pang, S.-Y.; Ma, J.; Liu, H., Oxidation of Phenolic Endocrine Disrupting Chemicals by Potassium Permanganate in Synthetic and Real Waters. *Environ. Sci. Technol.* **2012,** *46*, (3), 1774-1781.
61. Li, C.; Li, X. Z.; Graham, N.; Gao, N. Y., The aqueous degradation of bisphenol A and steroid estrogens by ferrate. *Water Res.* **2008,** *42*, (1), 109-120.
62. Chen, J.; Qu, R.; Pan, X.; Wang, Z., Oxidative degradation of triclosan by potassium permanganate: Kinetics, degradation products, reaction mechanism, and toxicity evaluation. *Water Res.* **2016,** *103*, 215-223.
63. Hua, G.; Reckhow, D. A.; Abusallout, I., Correlation between SUVA and DBP formation during chlorination and chloramination of NOM fractions from different sources. *Chemosphere* **2015,** *130*, 82-89.
64. Zhao, Y.; Anichina, J.; Lu, X.; Bull, R. J.; Krasner, S. W.; Hrudey, S. E.; Li, X.-F., Occurrence and formation of chloro- and bromo-benzoquinones during drinking water disinfection. *Water Res.* **2012,** *46*, (14), 4351-4360.
65. Dickenson, E. R. V.; Summers, R. S.; Croué, J.-P.; Gallard, H., Haloacetic acid and Trihalomethane Formation from the Chlorination and Bromination of Aliphatic β-Dicarbonyl Acid Model Compounds. *Environ. Sci. Technol.* **2008,** *42*, (9), 3226-3233.
66. Bond, T.; Henriet, O.; Goslan, E. H.; Parsons, S. A.; Jefferson, B., Disinfection Byproduct Formation and Fractionation Behavior of Natural Organic Matter Surrogates. *Environ. Sci. Technol.* **2009,** *43*, (15), 5982-5989.

67. Tentscher, P. R.; Bourgin, M.; von Gunten, U., Ozonation of Para-Substituted Phenolic Compounds Yields p-Benzoquinones, Other Cyclic α,β-Unsaturated Ketones, and Substituted Catechols. *Environ. Sci. Technol.* **2018,** *52*, (8), 4763-4773.
68. Held, A. M.; Halko, D. J.; Hurst, J. K., Mechanisms of chlorine oxidation of hydrogen peroxide. *J. Am. Chem. Soc.* **1978,** *100*, (18), 5732-5740.
69. USEPA, Disinfectants and Disinfection Byproducts final rule. In Federal Register: 1998; Vol. 63, pp 69390-69476.
70. Muellner, M. G.; Wagner, E. D.; McCalla, K.; Richardson, S. D.; Woo, Y.-T.; Plewa, M. J., Haloacetonitriles vs. Regulated Haloacetic Acids: Are Nitrogen-Containing DBPs More Toxic? *Environ. Sci. Technol.* **2007,** *41*, (2), 645-651.
71. Rook, J. J., Chlorination reactions of fulvic acids in natural waters. *Environ. Sci. Technol.* **1977,** *11*, (5), 478-482.
72. Shah, A. D.; Mitch, W. A., Halonitroalkanes, Halonitriles, Haloamides, and N-Nitrosamines: A Critical Review of Nitrogenous Disinfection Byproduct Formation Pathways. *Environ. Sci. Technol.* **2012,** *46*, (1), 119-131.
73. Dotson, A.; Westerhoff, P., Occurrence and removal of amino acids during drinking water treatment. *J. Am. Water Works Ass.* **2009,** *101*, (9), 101-115.
74. Zheng, L.; Zhao, M.; Xiao, C.; Zhao, Q.; Su, G., Practical problems when using ABTS assay to assess the radical-scavenging activity of peptides: Importance of controlling reaction pH and time. *Food Chem.* **2016,** *192*, 288-294.
75. Hoigné, J.; Bader, H., Rate constants of reactions of ozone with organic and inorganic compounds in water–II. *Water Res.* **1983,** *17*, (2), 185-194.
76. Pryor, W. A.; Giamalva, D. H.; Church, D. F., Kinetics of ozonation. 2. Amino acids and model compounds in water and comparisons to rates in nonpolar solvents. *J. Am. Chem. Soc.* **1984,** *106*, (23), 7094-7100.
77. Sharma, V. K.; Bielski, B. H. J., Reactivity of ferrate(VI) and ferrate(V) with amino acids. *Inorg. Chem.* **1991,** *30*, (23), 4306-4310.
78. Hoigné, J.; Bader, H., Kinetics of reactions of chlorine dioxide (OClO) in water-I. Rate constants for inorganic and organic compounds. *Water Res.* **1994,** *28*, (1), 45-55.
79. de Andres, J.; Brillas, E.; Garrido, J. A.; Perez-Benito, J. F., Kinetics and mechanisms of the oxidation by permanganate of L-alanine. *J. Chem. Soc. Perk. T. 2* **1988**, (2), 107-112.
80. Coble, P. G.; Green, S. A.; Blough, N. V.; Gagosian, R. B., Characterization of dissolved organic matter in the Black Sea by fluorescence spectroscopy. *Nature* **1990,** *348*, 432.
81. Coble, P. G., Characterization of marine and terrestrial DOM in seawater using excitation-emission matrix spectroscopy. *Mar. Chem.* **1996,** *51*, (4), 325-346.
82. Jia, A.; Wu, C.; Duan, Y., Precursors and factors affecting formation of haloacetonitriles and chloropicrin during chlor(am)ination of nitrogenous organic compounds in drinking water. *J. Hazard. Mater.* **2016,** *308*, 411-418.
83. Stewart, D. J.; Napolitano, M. J.; Bakhmutova-Albert, E. V.; Margerum, D. W., Kinetics and Mechanisms of Chlorine Dioxide Oxidation of Tryptophan. *Inorg. Chem.* **2008,** *47*, (5), 1639-1647.
84. Lee, Y.; Yoon, J.; von Gunten, U., Kinetics of the Oxidation of Phenols and Phenolic Endocrine Disruptors during Water Treatment with Ferrate (Fe(VI)). *Environ. Sci. Technol.* **2005,** *39*, (22), 8978-8984.
85. Casbeer, E. M.; Sharma, V. K.; Zajickova, Z.; Dionysiou, D. D., Kinetics and Mechanism of Oxidation of Tryptophan by Ferrate(VI). *Environ. Sci. Technol.* **2013,** *47*, (9), 4572-4580.

86. Kim, M. S.; Lee, H.-J.; Lee, K.-M.; Seo, J.; Lee, C., Oxidation of Microcystins by Permanganate: pH and Temperature-Dependent Kinetics, Effect of DOM Characteristics, and Oxidation Mechanism Revisited. *Environ. Sci. Technol.* **2018,** *52*, (12), 7054-7063.
87. Plewa, M. J.; Wagner, E. D.; Muellner, M. G.; Hsu, K.-M.; Richardson, S. D., Comparative Mammalian Cell Toxicity of N-DBPs and C-DBPs. In *Disinfection By-Products in Drinking Water*, American Chemical Society: 2008; Vol. 995, pp 36-50.

Every reasonable effort has been made to acknowledge the owners of copyright material. I would be pleased to hear from any copyright owner who has been omitted or incorrectly acknowledged.

Chapter 4. In Situ Formation of Free Chlorine during ClO_2 treatment: Implications on the Formation of Disinfection Byproducts

Valentin Rougé, Sébastien Allard, Jean-Philippe Croué and Urs von Gunten

Environmental Science & Technology, Volume 52, 29 October 2018, Pages 13421-13429

DOI: https://doi.org/10.1021/acs.est.8b04415

Statement of Contribution to Co-authored Published Paper

This Chapter includes the co-authored paper "In Situ Formation of Free Chlorine during ClO_2 treatment: Implications on the Formation of Disinfection Byproducts", published in Environmental Science & Technology. The bibliographic details of the co-authored paper, including all authors are:

Rougé, V.; Allard, S.; Croué, J.-P.; von Gunten, U., In Situ Formation of Free Chlorine During ClO_2 Treatment: Implications on the Formation of Disinfection Byproducts. *Environmental Science & Technolo*gy **2018**, 52, (22), 13421-13429.

I, Valentin Rougé, as the primary author, conducted all the experimental work and data analysis, including creating figures and tables, and writing and editing the manuscript.

I, as a Co-Author, endorsed that this level of contribution by the candidate indicated above is appropriate.

Sébastien Allard

Jean-Philippe Croué

Urs von Gunten

4.1 Abstract

Chlorine dioxide (ClO_2) is commonly used as an alternative disinfectant to chlorine in drinking water treatment because it produces limited concentrations of halogenated organic disinfection byproducts. During drinking water treatment, the primary ClO_2 byproducts are the chlorite (50–70%) and the chlorate ions (0–30%). However, a significant portion of the ClO_2 remains unaccounted for. This study demonstrates that when ClO_2 was reacting with phenol, one mole of free available chlorine (FAC) was produced per two moles of consumed ClO_2. The *in situ* formed FAC completed the mass balance on Cl for inorganic ClO_2 byproducts (FAC + ClO_2^- +ClO_3^-). When reacting with organic matter extracts at near neutral conditions (pH 6.5–8.1), ClO_2 also yielded a significant amount of FAC (up to 25%). Up to 27% of this *in situ* formed FAC was incorporated in organic matter forming adsorbable organic chlorine, which accounted for up to 7% of the initial ClO_2 dose. Only low concentrations of regulated trihalomethanes were produced because of an efficient mitigation of their precursors by ClO_2 oxidation. Conversely, dichloroacetonitrile formation from ClO_2-induced generation of FAC was higher than from addition of FAC in absence of ClO_2. Overall, these findings provide important information on the formation of FAC and disinfection byproducts during drinking water treatment with ClO_2.

4.2 Introduction

Chlorine dioxide (ClO_2) is a powerful oxidant and a common alternative disinfectant for chlorine with limited formation of organic halogenated disinfection byproducts (DBPs).[1] However, it inevitably forms chlorite ion (ClO_2^-) by a 1-electron transfer from reactions with water matrix components (eq 4-1),[2] and, to some extent, chlorate ion (ClO_3^-).

$$ClO_2 + e^- \rightarrow ClO_2^- \qquad E_0 = 0.954\ V \qquad \text{eq 4-1}$$

ClO_2^- is a widely regulated DBP, with a World Health Organization (WHO) guideline of 0.7 mg L^{-1}.[3] It is proposed by the European Commission to set an even lower value for ClO_3^- and ClO_2^- of 0.25 mg L^{-1}.[4] Unlike chlorine,[5] ClO_2 is unable to directly halogenate organic compounds. However, although generally at much lower concentrations than the DBPs produced from chlorination, ClO_2 still produces its own set of DBPs such as haloacetic acids, haloketones, and a large fraction of unknown total organic halogen species (UTOX).[6-8] The formation of halogenated DBPs can be partially explained by the method applied to generate ClO_2, such as the oxidation of ClO_2^- by chlorine or the reduction of ClO_3^- by chloride ion (Cl^-), leading to chlorine impurities.[2, 9] However, several studies have reported an *in situ* formation of hypochlorous acid (HOCl) when ClO_2 reacts with phenolic compounds through the following mechanism:[10-13]

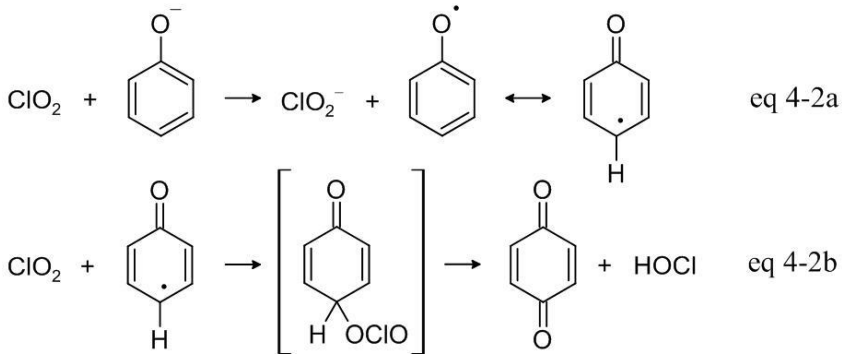

This two-step mechanism, originally proposed by Wajon et al.,[10] involves a one-electron transfer between the phenolate and ClO_2 to produce a phenoxyl radical and ClO_2^- (eq 4-2a). In a second step, instead of a second one-electron transfer, a phenoxyl-OClO adduct is formed which decays rapidly and releases HOCl and a quinone (eq 4-2b). This step involves a transfer of three electrons and the oxidation

state of chlorine is reduced from +IV to +I. In addition to the average two electrons transferred to ClO_2, the released HOCl can further react through another two-electrons oxidation process in which the oxidation state of chlorine is reduced from +I to -I (Cl^-).[14] Therefore, the overall oxidation capacity of ClO_2 is potentially higher than expected from eq 4-1.

This mechanism is supported by a substoichiometric transformation of ClO_2 to ClO_2^-, and the formation of chlorinated compounds as well as quinones from the reaction of model compounds with chlorine-free ClO_2 solutions.[10, 15-17] Similar reaction pathways have also been suggested for amino acids,[13, 17, 18] guanosine,[16] anilines,[19] indene[15] and lignin compounds.[20, 21] Furthermore, spectral evidence of the formation of a transient phenoxyl-OClO adduct has been provided,[13, 17] and the formation of HOCl from the reaction of ClO_2 with phenol and pulp lignins under acidic conditions was previously quantified.[22, 23] In a recent study,[23] the *in situ* formation of HOCl in presence of phenol and bromide ion (Br^-) was demonstrated by quantifying the formed bromophenols. Furthermore, the authors showed that the *in situ* formation of HOCl enhanced the transformation of atenolol and metoprolol in wastewater, which are otherwise recalcitrant to ClO_2 oxidation.

The present study investigates whether the mechanisms of HOCl formation from chlorine dioxide are relevant under drinking water conditions and if the production of halogenated DBPs can be linked to the intermediate formation of HOCl during ClO_2 treatment. The HOCl and OCl^- species, coexisting in solution at near neutral pH, will be referred as free available chlorine (FAC). The aim, in a first step, is to provide a comprehensive mechanistic understanding of the *in situ* formation of FAC from the reaction of ClO_2 with (1) phenol, used as a model system, and (2) different NOM extracts mimicking drinking water conditions. In a second step, the implications of the *in situ* production of HOCl were explored in terms of formation of halogenated DBPs from model compounds, as well as in synthetic and real water matrices for a large range of dissolved organic carbon (DOC) concentrations (2.6–9.2 mgC L^{-1}), NOM types (SUVA ranging from 1.6 to 4.8 L mgC m^{-1}), pH (6.5–8.1) and Br^- concentration (0–235 µg L^{-1}).

4.3 Materials and methods

4.3.1 Chemicals and reagents

Sodium chlorite (80%) and a sodium hypochlorite solution (10–15%) were purchased from Sigma-Aldrich. The impurities in the sodium chlorite and sodium hypochlorite were found to be mostly Cl^- and traces of ClO_3^- and are given in Table A-4-1. All other chemicals were of analytical grade quality (≥ 98%). Solutions were prepared with ultrapure water (Purelab Ultra, Elga, UK). The organic matter extracts (Table A-4-2), were purchased from the International Humic Substances Society (IHSS). The real waters were sampled from shallow (P100) and deeper bores (P105 and P65) located in Pinjar, Western Australia (Table A-4-2).

4.3.2 Preparation of oxidant solutions

FAC stock solutions were prepared from a sodium hypochlorite solution standardized by direct UV measurement at 292 nm (ε_{292} = 362 M^{-1} cm^{-1}).[24] ClO_2 was produced by mixing solutions of sodium persulfate (40 g L^{-1}) and sodium chlorite (80 g L^{-1}) under N_2 bubbling for about 1 h.[25, 26] The ClO_2 produced was retrieved in chilled ultrapure water and standardized by direct UV measurement at 359 nm (ε_{359} = 1230 M^{-1} cm^{-1}).[24] The concentration of FAC in the ClO_2 stock, determined by ABTS (2,2'-azino-bis(3-ethylbenzothiazoline-6-sulfonic acid) diammonium salt) measurements was < 1% (all the percentages expressed in the rest of the paper represent molar percentages unless specified otherwise).

4.3.3 FAC formation from phenol and NOM

Solutions of either phenol (10–40 μM) or NOM extracts (3.0 mgC L^{-1}) were prepared in phosphate buffers (25 mM for phenol and 10 mM for NOM extracts). The pH (7.5 for phenol and 8.1 for NOM extracts) was adjusted by the addition of NaOH or HCl (1 M). NH_4Cl was added in large excess, 20 times the phenol concentration or 0.4 mM (21.4 mg L^{-1}) in NOM experiments, before the addition of ClO_2. ClO_2 concentration was 2 to 4 times the phenol concentration or 7.5–200 μM in NOM experiments. NH_4Cl was added to quench the *in situ* formed FAC as monochloramine (NH_2Cl) and allow its measurement. After addition of ClO_2 and 10 s of vigorous mixing, the solution was split into smaller volumes (5 or 12 mL) without headspace (< 10% of total volume) and protected from light at room temperature (20 ± 2°C). In NOM extract experiments,

pH 8.1 was chosen to maximize the stability of the formed NH_2Cl.[14] Suwannee River (SRNOM) and Upper Mississippi River (UMRNOM) extracts were used for the FAC formation measurements.

4.3.4 Disinfection byproducts formation from model compounds and NOM

Solutions of either phenol (40 µM) in 25 mM phosphate buffer at pH 7.5 or NOM extracts (3.0 mgC L^{-1}) in 10 mM phosphate buffer at pH 6.5 or 8.1 were dosed with ClO_2 (80 µM in phenol and 7.5–200 µM in NOM experiments). For phenol, after full consumption of ClO_2 (1 min after its addition), 2 µM of tryptophan or resorcinol, used as DBP precursors, was added to the mixture. Samples of 60 mL (for the model compounds) or 200 mL (for the NOM extracts) were kept without headspace (< 10% of total volume) and protected from light at room temperature (20 ± 2°C) from 1 min to 24 h. The oxidant residual was then measured and quenched before analyzing trihalomethanes (THMs), haloacetonitriles (HANs) and adsorbable organic halogens (AOX). The quenching procedure is given in Text A-4-1. As a comparison, these solutions were also dosed with FAC (40 µM in phenol and 5.3–15 µM in NOM). The same experiments were also conducted in presence of glycine (0.4 mM, 30 mg L^{-1}) to quench the *in situ* formed or dosed FAC. SRNOM, UMRNOM, Pony Lake Fulvic Acid (PLFA) and Nordic Lake Fulvic Acid (NLFA) as well as real waters (the main water quality parameters are given in Table A-4-2) were used for the DBPs formation experiments.

4.3.5 Analytical methods

THMs and HANs were analyzed by headspace GC-MS with a method adapted from previously published methods, of which details are given in Text A-3-1.[27, 28] The AOX was measured by combustion and ion chromatography after adsorbing samples on activated carbon.[29] The benzoquinone concentration in the ClO_2/phenol experiments was estimated using its absorbance at 244 nm (ε_{244} = 19204 M^{-1} cm^{-1}).[30] Interferences due to phenol residual were negligible (Figure A-4-1a and Text A-4-2). The concentration of the different oxidants was measured by ABTS-based methods (Text A-4-3).[31] ClO_2^-, ClO_3^- and Cl^- ions were measured by ion chromatography using an AS9-HC column with a Na_2CO_3 eluent (9 mM, 1 mL min^{-1}).[32]

The electron donating capacity (EDC), a proxy for antioxidant capacity of NOM,[33, 34] and the UV absorbance at 254 nm (UVA) were measured on an Agilent 1100 series

system using a size-exclusion chromatography (SEC) (Text A-3-2, Chapter 2).[35, 36] The relative EDC and UVA results are presented as the EDC or UVA signal of the samples divided by the EDC or UVA signal of a 3.0 mgC L^{-1} SRNOM solution.

4.4 Results and discussion

4.4.1 *In situ* formation of FAC from ClO_2 reaction with phenol and NOM

4.4.1.1 Phenol

At pH 7.5 phenol reacts significantly faster with ClO_2 (k_{app} = 1.6 x 10^5 M^{-1} s^{-1})[37] than FAC (k_{app} = 3.7 x 10^1 M^{-1} s^{-1}).[38] Nevertheless, to avoid any loss of FAC by reaction with phenol, the *in situ* produced FAC was quenched by reaction with ammonia to NH_2Cl. The reaction of FAC with ammonia (k_{app} = 2.7 x 10^4 M^{-1} s^{-1})[39] is much faster than with ClO_2^- (k_{app} = 1.8 x 10^{-2} M^{-1} s^{-1})[40] and phenol ($[NH_4^+] = 20 \times [\text{phenol}]$). NH_2Cl is more stable in solution since it is about 3 orders of magnitude less reactive with phenol (k_{app} = 1.6 x 10^{-2} M^{-1} s^{-1} at pH 7.2)[41] than FAC. Quenching the FAC as NH_2Cl also prevented the catalytic disproportionation of ClO_2.[42]

In accordance with the kinetic and mechanistic information in literature (eq 4-2a and eq 4-2b), the oxidation of phenol by ClO_2 was completed within minutes while benzoquinone was formed (Figure A-4-1). As shown in Figure 4-1, for a phenol concentration of 10 µM and a ClO_2/phenol ratio of 2, 11.0 ± 0.2 µM of FAC (as NH_2Cl), 8.9 ± 0.1 µM of benzoquinone and 11.5 ± 0.2 µM of ClO_2^- were formed. Similarly, for 30 µM of phenol, 35 ± 2 µM of FAC (as NH_2Cl), 28.2 ± 0.5 µM of benzoquinone and 33 ± 1 µM of ClO_2^- were formed. Furthermore, the same concentration of FAC was produced with a two-fold excess of ClO_2 (23 ± 2 µM) compared to a four-fold excess (24 ± 2 µM), (Figure 4-1). The final concentrations of ClO_2^-, benzoquinone and FAC were almost equimolar to the initial phenol concentration and two moles of ClO_2 per mole of phenol were consumed. These results are consistent with a previous study reporting that about 40% of FAC was formed per mole of ClO_2 consumed, by measuring the formed bromophenols in presence of Br^- and in large excess of phenol at pH 4.[23] Our results further confirm the mechanism presented in eq 4-2a and eq 4-2b with about a 50% FAC yield per mole of ClO_2 consumed at near neutral pH.

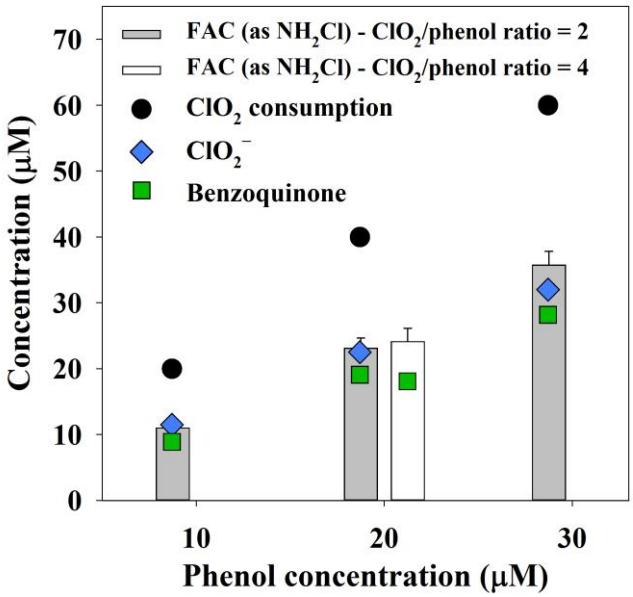

Figure 4-1. Formation of FAC and the main products from the reaction of ClO_2 with phenol. FAC, ClO_2 consumption, ClO_2^- and benzoquinone values are shown for a ClO_2/phenol ratio of 2. FAC and benzoquinone are also shown for a ClO_2/phenol ratio of 4. $[ClO_2]$ = 20–80 µM, $[NH_4^+]$ = 20 × [phenol], [phenol] = 10–30 µM, pH 7.5, 25 mM phosphate. Error bars represent the range of results of duplicate experiments.

4.4.1.2 SRNOM & UMRNOM

To evaluate the *in situ* formation of FAC from a more complex matrix at pH 8.1, synthetic waters containing SRNOM and UMRNOM were treated with ClO_2. Figure 4-2 shows the formation of FAC (measured as NH_2Cl) as a function of time for the reaction between ClO_2 and SRNOM, in presence of ammonia. A very fast initial FAC formation, similar to the ClO_2 reaction with phenol (blue crosses), was observed in the first 10 min. Following this fast reaction phase, a slower FAC formation occurred with a maximum concentration reached within 400 min (Figure 4-2). The FAC formation was anticorrelated to the consumption of ClO_2 (Figure A-4-2). Similar FAC and ClO_2 trends were observed with UMRNOM, with an overall ClO_2 consumption and FAC formation lower than SRNOM (Figure A-4-3). The FAC formation increased with increasing ClO_2 doses up to a plateau of about 15 µM and 11 µM for SRNOM and UMRNOM, respectively (insert of Figure 4-2). For SRNOM, at ClO_2 concentrations < 50 µM, a depletion of the FAC was observed (Figure 4-2). While the decrease was slow at 32.5 µM of ClO_2, it was very fast for 15 µM, which likely led to an underestimation of the FAC formed at lower ClO_2 doses. This decrease was likely due to the reaction of NH_2Cl with NOM reactive moieties.[43] For higher ClO_2 doses NH_2Cl

was stable in solution since these reactive moieties were probably oxidized directly by ClO_2.

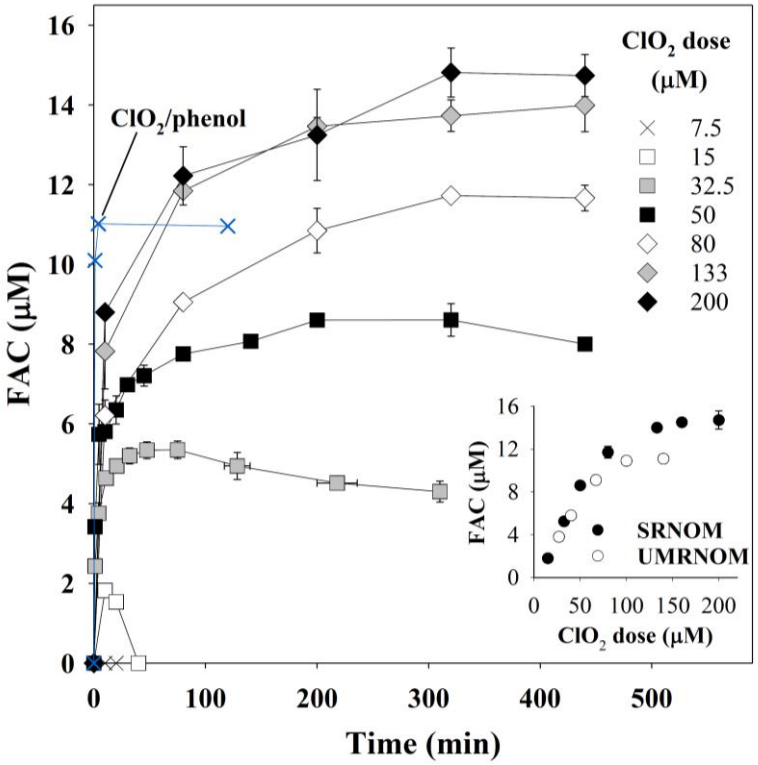

Figure 4-2. Kinetics of *in situ* FAC formation from the reaction of ClO_2 with SRNOM for various ClO_2 doses. The blue crosses represent the FAC formation from the reaction between ClO_2 and phenol (20/10 μM). Insert: maximum *in situ* FAC formed from SRNOM (closed circles) and UMRNOM (open circles) as a function of the ClO_2 dose. $[ClO_2]$ = 7.5–200 μM, $[NH_4^+]$ = 150 μM, [NOM] = 3.0 mgC L^{-1}, pH 8.1, 10 mM phosphate. Error bars represent the range of results of duplicate experiments. Experiments with UMRNOM were not duplicated.

The initial fast increase of FAC suggests, by comparison with the ClO_2/phenol reaction, that phenolic precursors within the NOM were primarily reacting with ClO_2 to form FAC. Beyond 10 min, the slower FAC increase was probably due to the oxidation of less reactive, less activated aromatic precursors. This hypothesis is supported by the negative effect of electron withdrawing substituents on the kinetics of the reactions of ClO_2 with phenolic compounds.[12, 44]

As suggested by the experiments with phenol (Figure 4-1) and previous studies,[10-13] phenolic compounds potentially play a significant role in the formation of FAC. The phenolic content of SRNOM and UMRNOM are 2.5 and 0.8 μeq mgC^{-1}, respectively.[45] However, the formation of FAC from SRNOM and UMRNOM is much higher with 5 and 3.7 μmolCl mgC^{-1}, respectively. Considering a reaction mechanism

analogous to that shown in eq 4-2a and eq 4-2b, the phenolic contents are low compared to the *in situ* FAC formation. These observations are in agreement with previous studies,[15-17] suggesting that phenolic compounds are not the only FAC precursors, wherefore the phenolic content has its limitations as a surrogate for *in situ* FAC formation.

4.4.1.3 Formation of inorganic products from the ClO_2-SRNOM reaction

The inorganic products ClO_2^-/ClO_3^- after 24 h and the maximum *in situ* FAC formation (insert of Figure 4-2) were measured. The sum of ClO_2^-, ClO_3^- and FAC was accounting for 78 to 103% of the consumed ClO_2 (Figure 4-3). For ClO_2 doses > 15 µM, the percentage recovery ranged from 97% to 103%. The lower recovery for lower ClO_2 doses could be explained by a fast degradation of FAC (as NH_2Cl) as observed in Figure 4-2. For ClO_2 doses > 15 µM, the ClO_2/SRNOM reaction led to the formation of 71–82% of ClO_2^-, 1–15% of ClO_3^- and 14–17% of FAC (Figure 4-3). After 400 min of reaction, the FAC yields (Δ[FAC]/Δ[ClO_2]) could reach up to 22% and 25% for SRNOM and UMRNOM, respectively (Figure A-4-4a).

The yields of ClO_2^- and ClO_3^- were consistent with values typically reported for real water treatment conditions,[46, 47] where a significant portion of the ClO_2 usually remains unaccounted for. The results from the ClO_2/NOM experiments demonstrate that FAC is an additional byproduct, which completes the mass balance for inorganic chlorine species. The large increase of ClO_3^- (from 5 to 15%) for ClO_2 doses > 133 µM suggests that for these conditions, ClO_2 was no longer reacting with organic moieties, since ClO_3^- arises from side reactions.[2, 48] This was supported by the ClO_2 consumption reaching a plateau (Figure A-4-4b) and by the *in situ* FAC formation reaching its maximum (insert of Figure 4-2). Furthermore, the EDC (a proxy for the availability of electrons in NOM)[33] was reaching its minimum for ClO_2 doses ≥ 133 µM while the UVA was still significantly decreasing (Figure A-4-5). This indicates that a significant fraction of UV-absorbing compounds is present in solution, with a poor reactivity with ClO_2. In general, UVA is used to represent the change in NOM characteristics or reactivity during oxidation processes. However, the variation of NOM characteristics observed by EDC measurements are larger than by UVA analysis and exhibit different behaviors during oxidation processes.[34, 35, 49] In the

present study, EDC might be a better surrogate than UVA for reactive organic moieties and subsequent *in situ* FAC formation during ClO_2 treatment.

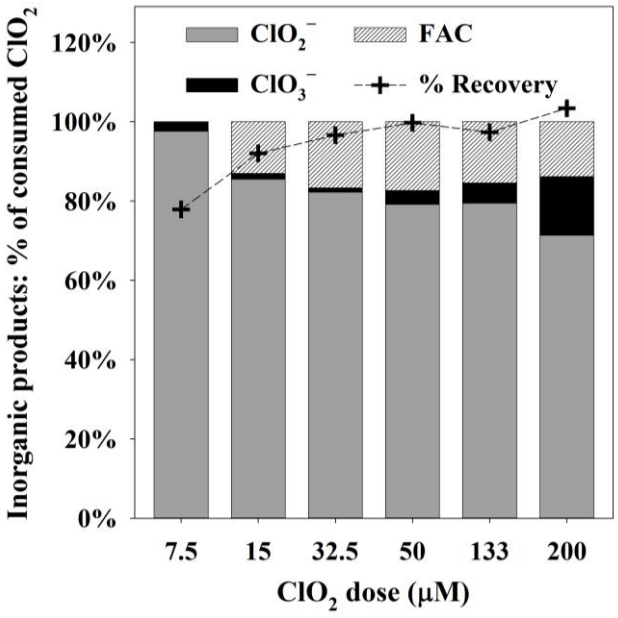

Figure 4-3. Percentage distribution of inorganic byproducts from the reactions of ClO_2 with SRNOM and mass balance on chlorine species. [ClO_2] = 7.5–200 μM, [NOM] = 3.0 mgC L^{-1}, pH 8.1, 10 mM phosphate.

4.4.2 Formation of DBPs from ClO_2 reactions with model compounds and NOM

4.4.2.1 Model compounds

It has been demonstrated that ClO_2/phenol mixtures produce one mole of FAC per mole of phenol for ClO_2 concentrations ≥ phenol (Figure 4-1). The *in situ* pre-formed FAC from the ClO_2/phenol mixture was reacted with two model compounds, resorcinol and tryptophan, which were added after ClO_2 was fully consumed (1 min). Resorcinol was chosen as it is a widely studied THMs precursor,[5, 50-52] while tryptophan is a precursor of HANs,[50] a class of non-regulated nitrogenous DBPs, which are more toxic than the THMs.[53] The formed THMs and HANs were compared to their formation potential from an equivalent concentration of dosed FAC (Figure A-4-6). The *in situ* formed FAC from the ClO_2/phenol mixture produced 0.8 mole and 0.08 mole of chloroform (TCM) per mole of resorcinol and tryptophan, respectively. 0.02 mole of dichloroacetonitrile (DCAN) per mole of tryptophan was also produced while no HAN was detected from resorcinol due to the absence of nitrogenous moieties. These concentrations were very similar to the DBPs produced by dosed FAC, 1.03 mole and 0.13 mole of TCM per mole of resorcinol and tryptophan, respectively, and 0.03 mole of DCAN per mole of tryptophan

(Figure A-4-6). These results are consistent with reported DBP formation potentials during chlorination of resorcinol and tryptophan.[5, 50-52, 54, 55] The presence of glycine, which reacts very quickly with FAC[39] but not with ClO_2,[37] was efficiently mitigating the formation of DBPs with both dosed FAC and the *in situ* formed FAC. This supports the hypothesis that FAC is the chlorine species involved in the formation of halogenated DBPs during ClO_2 treatment.

4.4.2.2 SRNOM

Doses of ClO_2 ranging from 7.5 to 200 µM were applied to SRNOM at pH 8.1 (Figure 4-4) and pH 6.5 (Figure A-4-7) to investigate the formation of organic halogenated DBPs, i.e. HANs, THMs and AOCl.

TCM and DCAN were detected at very low concentrations (≤ 26 nM, ≤ 3.1 µg L^{-1}) while significant concentrations of AOCl were produced (up to 2.1 µM, 74 µg L^{-1} as Cl). Traces of trichloroacetonitrile (< 1 nM, < 0.1 µg L^{-1}) were also detected. Increasing the ClO_2 dose from 7.5 to 50 µM increased the AOCl, TCM and DCAN formation (Figure 4-4 and A-4-7). For higher ClO_2 doses, the DBP concentrations decreased except for DCAN at pH 8.1. The pH did not significantly affect AOCl formation, while TCM and DCAN concentrations were higher at pH 6.5 (Figure 4-4 and A-4-7). The overall higher DCAN concentration measured at pH 6.5 than at pH 8.1 is consistent with its base-catalyzed degradation.[56]

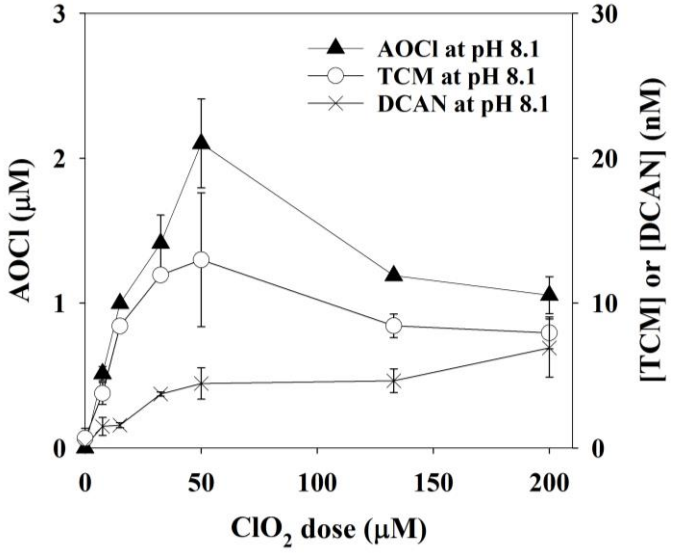

Figure 4-4. Disinfection byproducts formation from the reaction of ClO_2 with SRNOM for varying ClO_2 doses. [ClO_2] = 7.5–200 µM, [SRNOM] = 3.0 mgC L^{-1}, pH 8.1, 10 mM phosphate, 24 h reaction time. Error bars represent the range of results of duplicate experiments.

The DBP concentrations are comparable to a previous study conducted using Suwannee River Fulvic Acid (SRFA).[57] A decrease in DBP concentrations at higher ClO_2 doses was previously reported,[8] and corresponded to the trend of the *in situ* FAC formation from the reaction between ClO_2 and SRNOM (insert of Figure 4-2). At low ClO_2 doses, increasing the ClO_2 increased the formation of FAC and consequently the DBPs. Once all the FAC precursors were consumed, increasing the dose of ClO_2 did not form additional FAC. Moreover, under these conditions, the *in situ* formed FAC and ClO_2 are competing for reactive DOM moieties. At higher ClO_2 doses, more DBP precursor moieties were consumed by ClO_2 while similar FAC concentrations were generated. Overall, this leads to a decrease of the DBP concentrations. A shift of DBP speciation toward more polar compounds might lead to a decrease of DBP recovery during extraction with activated carbon and a potential decrease of AOCl. However, several publications showed that polar DBPs, such as haloacetic acids, were efficiently recovered at acidic pH.[58, 59] The formation of polar compounds is not expected to significantly affect the AOCl measurement and therefore the substantial mitigation of AOCl (from 2.1 to 1.1 µM) is mainly due to ClO_2 pre-oxidation.

4.4.2.3 Comparison between in situ formed FAC and dosed FAC

The formation of DBPs from SRNOM was determined for both ClO_2 (*in situ* formed FAC) and a reference experiment with dosed FAC at pH 8.1 (Figure 4-5a). As shown in Figure 4-2, a ClO_2 dose of 50 µM produced 8.6 µM of FAC. Therefore, the DBPs produced by reaction of 50 µM of ClO_2 were compared to 8.6 µM of FAC dosed in SRNOM (Figure 4-5a). Control experiments in presence of glycine were also carried out. The effect of the addition of Cl^- along with FAC was estimated to be insignificant based on Cl_2 and HOCl reactivity with phenol (Text A-4-4).[60] Similar experiments were carried out with ClO_2 doses ranging from 32.5 to 200 µM and FAC doses ranging from 5.3 to 15 µM. The percentage of chlorine-incorporation into SRNOM was then determined as the ratio of AOCl produced per mole of FAC measured (during ClO_2 experiments) or dosed (during FAC experiments) (Figure 4-5b).

For 50 µM ClO_2 and 8.6 µM dosed FAC the same concentration of AOCl was produced (2.1–2.3 µM, 74–82 µg L^{-1} as Cl) while ClO_2 produced less TCM (8.4 nM, 1.0 µg L^{-1}) and more DCAN (3.4 nM, 0.3 µg L^{-1}) compared to the equivalent FAC dose (107 nM TCM (12.8 µg L^{-1}) and 1.4 nM DCAN (0.2 µg L^{-1})) (Figure 4-5a).

Similar to a previous study, the levels of TCM formed by ClO_2 and dosed FAC represented 1 and 14% of the AOCl, respectively.[57]

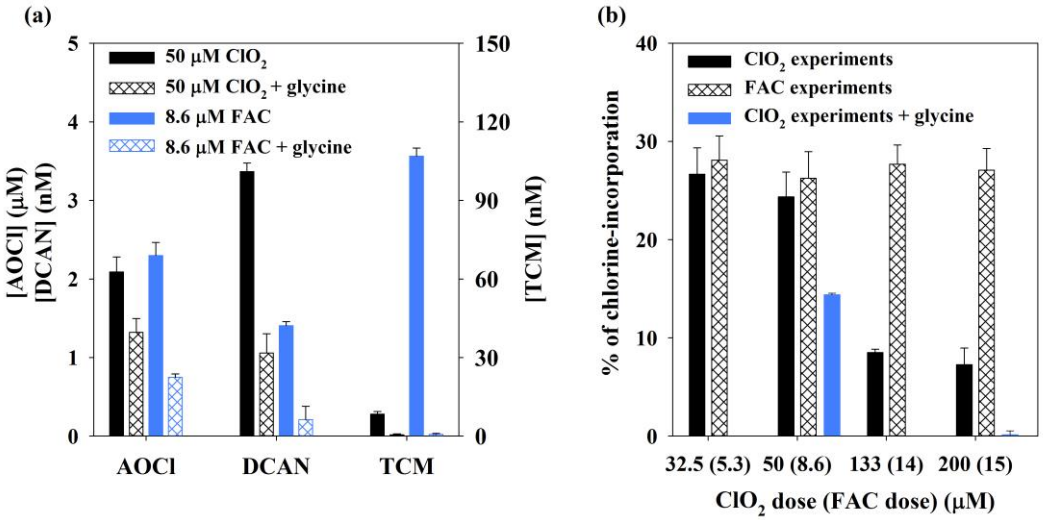

Figure 4-5. Comparison between ClO_2 (*in situ* formed FAC) and dosed FAC. (a) DBPs formed by reaction of 50 µM ClO_2 and 8.6 µM dosed FAC, without (filled bars) and with glycine (patterned bars). (b) Percentage of chlorine incorporation into SRNOM during ClO_2 (*in situ* formed FAC) and FAC experiments. The chlorine incorporation is also represented for 50 and 200 µM ClO_2 in presence of glycine. For all graphs: $[ClO_2]$ = 32.5–200 µM, [FAC] = 5.3–15 µM, [SRNOM] = 3.0 mgC L^{-1}, pH 8.1, 10 mM phosphate, 24 h reaction time. Error bars represent the range of results of duplicate analyses.

The lower formation of TCM by ClO_2 compared to dosed FAC is explained by the high reactivity of ClO_2 towards TCM precursors. As an example, at pH 8.1, resorcinol has about a 100 times higher apparent second order rate constants for the reaction with ClO_2 than with FAC.[37, 61] Conversely, the higher formation of DCAN in the ClO_2 experiment compared to a simple dosage of FAC is explained by the low reactivity of ClO_2 with nitrogenous compounds. Many amino acids have a low reactivity with ClO_2,[62] as illustrated by the glycine used to quench FAC in our experiments. For example, histidine and alanine react slowly with ClO_2 while forming HANs in presence of FAC.[62-64] Overall, ClO_2 will preferentially oxidize some of the reactive sites, such as THM precursors, leaving more of the *in situ* formed FAC to react with N-containing moieties, leading to a higher DCAN formation. Furthermore, previous work on tyrosine-based amino acids showed that ClO_2 oxidation could enhance the DCAN formation during chlorination.[65] The similar levels of AOCl produced from 8.6 µM FAC and 50 µM ClO_2 (Figure 4-5a) support that organic chlorinated DBPs formed during ClO_2 treatment originate from the *in situ* formed FAC.

The chlorine-incorporation during ClO_2 experiments decreased from 27 to 7% of the formed FAC with increasing ClO_2 doses from 32.5 to 200 µM (Figure 4-5b). In contrast, for dosed FAC concentrations ranging from 5.3 to 15 µM (corresponding to the *in situ* FAC formation in the ClO_2 experiments), the chlorine-incorporation was constant with percentages ranging from 26 to 28%, consistent with typical chlorine-incorporation during chlorination in water treatment.[57, 66, 67] For the lower ClO_2 doses (32.5 and 50 µM), the chlorine-incorporation was similar for FAC and ClO_2 experiments (Figure 4-5b). At these doses, ClO_2 degraded part of the AOCl precursors but they were still in excess compared to the *in situ* formed FAC. Therefore, comparable results were obtained for the FAC and ClO_2 experiments. At higher ClO_2 doses, the decrease in chlorine-incorporation could be explained by a gradual abatement of the reactive moieties by ClO_2, i.e., a large fraction of the AOCl precursors was degraded by ClO_2, preventing the formation of AOCl. Hence the chlorine-incorporation was mitigated compared to the FAC experiments. This behavior is clearly illustrated by an efficient EDC abatement of up to 80% for ClO_2 doses ranging from 5.3 to 50 µM followed by a less efficient additional abatement of 10% for a ClO_2 dose of 133 µM and no further abatement for a ClO_2 dose of 200 µM (Figure A-4-5). As mentioned above for the inorganic byproducts distribution, the UVA measurement exhibits a different behavior with a continuous decrease for ClO_2 doses ranging from 50 µM to 200 µM and a much lower abatement of the relative UVA (< 50%) (Figure A-4-5).

To verify that the DBPs were formed by reaction of NOM with *in situ* formed FAC and not with ClO_2, samples were quenched with glycine (Figure 4-5a). The formation of DCAN and TCM for both ClO_2 and dosed FAC was efficiently mitigated (≤ 1 nM, ≤ 0.1 µg L^{-1}) while AOCl formation was only partially inhibited in the presence of glycine. The AOCl reached 1.3 µM (47 µg L^{-1} as Cl) and 0.7 µM (27 µg L^{-1} as Cl) for ClO_2 and dosed FAC, respectively. It has been verified that *N*-chloroglycine alone does not contribute to AOCl. Furthermore, in absence of glycine, most of the AOCl was formed within 30 min whereas in presence of glycine AOCl formation increased up to 24 h (Figure A-4-8). These results suggest that AOCl resulted from the reaction of *N*-chloroglycine (formed by reaction between FAC and glycine) with NOM and not from ClO_2 since the latter was fully consumed in 30 min (Figure A-4-2). When the ClO_2 dose was increased to 200 µM, no AOCl was formed in the presence of glycine

(Figure 4-5b). This can be explained by a significant abatement of the reactive NOM moieties, confirmed by the significant abatement of EDC (Figure A-4-5).

4.4.2.4 Effect of NOM type on formation of DBPs

The same dose of ClO_2 (15 µM, 1 mg L^{-1}) was applied to four synthetic waters (PLFA, UMRNOM, SRNOM, NLFA) and three real waters (P105, P65, P100) (Table A-4-2). All the synthetic waters were prepared with 3.0 mgC L^{-1} while the real waters had DOC concentrations ranging from 2.6 to 9.2 mgC L^{-1}, SUVAs between 1.6 and 3.6 L mgC^{-1} m^{-1} and contained Br^- concentrations ranging from 135 to 235 µg L^{-1}. The sample from a shallow bore, P100, presented higher SUVA and DOC content as well as lower pH (6.5 vs 7.2–7.4) and Br^- concentrations compared to the deeper bores, P105 and P65 (Table A-4-2). The ClO_2 dose was chosen to be representative of a pre-oxidation step for real drinking water treatment conditions where ClO_2^- formation is the limiting factor (< 12 µM, < 0.8 mg L^{-1}).[68]

The formation of AOX (AOCl/AOBr) ranged from 0.7 µM for PLFA to 4.0 µM for P100 (21–138 µg L^{-1} as Cl) (Figure 4-6), while the THM and DCAN levels were very low, ≤ 11.9 nM (1.4 µg L^{-1}) for THMs (Figure A-4-9) and ≤ 2.8 nM (0.3 µg L^{-1}) for DCAN (Figure A-4-10a).

The AOX formation during ClO_2 treatment was correlated with the EDC and UVA of the tested waters (r^2 = 0.849 and 0.777, respectively), while the SUVA gave a poor correlation (r^2 = 0.170) (Figure A-4-11). The correlation between UVA and AOX formation is consistent with previous chlorination studies.[69, 70] THM formation was also correlated to the EDC and UVA except for P100 for which the lowest amount of THMs was produced while its UVA and EDC indicated a high reactivity (Figure A-4-9). In this sample, the *in situ* formed free available chlorine or bromine was distributed over many sites, indicated by the high AOX, and therefore was probably fully consumed before multi-halogenation of the same site, leading to THM formation, could occur. Finally, for synthetic waters, DCAN increased with the nitrogen content and the ratio of DCAN/AOX was strongly correlated to the N/C ratio (r^2 = 0.999) (Figure A-4-10b), as previously demonstrated for the chlorination of humic and fulvic extracts.[69]

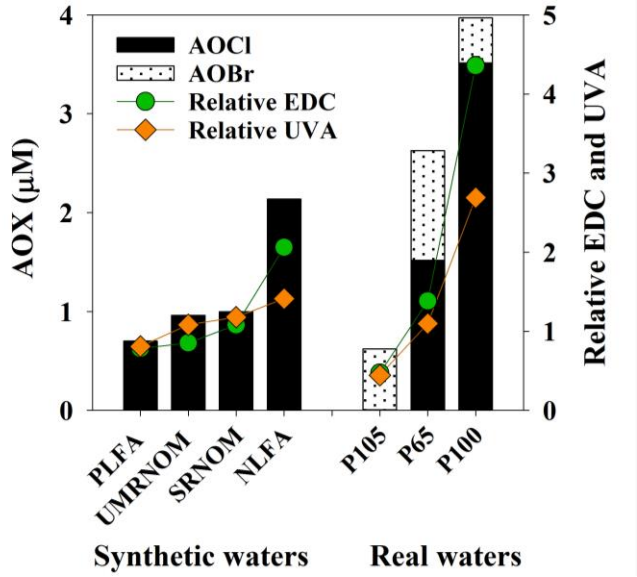

Figure 4-6. AOX formed from the reactions of ClO_2 with synthetic (PLFA, UMRNOM, SRNOM, NLFA) and real waters (P105, P65, P100) compared to the relative EDC and UVA of the untreated sample. The relative EDC and UVA were calculated as the EDC or UVA signal of the samples divided by the EDC or UVA signal of an unbuffered 3.0 mgC L^{-1} SRNOM solution, respectively. [ClO_2] = 15 µM, 24 h reaction time, NOM characteristics and characteristic of the real water samples are given in Table A-4-2. No Br^- was spiked into synthetic waters while real waters contained 135–235 µg L^{-1}.

4.4.3 Practical implications

ClO_2 is commonly used as an alternative to chlorine or as pre-oxidant because it produces less THMs or other halogenated organic DBPs due to its different mode of action (eq 4-1). However, this study demonstrates that under drinking water treatment conditions, ClO_2 degradation induces *in situ* formation of FAC, leading to substantial levels of AOX. At low ClO_2 doses, typically used in pre-oxidation (15 µM, 1 mg L^{-1}), 7% of the dosed ClO_2 was forming AOCl. Although FAC could not accurately be determined at this ClO_2 dose, it is estimated that about 20–25% of the ClO_2 would produce FAC and 25–30% of this *in situ* formed FAC would be incorporated to SRNOM. Experiments in synthetic and real waters showed that AOX formation depended on the EDC and UVA in more complex matrices (Figure 4-6 and A-4-11). Furthermore, while ClO_2 is known to be unreactive toward Br^-,[37] the *in situ* formed FAC can oxidize Br^- to free available bromine and produce brominated DBPs. The Br^-/DOC ratio is an important indicator of AOBr formation (Figure A-4-12).

The THMs levels produced by ClO_2 are negligible and not likely to be an issue for drinking water suppliers, while the AOX yields (up to 7%) from ClO_2 remain much

lower compared to FAC (typically between 21 and 29%).[57, 66, 67] However, when ClO_2 is used as a pre-oxidant, the AOX produced from the *in situ* formed FAC could partially counteract the mitigating effect of pre-oxidation on AOX formation and enhance the formation of lower molecular weight DBPs during subsequent chlorination. The incorporation of bromine in NOM for bromide-containing natural waters also has to be considered as brominated DBPs are generally more toxic than their chlorinated analogues.[71]

4.5 References

1. Black & Veatch Corporation, Chlorine Dioxide. In *White's Handbook of Chlorination and Alternative Disinfectants*, 5th ed.; John Wiley & Sons, Inc.: Hoboken, 2010; pp 700-766.
2. Gordon, G.; Kieffer, R. G.; Rosenblatt, D. H., The Chemistry of Chlorine Dioxide. In *Progress in Inorganic Chemistry*, Lippard, S.J., Ed. John Wiley & Sons, Inc.: New York, 1972; Vol. 15, pp 201-286.
3. WHO, Guidelines for Drinking-Water Quality. In 4th ed.; WHO, Ed. Geneva, 2017.
4. European Commission, Proposal for a directive of the european parliament and of the council on the quality of water intended for human consumption. In *2017/0332*: Brussels, 2017.
5. Boyce, S. D.; Hornig, J. F., Reaction pathways of trihalomethane formation from the halogenation of dihydroxyaromatic model compounds for humic acid. *Environ. Sci. Technol.* **1983,** *17*, (4), 202-211.
6. Richardson, S. D.; Thruston, A. D., Jr.; Caughran, T. V.; Chen, P. H.; Collette, T. W.; Schenck, K. M.; Lykins, B. W., Jr.; Rav-acha, C.; Glezer, V., Identification of New Drinking Water Disinfection by - Products from Ozone, Chlorine Dioxide, Chloramine, and Chlorine. *Water Air Soil Pollut.* **2000,** *123*, (1-4), 95-102.
7. Hua, G.; Reckhow, D. A., Comparison of disinfection byproduct formation from chlorine and alternative disinfectants. *Water Res.* **2007,** *41*, (8), 1667-1678.
8. Chang, C.-Y.; Hsieh, Y.-H.; Hsu, S.-S.; Hu, P.-Y.; Wang, K.-H., The formation of disinfection byproducts in water treated with chlorine dioxide. *J. Hazard. Mater.* **2000,** *79*, (1–2), 89-102.
9. Aieta, E. M.; Berg, J. D., A Review of Chlorine Dioxide in Drinking Water Treatment. *J. Am. Water Works Assoc.* **1986,** *78*, (6), 62-72.
10. Wajon, J. E.; Rosenblatt, D. H.; Burrows, E. P., Oxidation of phenol and hydroquinone by chlorine dioxide. *Environ. Sci. Technol.* **1982,** *16*, (7), 396-402.
11. Ganiev, I. M.; Suvorkina, E. S.; Kabal'nova, N. N., Reaction of chlorine dioxide with phenol. *Russ. Chem. Bull.* **2003,** *52*, (5), 1123-1128.
12. Aguilar, C. A. H.; Narayanan, J.; Manoharan, M.; Singh, N.; Thangarasu, P., A Much-Needed Mechanism and Reaction Rate for the Oxidation of Phenols with ClO_2: A Joint Experimental and Computational Study. *Aust. J. Chem.* **2013,** *66*, (7), 814-824.
13. Napolitano, M. J.; Green, B. J.; Nicoson, J. S.; Margerum, D. W., Chlorine Dioxide Oxidations of Tyrosine, N-Acetyltyrosine, and Dopa. *Chem. Res. Tox.* **2005,** *18*, (3), 501-508.
14. Black & Veatch Corporation, Chemistry of Aqueous Chlorine. In *White's Handbook of Chlorination and Alternative Disinfectants*, 5th ed.; John Wiley & Sons, Inc.: Hoboken, 2010; pp 68-173.
15. Rav-Acha, C.; Choshen, E., Aqueous reactions of chlorine dioxide with hydrocarbons. *Environ. Sci. Technol.* **1987,** *21*, (11), 1069-1074.
16. Napolitano, M. J.; Stewart, D. J.; Margerum, D. W., Chlorine Dioxide Oxidation of Guanosine 5‘-Monophosphate. *Chem. Res. Tox.* **2006,** *19*, (11), 1451-1458.
17. Stewart, D. J.; Napolitano, M. J.; Bakhmutova-Albert, E. V.; Margerum, D. W., Kinetics and Mechanisms of Chlorine Dioxide Oxidation of Tryptophan. *Inorg. Chem.* **2008,** *47*, (5), 1639-1647.

18. Ison, A.; Odeh, I. N.; Margerum, D. W., Kinetics and Mechanisms of Chlorine Dioxide and Chlorite Oxidations of Cysteine and Glutathione. *Inorg. Chem.* **2006,** *45*, (21), 8768-8775.
19. Aguilar, C. A. H.; Narayanan, J.; Singh, N.; Thangarasu, P., Kinetics and mechanism for the oxidation of anilines by ClO_2: a combined experimental and computational study. *J. Phys. Org. Chem.* **2014,** *27*, (5), 440-449.
20. Nie, S.; Liu, X.; Wu, Z.; Zhan, L.; Yin, G.; Yao, S.; Song, H.; Wang, S., Kinetics study of oxidation of the lignin model compounds by chlorine dioxide. *Chem. Eng. J.* **2014,** *241*, (Supplement C), 410-417.
21. Ni, Y.; Shen, X.; van Heiningen, A. R. P., Studies on the Reactions of Phenolic and Non-Phenolic Lignin Model Compounds with Chlorine Dioxide. *J. Wood Chem. Technol.* **1994,** *14*, (2), 243-262.
22. Kolar, J. J.; Lindgren, B. O.; Pettersson, B., Chemical reactions in chlorine dioxide stages of pulp bleaching. *Wood Sci. and Technol.* **1983,** *17*, (2), 117-128.
23. Terhalle, J.; Kaiser, P.; Jütte, M.; Buss, J.; Yasar, S.; Marks, R.; Uhlmann, H.; Schmidt, T. C.; Lutze, H. V., Chlorine dioxide–Pollutant transformation and formation of hypochlorous acid as a secondary oxidant. *Environ. Sci. Technol.* **2018**, *52*, (17), 9964-9971.
24. Furman, C. S.; Margerum, D. W., Mechanism of Chlorine Dioxide and Chlorate Ion Formation from the Reaction of Hypobromous Acid and Chlorite Ion. *Inorg. Chem.* **1998,** *37*, (17), 4321-4327.
25. Granstrom, M. L.; Lee, G. F., Generation and Use of Chlorine Dioxide in Water Treatment. *J. Am. Water Works Assoc.* **1958,** *50*, (11), 1453-1466.
26. Gates, D. J., *The Chlorine Dioxide Handbook*. American Water Works Association: 1998.
27. Allard, S.; Charrois, J. W. A.; Joll, C. A.; Heitz, A., Simultaneous analysis of 10 trihalomethanes at nanogram per liter levels in water using solid-phase microextraction and gas chromatography mass-spectrometry. *J. Chromatogr. A* **2012,** *1238*, 15-21.
28. Kristiana, I.; Joll, C.; Heitz, A., Analysis of halonitriles in drinking water using solid-phase microextraction and gas chromatography–mass spectrometry. *J. Chromatogr. A* **2012,** *1225*, 45-54.
29. Langsa, M.; Allard, S.; Kristiana, I.; Heitz, A.; Joll, C. A., Halogen-specific total organic halogen analysis: Assessment by recovery of total bromine. *J. Environ. Sci.***2017,** *58*, 340-348.
30. Wilke, T.; Schneider, M.; Kleinermanns, K., 1,4-Hydroquinone is a Hydrogen Reservoir for Fuel Cells and Recyclable via Photocatalytic Water Splitting. *Open J. Phys. Chem.* **2013,** *3*, 97-102.
31. Pinkernell, U.; Nowack, B.; Gallard, H.; Von Gunten, U., Methods for the photometric determination of reactive bromine and chlorine species with ABTS. *Water Res.* **2000,** *34*, (18), 4343-4350.
32. USEPA, Method 326.0: Determination of Inorganic Oxyhalide Disinfection Byproducts in Drinking Water Using Ion Chromatography Incorporating the Addition of a Suppressor Acidified Postcolumn Reagent for Trace Bromate Analysis, 2002.
33. Aeschbacher, M.; Graf, C.; Schwarzenbach, R. P.; Sander, M., Antioxidant properties of humic substances. *Environ. Sci. Technol.* **2012,** *46*, (9), 4916-4925.
34. Wenk, J.; Aeschbacher, M.; Salhi, E.; Canonica, S.; Von Gunten, U.; Sander, M., Chemical oxidation of dissolved organic matter by chlorine dioxide, chlorine, and ozone: Effects on its optical and antioxidant properties. *Environ. Sci. Technol.* **2013,** *47*, (19), 11147-11156.

35. Chon, K.; Salhi, E.; von Gunten, U., Combination of UV absorbance and electron donating capacity to assess degradation of micropollutants and formation of bromate during ozonation of wastewater effluents. *Water Res.* **2015,** *81*, 388-397.
36. Önnby, L.; Walpen, N.; Salhi, E.; Sander, M.; von Gunten, U., Two analytical approaches quantifying the electron donating capacities of dissolved organic matter to monitor its oxidation during chlorination and ozonation. *Water Res.* **2018**, *144*, 677-689.
37. Hoigné, J.; Bader, H., Kinetics of reactions of chlorine dioxide (OClO) in water-I. Rate constants for inorganic and organic compounds. *Water Res.* **1994,** *28*, (1), 45-55.
38. Gallard, H.; von Gunten, U., Chlorination of Phenols: Kinetics and Formation of Chloroform. *Environ. Sci. Technol.* **2002,** *36*, (5), 884-890.
39. Deborde, M.; von Gunten, U., Reactions of chlorine with inorganic and organic compounds during water treatment–Kinetics and mechanisms: A critical review. *Water Res.* **2008,** *42*, (1–2), 13-51.
40. Peintler, G.; Nagypal, I.; Epstein, I. R., Systematic design of chemical oscillators. 60. Kinetics and mechanism of the reaction between chlorite ion and hypochlorous acid. *J. Phys. Chem.* **1990,** *94*, (7), 2954-2958.
41. Heeb, M. B.; Kristiana, I.; Trogolo, D.; Arey, J. S.; von Gunten, U., Formation and reactivity of inorganic and organic chloramines and bromamines during oxidative water treatment. *Water Res.* **2017,** *110*, (Supplement C), 91-101.
42. Wang, L.; Margerum, D. W., Hypohalite Ion Catalysis of the Disproportionation of Chlorine Dioxide. *Inorg. Chem.* **2002,** *41*, (23), 6099-6105.
43. Nihemaiti, M.; Le Roux, J.; Hoppe-Jones, C.; Reckhow, D. A.; Croué, J.-P., Formation of Haloacetonitriles, Haloacetamides, and Nitrogenous Heterocyclic Byproducts by Chloramination of Phenolic Compounds. *Environ. Sci. Technol.* **2017,** *51*, (1), 655-663.
44. Tratnyek, P. G.; Hoigné, J., Kinetics of reactions of chlorine dioxide (OCIO) in water-II. Quantitative structure-activity relationships for phenolic compounds. *Water Res.* **1994,** *28*, (1), 57-66.
45. I.H.S.S http://humic-substances.org
46. Korn, C.; Andrews, R. C.; Escobar, M. D., Development of chlorine dioxide-related byproduct models for drinking water treatment. *Water Res.* **2002,** *36*, (1), 330-342.
47. Werdehoff, K. S.; Singer, P. C., Chlorine Dioxide Effects on THMFP, TOXFP, and the Formation of Inorganic Byproducts. *J. Am. Water Works Assoc.* **1987,** *79*, (9), 107-113.
48. Odeh, I. N.; Francisco, J. S.; Margerum, D. W., New Pathways for Chlorine Dioxide Decomposition in Basic Solution. *Inorg. Chem.* **2002,** *41*, (24), 6500-6506.
49. Walpen, N.; Schroth, M. H.; Sander, M., Quantification of Phenolic Antioxidant Moieties in Dissolved Organic Matter by Flow-Injection Analysis with Electrochemical Detection. *Environ. Sci. Technol.* **2016,** *50*, (12), 6423-6432.
50. Bond, T.; Henriet, O.; Goslan, E. H.; Parsons, S. A.; Jefferson, B., Disinfection Byproduct Formation and Fractionation Behavior of Natural Organic Matter Surrogates. *Environ. Sci. Technol.* **2009,** *43*, (15), 5982-5989.
51. Chaidou, C. I.; Georgakilas, V. I.; Stalikas, C.; Saraçi, M.; Lahaniatis, E. S., Formation of chloroform by aqueous chlorination of organic compounds. *Chemosphere* **1999,** *39*, (4), 587-594.

52. Norwood, D. L.; Johnson, J. D.; Christman, R. F.; Hass, J. R.; Bobenrieth, M. J., Reactions of chlorine with selected aromatic models of aquatic humic material. *Environ. Sci. Technol.* **1980,** *14*, (2), 187-190.
53. Muellner, M. G.; Wagner, E. D.; McCalla, K.; Richardson, S. D.; Woo, Y.-T.; Plewa, M. J., Haloacetonitriles vs. Regulated Haloacetic Acids: Are Nitrogen-Containing DBPs More Toxic? *Environ. Sci. Technol.* **2007,** *41*, (2), 645-651.
54. de Laat, J.; Merlet, N.; Dore, M., Chlorination of organic compounds: chlorine demand and reactivity in relationship to the trihalomethane formation. Incidence of ammoniacal nitrogen. *Water Res.* **1982,** *16*, (10), 1437-1450.
55. Hureiki, L.; Croué, J. P.; Legube, B., Chlorination studies of free and combined amino acids. *Water Res.* **1994,** *28*, (12), 2521-2531.
56. Reckhow, D. A.; MacNeill, A. L.; Platt, T. L.; MacNeill, A. L.; McClellan, J. N., Formation and degradation of dichloroacetonitrile in drinking waters. *J. Water Supply Res. Technol. Aqua* **2001,** *50*, (1), 1-13.
57. Zhang, X.; Echigo, S.; Minear, R. A.; Plewa, M. J., Characterization and Comparison of Disinfection Byproducts of Four Major Disinfectants. In *Natural Organic Matter and Disinfection Byproducts*, American Chemical Society: 2000; Vol. 761, pp 299-314.
58. Kristiana, I.; McDonald, S.; Tan, J.; Joll, C.; Heitz, A., Analysis of halogen-specific TOX revisited: Method improvement and application. *Talanta* **2015,** *139*, (Supplement C), 104-110.
59. Hua, G.; Reckhow, D. A., Determination of TOCl, TOBr and TOI in drinking water by pyrolysis and off-line ion chromatography. *Anal. Bioanal. Chem.* **2006,** *384*, (2), 495-504.
60. Lau, S. S.; Abraham, S. M.; Roberts, A. L., Chlorination Revisited: Does Cl– Serve as a Catalyst in the Chlorination of Phenols? *Environ. Sci. Technol.* **2016,** *50*, (24), 13291-13298.
61. Rebenne, L. M.; Gonzalez, A. C.; Olson, T. M., Aqueous Chlorination Kinetics and Mechanism of Substituted Dihydroxybenzenes. *Environ. Sci. Technol.* **1996,** *30*, (7), 2235-2242.
62. Tan, H.-k.; Wheeler, W. B.; Wei, C.-i., Reaction of chlorine dioxide with amino acids and peptides: Kinetics and mutagenicity studies. *Mutat. Res.* **1987,** *188*, (4), 259-266.
63. Li, C.; Gao, N.; Chu, W.; Bond, T.; Wei, X., Comparison of THMs and HANs formation potential from the chlorination of free and combined histidine and glycine. *Chem. Eng. J.* **2017,** *307*, 487-495.
64. Bond, T.; Mokhtar Kamal, N. H.; Bonnisseau, T.; Templeton, M. R., Disinfection byproduct formation from the chlorination and chloramination of amines. *J. Hazard. Mater.* **2014,** *278*, 288-296.
65. Yao, D.; Chu, W.; Bond, T.; Ding, S.; Chen, S., Impact of ClO_2 pre-oxidation on the formation of CX3R-type DBPs from tyrosine-based amino acid precursors during chlorination and chloramination. *Chemosphere* **2018,** *196*, 25-34.
66. Langsa, M.; Heitz, A.; Joll, C. A.; von Gunten, U.; Allard, S., Mechanistic Aspects of the Formation of Adsorbable Organic Bromine during Chlorination of Bromide-containing Synthetic Waters. *Environ. Sci. Technol.* **2017,** *51*, (9), 5146-5155.
67. Hua, G.; Reckhow, D. A.; Kim, J., Effect of bromide and iodide ions on the formation and speciation of disinfection byproducts during chlorination. *Environ. Sci. Technol.* **2006,** *40*, (9), 3050-3056.

68. USEPA, Disinfectants and Disinfection Byproducts final rule. In Federal Register: 1998; Vol. 63, pp 69390-69476.
69. Reckhow, D. A.; Singer, P. C.; Malcolm, R. L., Chlorination of humic materials: byproduct formation and chemical interpretations. *Environ. Sci. Technol.* **1990,** *24*, (11), 1655-1664.
70. Archer, A. D.; Singer, P. C., Effect of SUVA and enhanced coagulation on removal of TOX precursors. *J. Am. Water Works Assoc.* **2006,** *98*, (8), 97-107.
71. Wagner, E. D.; Plewa, M. J., CHO cell cytotoxicity and genotoxicity analyses of disinfection byproducts: An updated review. *J. Environ. Sci.***2017,** *58*, 64-76.

Every reasonable effort has been made to acknowledge the owners of copyright material. I would be pleased to hear from any copyright owner who has been omitted or incorrectly acknowledged.

Chapter 5. Optimizing ClO_2 Pre-oxidation by Predicting Chlorite Oxidation during Chlorination

The content of Chapter 5 and Appendix 5 is unable to be reproduced here as they are under embargo due to current consideration for publication in the journal *Water Research*, with the following contributing co-authors: Sébastien Allard and Urs von Gunten.

I, Valentin Rougé, as the primary author, conducted all the experimental work and data analysis, including creating figures and tables, and writing and editing the manuscript.

I, as a Co-Author, endorsed that this level of contribution by the candidate indicated above is appropriate.

Sébastien Allard

Urs von Gunten

5.1 Abstract

Chlorine dioxide (ClO_2) application is limited by the formation of the regulated chlorite (ClO_2^-). However, when ClO_2 is used as a pre-oxidant, the ClO_2^- can be oxidized by chlorine during subsequent disinfection. In this study, a conceptual kinetic model for the reaction of chlorine with ClO_2^- was developed to predict the abatement of ClO_2^- during the disinfection step. The reaction was highly dependent on pH and formed ClO_3^- and ClO_2 in ultrapure water. In presence of NOM, about 70% of the ClO_2^- was recovered as ClO_3^- while the *in situ* regenerated ClO_2 was not accumulating as a consequence of its fast reaction with NOM. The remaining 30% was proposed to be recovered as chlorine, released from the NOM/ClO_2 reaction. This indicates that the sum of the oxychloro species (ClO_2^- + ClO_3^-) was decreased by chlorination and suggests that NOM could be further oxidized by the *in situ* regenerated ClO_2. The ClO_2^- concentration after 24 h of disinfection could be accurately predicted under various controlled conditions, but was overestimated in real waters in which the chlorine/ClO_2^- reaction might be catalyzed by (in)organic acids. By decreasing the ClO_2^- concentration during chlorination, higher doses of ClO_2 (up to 2 mg L^{-1}) could be applied during the pre-oxidation step. Increasing the dose of ClO_2 while keeping the ClO_2^- below the guideline improved the mitigation of DBPs. In particular, > 75% of the haloacetonitriles were mitigated. This work provides a better understanding of the chlorine/ClO_2^- interactions in typical drinking water treatment conditions, which can be valuable to optimize the ClO_2 dose during pre-oxidation based on the water reactivity (represented by the chlorine demand), the pH and the contact time, therefore improving the DBP mitigation, while keeping the ClO_2^- levels within regulatory limits.

5.2 Introduction

Disinfection byproducts (DBPs) arise from the reaction of natural organic matter (NOM) with the applied disinfectant, commonly chlorine (HOCl).[1-3] Pre-oxidation with ClO_2 has been successfully used to reduce the formation of DBPs during chlorination.[4-6] However, ClO_2 application is limited by the formation of ClO_2^-, which is regulated at 0.8 mg L^{-1} by USEPA,[7] while the World Health Organization (WHO) provides a guideline 0.7 mg L^{-1}.[8] Furthermore, a lower value of 0.25 mg L^{-1} has been proposed for ClO_3^- and ClO_2^- by the European Commission.[9] Such a regulation would prevent the use of ClO_2 as pre-oxidation without a supplementary step to remove ClO_2^- .

Treatments with ferrous iron or activated carbon have been found to decrease the concentration of ClO_2^-.[10, 11] Moreover, when chlorine is used as a disinfectant, the reaction between chlorine and ClO_2^- can lead to the formation of ClO_3^- or regenerate ClO_2,[12, 13] therefore decreasing the levels of ClO_2^-. A decrease of the ClO_2^- concentration during the disinfection step would allow the use of higher ClO_2 doses during pre-oxidation, consequently enhancing DBP mitigation while meeting the regulatory requirements of ClO_2^- levels in the finished water. The *in situ* regeneration of ClO_2 may also be beneficial for the further oxidation of DBP precursors, as well as complementary disinfection.[14]

The reaction of ClO_2^- and HOCl has been extensively studied in concentrated conditions,[12, 13, 15-17] and different models have been developed. However, little attention has been paid on their interaction in conditions relevant to drinking water treatment. The depletion of ClO_2^- during disinfection was observed by Werdehoff and Singer,[5] and was shown to produce equimolar quantities of ClO_3^- at pH $\geq$ 7.[18, 19]

This study aims in a first part to model the HOCl/ClO_2^- reaction at pH (6.6–8.1) and concentrations representative of a disinfection step, in order to predict the doses of ClO_2 that can be applied during pre-oxidation, while keeping ClO_2^- under regulatory limits after disinfection. In a second part, the benefit of increasing ClO_2 doses beyond the typically used 1 mg L^{-1} is evaluated in real waters in terms of AOX, THM and HAN formation.

5.3 Materials and methods

5.3.1 Chemicals and reagents

Sodium chlorite (80%) and sodium hypochlorite solution (10–15%) were purchased from Sigma-Aldrich. Titration of sodium chlorite by direct UV measurement at 260 nm (ε_{260} = 154 M^{-1} cm^{-1})[20] gave a purity of 79% and the impurities were found to be mostly chloride ion and traces of chlorate (< 0.01 µM of ClO_3^- per µM of ClO_2^-). All other chemicals were of analytical grade purity (≥ 98%). Solutions were prepared with ultrapure water (Purelab Ultra, Elga, UK). The Upper Mississippi River (UMRNOM, cat. No. 1R110N) and Nordic Lake (NLFA, cat. No. 1R105F) organic matter extracts were purchased from the International Humic Substances Society. The real waters were groundwaters from Pinjar, Western Australia.

5.3.2 Preparation of oxidant solutions

Chlorine (referred as HOCl in this paper) stock solutions were prepared from a sodium hypochlorite solution standardized by direct UV measurement at 292 nm (ε_{292} = 362 M^{-1} cm^{-1}).[20] ClO_2 was produced by mixing solutions of sodium persulfate (40 g L^{-1}) and sodium chlorite (80 g L^{-1}) under N_2 bubbling for about 1 h.[21, 22] The ClO_2 produced was retrieved in chilled ultrapure water and standardized by direct UV measurement at 359 nm (ε_{359} = 1230 M^{-1} cm^{-1}).[20]

5.3.3 HOCl/ClO_2^-/NOM kinetics

Kinetic experiments were conducted with 23.7 µM of ClO_2^- (1.6 mg L^{-1}) and 65 µM of HOCl (4.5 mgCl_2 L^{-1}) in ultrapure water or in 3 mgC L^{-1} UMRNOM, at pH between 6.6 and 8.1 (10 mM phosphate). Solutions were prepared in 50 mL, vigorously mixed for 10 s after HOCl addition, and split into headspace-free amber vials (3 mL) until analysis of oxidants, ClO_2^- and ClO_3^-. Similar experiments with measurements after 24 h reaction were conducted with 23.7 µM of ClO_2^- (1.6 mg L^{-1}), 40–65 µM of HOCl (2.8–4.5 mgCl_2 L^{-1}) and NOM (UMRNOM or NLFA) concentrations between 1 and 5 mgC L^{-1}. HOCl doses were chosen to ensure a residual above 0.5 mgCl_2 L^{-1} after 24 h in all the experiments.

5.3.4 Real water pre-oxidation

ClO_2 was applied to 200 mL of 3 groundwaters (P120, P130, W20), of which characteristics are given in Table A-5-1, at doses of 1–1.5 mg L^{-1} (1–2 mg L^{-1} for W20). The samples were kept without headspace and in the dark until complete decay of ClO_2. An aliquot (0.2 mL) was taken for ClO_2^- and ClO_3^- analysis, and the rest was chlorinated for 24 h. The doses of chlorine were set to target a residual of 0.5–1 mgCl_2 L^{-1} without pre-oxidation. The same chlorine doses were applied in pre-oxidized samples. After chlorination, 0.2 mL was taken for ClO_2^- and ClO_3^- analysis, 20 mL for THM and HAN analysis and 150 mL was used for AOX measurement.

5.3.5 Analytical methods

The concentration of the different oxidants was measured by ABTS-based methods.[23] Samples for ClO_2^- and ClO_3^- analysis were diluted by 30 in ultrapure water containing 0.4 mM of ethylenediamine to quench the HOCl and stabilize the ClO_2^- and kept less than two days before analysis by ion chromatography.[24] THMs and HANs were analyzed by headspace GC-MS with a method adapted from previously published methods, of which details are given in Text A-3-1.[25, 26] The samples for AOX measurement were quenched by sodium sulfite (10% excess) before adsorption on activated carbon followed by combustion and ion chromatography.[27]

5.3.6 Model

Kintecus software was used to model systems containing HOCl, ClO_2^-, ClO_2 and NOM. The ClO_2/OCl^- reaction constants were used as given by Wang et al (Table A-5-2).[28] The rest of the model was developed in this study.

5.4 Results and discussion

5.4.1 HOCl/ClO_2^- reaction in ultrapure water

5.4.1.1 Models

Three existing models for the HOCl/ClO_2^- system, i.e., Peintler et al. (Model 1),[12] Jia et al. (Model 2)[13] and Gordon and Tachiyashiki (Model 3)[17] were compared with experimental data. The equations and rate constants of the tested models are shown in Table 5-1. Model 1 consists of a 3rd order reaction rate between ClO_2^-, HOCl and H_3O^+ to form an intermediate, Cl_2O_2 (eq 5-1). This intermediate is either producing (i) ClO_2 and Cl^- by reaction of Cl_2O_2 and a second ClO_2^- (eq 5-4) or (ii) ClO_3^- and Cl^- through Cl_2O_2 decomposition (eq 5-5). Alternatively, ClO_2^- is reacting with two HOCl, forming ClO_3^- (eq 5-3). A reaction of ClO_2^- and Cl_2 is also provided (eq 5-2), which is only significant when high concentrations of Cl^- are present in solution. Model 2 uses a reaction scheme similar to Model 1 with eq 5-6a, eq 5-7 and eq 5-8a corresponding to eq 5-1, eq 5-4 and eq 5-5, respectively. In contrast to Model 1, Cl_2O_2 intermediate decomposition was suggested to be base-assisted (eq 5-8a) and the HOCl/ClO_2^- reaction to be catalyzed by phosphate (eq 5-6b and eq 5-8b). Finally, Model 3 consists of one equation (eq 5-9) similar to eq 5-3 from Model 1. Due to the presence of Cl_2 in eq 5-2 and eq 5-9, the equilibrium between Cl_2, Cl^- and HOCl species was added to the models (Table A-5-3).

5.4.1.2 Comparison of the unmodified models

The HOCl/ClO_2^- reaction was followed during 24 h between pH 6.6 and 8.1 at concentrations relevant to a disinfection step in drinking water treatment, i.e. 65 µM of HOCl (4.6 mgCl_2 L^{-1}) and 24 µM of ClO_2^- (1.6 mg L^{-1}) (Figure 5-1). The concentration of ClO_2^- was chosen to be above the guideline provided by WHO (0.7 mg L^{-1}) and corresponds to a ClO_2 dosage of about 2 mg L^{-1} (29.7 µM). As shown in Figure 5-1, the reaction rate greatly decreased with increasing the pH. ClO_2^- was decreased by 51, 32 and 10% after 24 h at pH 6.6, 7.1 and 7.7, respectively. The reaction became negligible at pH > 7.7. The experimental results were compared to the three models from the literature (Table 5-1, Figure 5-1).

Table 5-1. Equations and rate constants for the three tested models. [a]Peintler et al.,[12] [b]Jia et al.,[13] [c]Gordon and Tachiyashiki.[17]

	Equations	Rate constants
Model 1[a]		
eq 5-1	$ClO_2^- + HOCl + H_3O^+ \rightarrow Cl_2O_2 + 2H_2O$	k1 = 1.12 x 10^6 M^{-2} s^{-1}
eq 5-2	$ClO_2^- + Cl_2 \rightarrow Cl_2O_2 + Cl^-$	k2 = 4.07 x 10^4 M^{-1} s^{-1}
eq 5-3	$ClO_2^- + 2HOCl \rightarrow ClO_3^- + Cl_2 + H_2O$	k3 = 2.1 x 10^3 M^{-2} s^{-1}
eq 5-4	$ClO_2^- + Cl_2O_2 \rightarrow 2ClO_2 + Cl^-$	k4 = 1 x 10^{10} M^{-1} s^{-1}
eq 5-5	$Cl_2O_2 + H_2O \rightarrow ClO_3^- + Cl^- + 2H^+$	k5/k4 = 1.85 x 10^{-5} M
Model 2[b]		
eq 5-6a	$ClO_2^- + HOCl + H_3O^+ \rightarrow Cl_2O_2 + 2H_2O$	k6a = 2.56 x 10^4 M^{-2} s^{-1}
eq 5-6b	$ClO_2^- + HOCl + H_2PO_4^- \rightarrow Cl_2O_2 + HPO_4^{2-}$	k6b = 1.36 x 10^1 M^{-2} s^{-1}
eq 5-7	$ClO_2^- + Cl_2O_2 \rightarrow 2ClO_2 + Cl^-$	k7 = 1 x 10^{10} M^{-1} s^{-1}
eq 5-8a	$Cl_2O_2 + OH^- \rightarrow HClO_3 + Cl^-$	k8a/k7 = 1.3 x 10^5
eq 5-8b	$Cl_2O_2 + HPO_4^{2-} + H_2O \rightarrow ClO_3^- + Cl^- + H_2PO_4^-$	k8a/k7 = 2 x 10^{-1}
Model 3[c]		
eq 5-9	$HClO_2 + 2HOCl \rightarrow ClO_3^- + Cl_2 + H_3O^+$	k9 = 4.37 x 10^9 M^{-2} s^{-1}

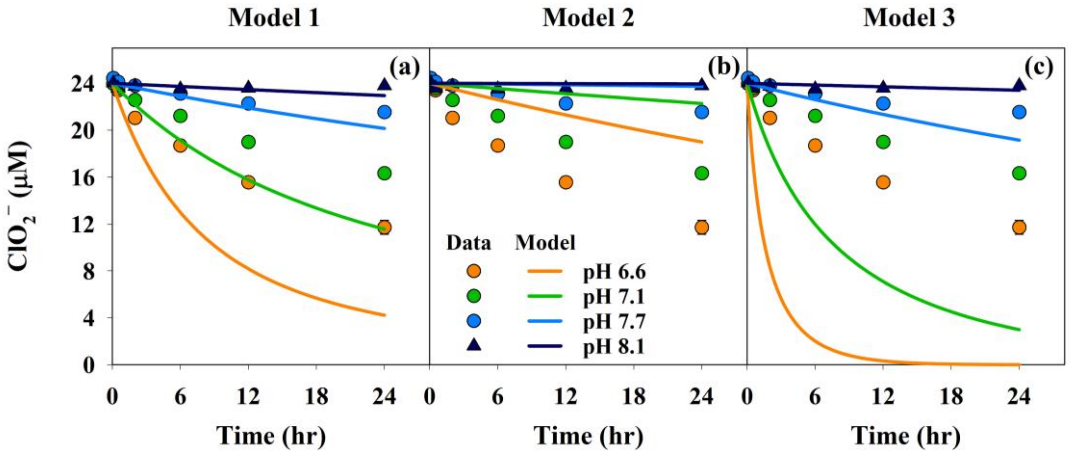

Figure 5-1. Oxidation of ClO_2^- overtime (circles) compared to the unmodified models (lines). The equations and constants are given in Table 5-1. [ClO_2^-]i = 23.7 μM, [HOCl]i = 65 μM, pH 6.6–8.1 (10 mM phosphate). Error bars represent duplicated experiments.

Model 1 and 3 predicted a ClO_2^- decrease faster than the experimental data while Model 2 underestimated the ClO_2^- decrease (Figure 5-1). The rate constants of Model 1 and 3 were determined in acetate (0.5 M) and phosphate buffer (1 M), respectively, while our experiments were done in 10 mM phosphate. Jia et al.[13] previously suggested that the $HOCl/ClO_2^-$ reaction was catalyzed by acetic acid and $H_2PO_4^-$, which may explain the faster ClO_2^- decrease predicted by Model 1 and 3.

5.4.1.3 Development of a conceptual kinetic model

In a first step, to improve the kinetic modelling, rate constants were modified by iteration to fit the ClO_2^- experimental data at pH 6.6. For Model 1 and 2, the rate constants related to the formation of the intermediate Cl_2O_2 were modified, i.e. k1 for Model 1, k6a or k6b for Model 2. In Model 1, k2 was not significantly impacting the model output and therefore was not modified. Once the "best fit" was obtained for pH 6.6, the fitted rate constants were used to model the experiments at pH 7.1, 7.7 and 8.1. The modified rate constants are presented in Table A-5-4 and the resulting fitting are presented in Figure 5-2 and A-5-1. A good fit was obtained with the modified k1 value (1.15×10^5 M^{-2} s^{-1}) in Model 1 for all pHs while Model 2 (results for k6b fitting are presented in Figure A-5-1) and 3 overestimated the impact of increasing the pH on $HOCl/ClO_2^-$ reaction with higher predicted concentrations of ClO_2^- compared to the experimental data (Figure 5-2).

Therefore, Model 1 was modified to build a conceptual kinetic model allowing to predict the behaviour of the different chlorine species and provide better mechanistic understanding of the $HOCl/ClO_2^-$ system.

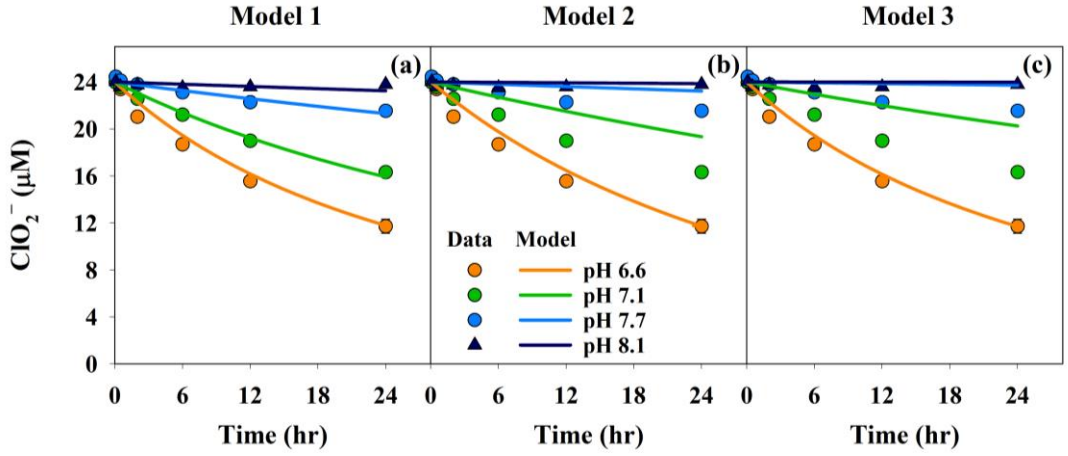

Figure 5-2. Oxidation of ClO_2^- overtime (circles) compared to the modified models (lines). Fitted constants were k1 for Model 1, k6a for Model 2, k9 for Model 3 and are shown in Table A-5-4. $[ClO_2^-]i$ = 23.7 µM, [HOCl]i = 65 µM, pH 6.6–8.1 (10 mM phosphate). Error bars represent duplicated experiments.

To further improve the conceptual model, the formation of ClO_3^- after 24 h was followed at pH 6.6–8.1 and k3 and k5/k4 were modified to fit the experimental data. As shown in Figure 5-3a (dashed red line) the concentration of ClO_3^- was overestimated by the updated model. Decreasing k3, decreased the modeled ClO_3^- but also increased the residual ClO_2^-. Therefore, k1 was slightly modified in parallel with k3 to fit ClO_2^- residual at pH 6.6 and the resulting model was compared with the ClO_2^- and ClO_3^- experimental data. Figure 5-3 shows the experimental and modeled data for ClO_3^- and ClO_2^- at different k1 and k3 combinations and different pHs after 24 h contact time. The best fit for ClO_2^- and ClO_3^- was found for k1 = 2.25 x 10^5 M^{-2} s^{-1} and k3 = 1.43 x 10^3 M^{-2} s^{-1} (dotted blue line).

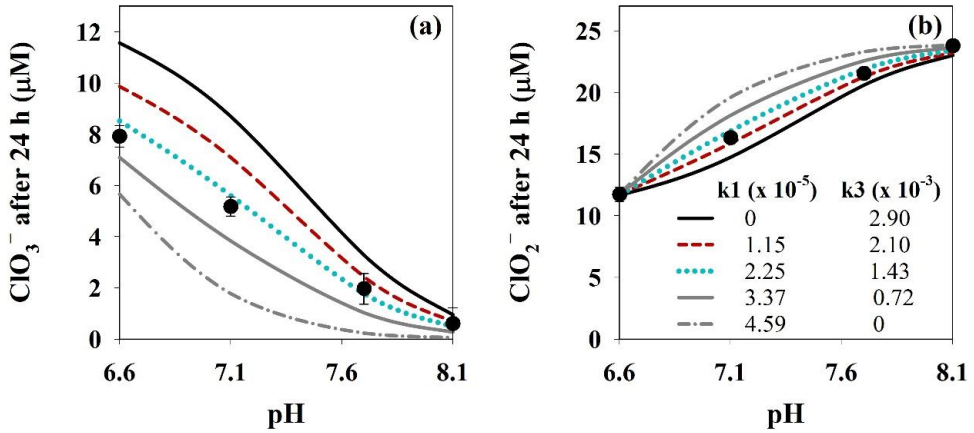

Figure 5-3. Fitting of k1 and k3 based on ClO_3^- formation after 24 h (a) and comparison with the ClO_2^- residual after 24 h (b). The dashed red line represents the model fitted in Figure 5-2a while the dotted blue line represents the selected model. Circles represent the duplicated experimental data. $[ClO_2^-]i$ = 23.7 µM, [HOCl]i = 65 µM, pH 6.6–8.1 (10 mM phosphate).

Finally, the impact of different k5/k4 ratios on the 24 h ClO_3^- formation was tested (Figure A-5-2). The k5/k4 ratio was varied between 0 (all ClO_3^- formed by eq 5-3) and 1.85 M x 10^{-5} M (provided in the original model, Table 5-1). The k5/k4 ratios was not affecting the ClO_3^- formation for pH ≥ 7.7, but did have an impact at pH 6.6–7.1 (Figure A-5-2). A k5/k4 ratio of 1.23 x 10^{-5} M was found to accurately fit the ClO_3^- data.

The finalized conceptual model, is shown in Table 5-2 (eq 5-1' to eq 5-5') and was used to predict the concentration of ClO_2^-, HOCl, ClO_3^- and ClO_2 between pH 6.6–8.1 (Figure 5-4). A good fit to the experimental data was obtained for ClO_2^-, HOCl and ClO_3^- while a significantly lower ClO_2 was measured at pH 6.6 compared to the model.

Table 5-2. Fitted HOCl/ClO_2^- reaction model.

	Equations	Rate constants
Fitted model		
eq 5-1'	$ClO_2^- + HOCl + H_3O^+ \rightarrow Cl_2O_2 + 2H_2O$	k1' = 2.25 x 10^5 M^{-2} s^{-1}
eq 5-2	$ClO_2^- + Cl_2 \rightarrow Cl_2O_2 + Cl^-$	k2 = 4.07 x 10^4 M^{-1} s^{-1}
eq 5-3'	$ClO_2^- + 2HOCl \rightarrow ClO_3^- + Cl_2 + H_2O$	k3' = 1.43 x 10^3 M^{-2} s^{-1}
eq 5-4	$ClO_2^- + Cl_2O_2 \rightarrow 2ClO_2 + Cl^-$	k4 = 1 x 10^{10} M^{-1} s^{-1}
eq 5-5'	$Cl_2O_2 + H_2O \rightarrow ClO_3^- + Cl^- + 2H_3O^+$	k5'/k4 = 1.23 x 10^{-5} M
eq 5-10	NOMfast + $HOCl/OCl^- \rightarrow$ Products	$k_{NOMfast}$ = 1.2 x 10^1 M^{-1} s^{-1}
eq 5-11	NOMslow + $HOCl/OCl^- \rightarrow$ Products	$k_{NOMslow}$ = 4.0 x 10^{-1} M^{-1} s^{-1}
eq 5-12	$2ClO_2$ + NOMslow $\rightarrow$ ClO_2^- + HOCl + NOMox	k12 = 1 x 10^9 M^{-2} s^{-1}

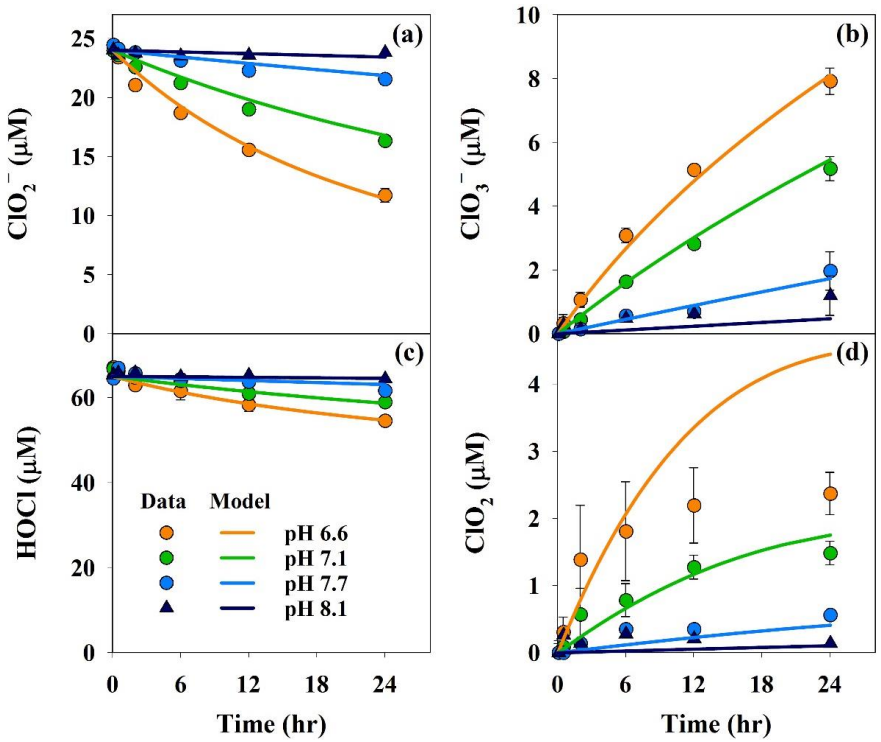

Figure 5-4. Comparison between the final conceptual model (lines) and experimental data (circles) for the oxidation of ClO_2^- (a), the reduction of HOCl (c) and the formation of ClO_3^- (b) and ClO_2 (d). The equations and contants are given in Table 5-2. [ClO_2^-]i = 23.7 μM, [HOCl]i = 65 μM, pH 6.6–8.1 (10 mM phosphate). Error bars represent duplicated experiments.

5.4.2 HOCl/ClO_2^- reaction in synthetic water

5.4.2.1 HOCl/NOM reaction

The HOCl decay in 3 mgC L^{-1} UMRNOM and in absence of ClO_2^- was modeled using a fast and a slow reacting fractions of NOM, similarly to previous studies (eq 5-10 and eq 5-11, Table 5-2).[29, 30] The sum of the fast and slow reacting fractions was based on the aromatic carbon concentration of the NOM calculated from the ^{13}C NMR carbon distribution of UMRNOM as 15.8 µM mgC^{-1} of aromatic carbons.[31] The 3 mgC L^{-1} of UMRNOM used for the HOCl/NOM fitting would therefore contain 48 µM of aromatic carbons.

The fast reacting fraction (NOMfast) was initially defined as the fraction reacting in the first 2 h (about 20 µM, 42% of the aromatic carbon for UMRNOM), and the HOCl/NOMfast rate constant ($k_{NOMfast}$) was adjusted to fit the decay of HOCl between 0 and 2 h (Figure 5-5a, black squares). The remaining aromatic carbon accounted for the slow reacting fraction (NOMslow, 28 µM, 58% of the aromatic carbon for UMRNOM) and the HOCl/NOMslow rate constant ($k_{NOMslow}$) was adjusted to fit the HOCl decay between 6–24 h, where the NOMfast fraction was exhausted. Once $k_{NOMfast}$ and $k_{NOMslow}$ were determined the NOMfast and NOMslow fractions were slightly refined to further improve the fitting and set to 37 and 63%, respectively. These fractions were consistent with the fractions used by Qualls and Johnson to model the short-term HOCl/NOM reaction.[29] The rate constants were 12 and 0.4 M^{-1} s^{-1} for $k_{NOMfast}$ and $k_{NOMslow}$, respectively (eq 5-10 and eq 5-11, Table 5-2) and the resulting fitting of HOCl/NOM reaction is shown in Figure 5-5a (black line). As the HOCl/UMRNOM reaction was found to be independent of pH (6.6–8.1, Figure A-5-3), the model was not accounting for the HOCl/OCl^- speciation. The reaction of HOCl with NLFA was modelled using the same fractions and rate constants of NOMfast and NOMslow, and an aromatic carbon concentration of 25.8 µM mgC^{-1} estimated from NLFA ^{13}C NMR carbon distribution.[31]

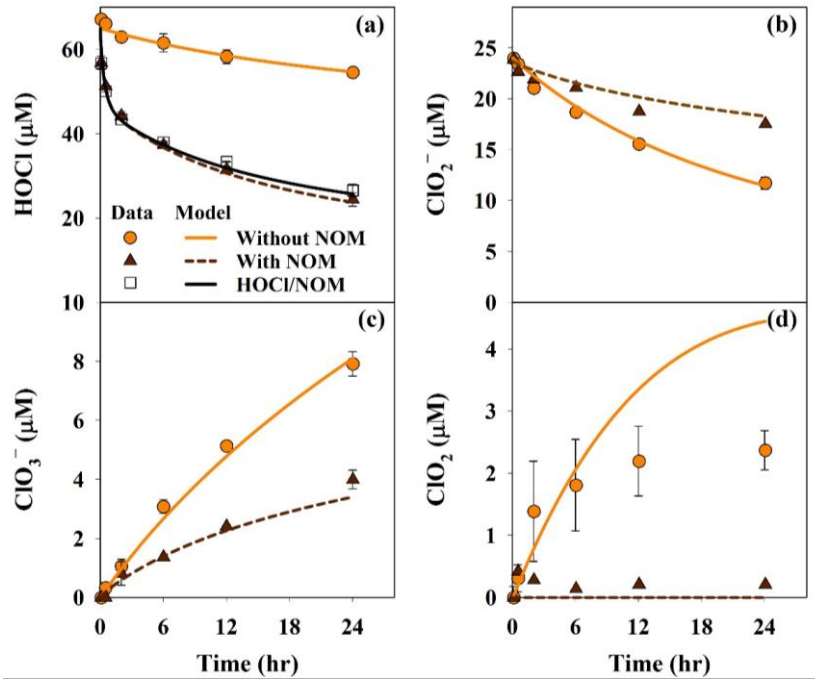

Figure 5-5. Impact of NOM on HOCl (a) and ClO_2^- (b) decrease as well as ClO_3^- (c) and ClO_2 (d) formation. The equations and contants are given in Table 5-2. [ClO_2^-]i = 23.7 μM, [HOCl]i = 65 μM, [UMRNOM] = 3 mgC L^{-1}, pH 6.6 (10 mM phosphate).

5.4.2.2 Impact of NOM on HOCl/ClO_2^- kinetic

The HOCl/ClO_2^- reaction was compared with and without 3 mgC L^{-1} of UMRNOM at pH 6.6 (Figure 5-5). In presence of NOM, ClO_2^- decreased from 23.7 μM to 17.5 μM after 24 h compared to 11.7 μM in absence of NOM (Figure 5-5b). This was due to the fast consumption of HOCl by NOM, reducing the exposure of ClO_2^- to HOCl. Consequently, ClO_3^- formation was mitigated, from 7.9 μM to 4.0 μM after 24 h (Figure 5-5c). In presence of NOM, ClO_2 was not detected as a result of its fast reaction with activated aromatic compounds which are major constituents of the NOM (Figure 5-5d).[32] The reaction of NOM and ClO_2 was previously shown to produce ClO_2^- and HOCl, the latter representing a maximum of 50% of the consumed ClO_2, as demonstrated by the reaction of ClO_2 with phenol.[33] Activated aromatics such as phenol are among the most reactive moieties toward ClO_2 while they are much less reactive with HOCl (for the reaction with phenol, $kClO_2/kHOCl > 2 \times 10^3$ at pH 6.6–8.1).[34, 35] Therefore eq 5-12 was added to the model:

$$2ClO_2 + NOMslow \rightarrow ClO_2^- + HOCl + NOMox \qquad \text{eq 5-12}$$

Since ClO_2 was gradually produced over the 24 h of our experiments (Figure 5-4), NOMslow fraction was used in eq 5-12. The rate constant ($k12 = 1 \times 10^9$ M^{-2} s^{-1}) was

set sufficiently high to prevent ClO_2 accumulation in the model (Figure A-5-4a). The slight impact of ClO_2 reaction with NOM on ClO_3^-, HOCl and ClO_2^- is also shown in Figure A-5-4 and was agreeing with the experimental data. The consumption of NOMslow by reaction with ClO_2 in the model was negligible and had little effect on the HOCl/NOMslow reaction. As shown in Figure 5-5b,c, the conceptual model accurately predicted ClO_2^- mitigation and ClO_3^- formation in presence of NOM.

5.4.2.3 Prediction of HOCl/ClO_2^- reaction

In order to validate the accuracy of the model under different experimental conditions, the 24 h decay of ClO_2^- and HOCl as well as the formation of ClO_3^- were measured at different concentrations of UMRNOM (1, 3 and 5 mgC L^{-1}) and NLFA (3 mgC L^{-1}), at pH 6.6 or 7.1 and with an initial HOCl dose of 40 or 65 µM. The concentrations of HOCl, ClO_2^- and ClO_3^- after 24 h were in good agreement with the predicted values (Figure 5-6).

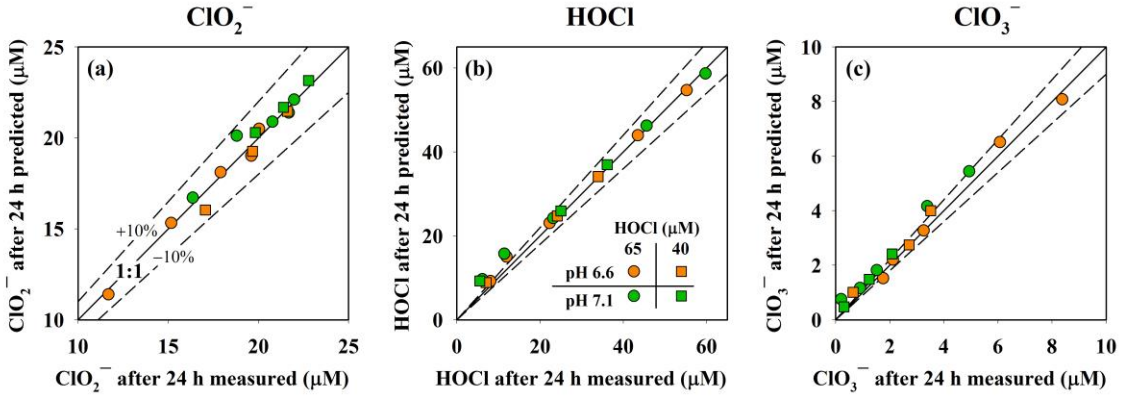

Figure 5-6. Predicted versus measured ClO_2^- (a), HOCl (b) and ClO_3^- (c) after 24 h. $[ClO_2^-]i$ = 23.7 µM, [HOCl]i = 40–65 µM, [UMRNOM] = 1–5 mgC L^{-1}, [NLFA] = 3 mgC L^{-1}, pH 6.6–7.1 (10 mM phosphate).

The ClO_2^- predicted values were within ± 10% of the measured values. Furthermore, 66–69% of the ClO_2^- was recovered as ClO_3^- for both measured and model results (Figure A-5-5), which supported the hypothesis that ClO_2^- was partially regenerating ClO_2, a fraction of which was reduced to HOCl (eq 5-12).

For waters where the aromatic carbon content is not available, the initial and final HOCl doses may be used to estimate an average HOCl dose. The average HOCl was calculated from the 24 h HOCl CT ([HOCl]average = CT/24, Figure A-5-6a). The HOCl/NOM model was used to correlate the average HOCl concentration and the HOCl demand over 24 h (Figure A-5-6b). For different initial HOCl doses (40–

100 μM) and aromatic carbon concentrations (15–120 μM) the following correlation was found (Figure A-5-6b):

$$[\mathrm{HOCl}]_{\mathrm{average}} = [\mathrm{HOCl}]_{\mathrm{initial}} - 0.85 \times ([\mathrm{HOCl}]_{\mathrm{initial}} - [\mathrm{HOCl}]_{\mathrm{final}}) \qquad \text{eq 5-13}$$

The predicted ClO_2^- and ClO_3^-, when using the model with a fixed average HOCl concentration, were also in good agreement with the measured data (Figure A-5-7).

5.4.3 ClO_2 pre-oxidation of real waters

5.4.3.1 ClO_2^- formation from ClO_2

ClO_2 doses ≥ 1 mg L^{-1} were applied to 3 groundwaters (P120, P130, W20) until full consumption of ClO_2, followed by 24 h chlorination (water characteristics are given in Table A-5-1). ClO_2 pre-oxidation produced 60–65% of ClO_2^- and no ClO_3^- in P120 and P130, consistently with typical ClO_2^- yields (bars, Figure 5-7).[5, 36] In W20, only 14–38% of the ClO_2 was recovered as ClO_2^- (red bars, Figure 5-7). It has been shown that a significant part of the ClO_2 can form HOCl during reactions with NOM, which may subsequently be reduced to Cl^- or incorporated as AOCl (not measured) and leading to ClO_2^- yields < 80%.[33] Reaction between ClO_2^- and the matrix may also occur, in particular, inorganics such as iron or sulfur species can reduce ClO_2^- to Cl^-.[37, 38] While the reduction of ClO_2^- to Cl^- was probably not significant in P120 and P130, the low ClO_2^- yields in W20 suggest that a large fraction of the ClO_2^- was reacting with the matrix. This was confirmed by the constant difference between the measured and estimated ClO_2^- (assuming a 65% yield, similarly to P120 and P130) accounting for 8–9 μM for all ClO_2 doses (1–2 mg L^{-1}). Therefore, 8–9 μM of ClO_2^- may have been consumed by the matrix in W20.

5.4.3.2 ClO_2^- decrease during chlorination.

After ClO_2 pre-oxidation, the ClO_2^- levels were above the WHO guideline (0.7 mg L^{-1}), i.e. 0.76–0.95 mg L^{-1} for 1.25 and 1.5 mg L^{-1} of ClO_2 in P120 and P130 (bars, Figure 5-7). In W20, the ClO_2^- was above regulation only for the highest ClO_2 dose (0.75 mg L^{-1} of ClO_2^-). After chlorination, ClO_2^- levels were decreased below 0.7 mg L^{-1} in all samples (diamonds, Figure 5-7). In comparison to the measured data, the predicted final ClO_2^- concentration was systematically overestimated by the model, suggesting that the HOCl/ClO_2^- reaction was faster in real water compared to synthetic water (circles, Figure 5-7). Acids such as $H_2PO_4^-$ or acetic acid were

previously shown to catalyze the HOCl/ClO_2^- reaction.[13] Similarly, the presence of bicarbonate in real waters may also catalyze the reaction and explain the faster reaction observed. For a dose of 1.5 mg L^{-1} of ClO_2, it was predicted by the model that the final ClO_2^- would be beyond the guideline value in P120 and P130 (10.9–11.8 µM, 0.74–0.80 mg L^{-1}, circles in Figure 5-7). However, the faster HOCl/ClO_2^- reaction decreased the ClO_2^- levels well below the guideline in those waters, i.e. 5.5 and 5.7 µM (0.37 and 0.38 mg L^{-1}) for P120 and P130, respectively (diamonds in Figure 5-7).

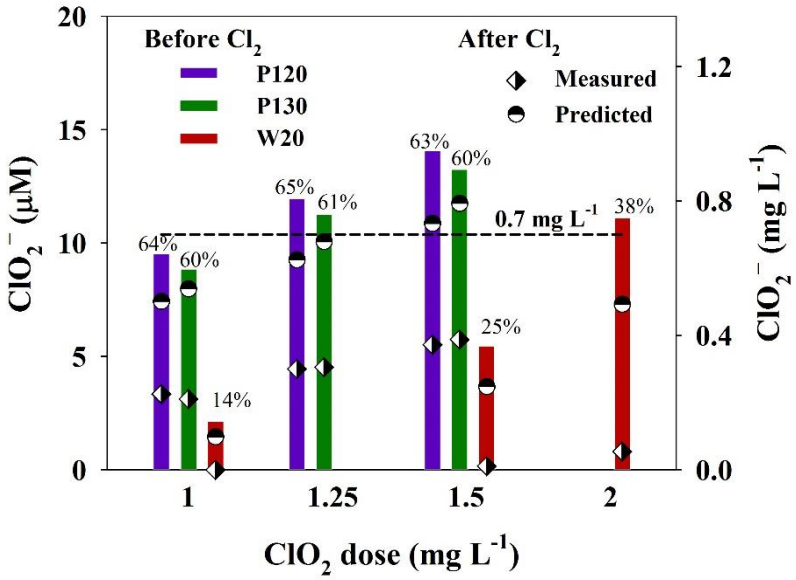

Figure 5-7. Formation of ClO_2^- after ClO_2 pre-oxidation of real waters (bars) and measured (diamonds) and predicted (circles) ClO_2^- residual after chlorination at different ClO_2 doses. The percentages represent the yield of ClO_2^- compared to the ClO_2 dose. [ClO_2] = 15–30 µM (1–2 mg L^{-1}), [HOCl] = 52–124 µM (3.7–8.8 mgCl_2 L^{-1}), 24 h reaction time, characteristics of the real water samples are given in Table A-5-1.

Consequently to the ClO_2^- decrease, ClO_3^- was formed in all samples. Similarly, to the experiments in synthetic waters, the measured ClO_3^- accounted for 70% of the oxidized ClO_2^- (Figure A-5-8). Although the reaction rate was underestimated in real waters, the predicted yield of ClO_3^- was also representing 70% of the oxidized ClO_2^- (Figure A-5-8). These results further support that part of the *in situ* generated ClO_2 from the HOCl/ClO_2^- reaction was not reduced to ClO_2^- but was producing HOCl. Furthermore, the partial oxidation of ClO_2^- to ClO_3^- indicates that the sum of oxychloro species (ClO_2^- + ClO_3^-) was decreasing during chlorination, which can be of interest if ClO_3^- becomes regulated.

5.4.3.3 DBP formation

AOX, THMs and HANs were analyzed after chlorination (Figure 5-8). The DOC of the real waters was ranging from 6.8 mgC L^{-1} (W20) > 4.2 mgC L^{-1} (P130) > 3 mgC L^{-1} (P120) (Table A-5-1). Without pre-oxidation (0 mg L^{-1} ClO_2), the levels of DBPs were increasing with increasing carbon concentration. Chlorination of W20, P130 and P120 produced 29.7, 11.6 and 8.5 µM of AOX, respectively (Figure 5-8a). THMs and HANs followed the same order with 1.77, 0.84 and 0.44 µM of THMs and 186, 99 and 58 nM of HANs produced in W20, P130 and P120, respectively (Figure 5-8b,c).

All three waters contained significant levels of bromide (190–260 µg L^{-1}, Table A-5-1). Without pre-oxidation, most of the bromide was incorporated in the NOM with 81, 84 and 89% of the bromide recovered as AOBr in P120, P130 and W20, respectively (Figure 5-8a). For the THMs and HANs, the formation of brominated DBPs was affected by the bromide to DOC ratio.[39, 40] For W20, which had a low Br^-/DOC ratio (219 µgBr^- L^{-1}versus 6.8 mgC L^{-1}), TCM and the sum of TCAN and DCAN represented 70% and 81% of the THMs and HANs, respectively (Figure 5-8b,c). By comparison, P120 and P130 had a higher Br^-/DOC ratio (190 and 260 µgBr^- L^{-1} versus 3 and 4.2 mgC L^{-1}, respectively), which led to the formation of higher levels of brominated DBPs (Figure 5-8b,c).

A pre-oxidation treatment of 1 mg L^{-1} of ClO_2 decreased the AOX formation by 28%, 21% and 11% in P120, P130 and W20, respectively (Figure 5-8a). The THM formation was decreased by 11% in P120 and by ≤ 2% in P130 and W20 (Figure 5-8b). The HAN formation was reduced by 73%, 71% and 50% in P120, P130 and W20, respectively (Figure 5-8c).

Using ClO_2 doses higher than 1 mg L^{-1} improved the AOX mitigation in P120 and W20 with up to 35% and 17% reduction, respectively (Figure 5-8a). However, no significant improvement was observed in P130. The THM mitigation was significantly improved in P120 and P130 with up to 37% and 21% reduction, respectively, while the mitigation was negligible in W20, even at 2 mg L^{-1} (3%) (Figure 5-8b). Finally, increasing the ClO_2 dose improved the HAN mitigation up to 81%, 75% and 79%, in P120, P130 and W20, respectively (Figure 5-8c).

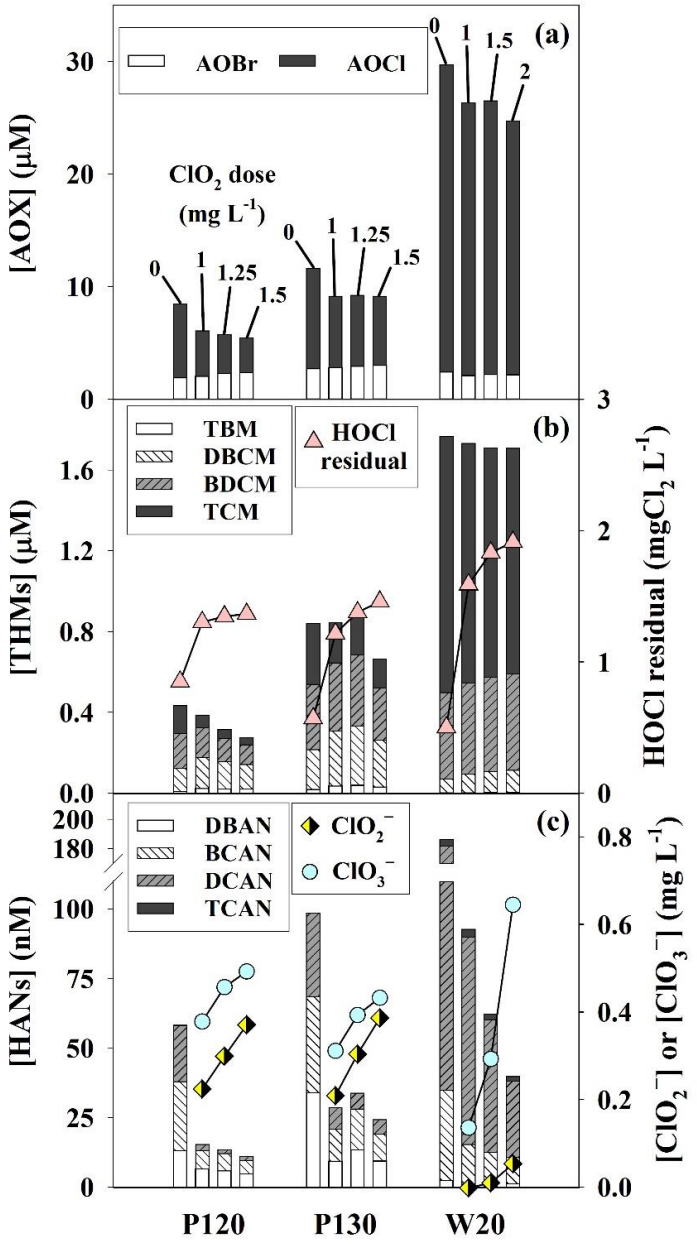

Figure 5-8. AOX (a), THMs (b) and HANs (c) formed after chlorination of real waters with or without ClO_2 pre-oxidation. The HOCl demand (triangle) as well as ClO_2^- (circles) and ClO_3^- (diamonds) after chlorination are also shown. [ClO_2] = 15–30 μM (1–2 mg L^{-1}), [HOCl] = 52–124 μM (3.7–8.8 mgCl_2 L^{-1}), 24 h reaction time, characteristic of the real water samples are given in Table A-5-1.

It was previously shown that pre-oxidation was less efficient on brominated DBPs (Br-DBPs), and can enhance their formation (c.f Chapter 6).[4, 41] The AOBr was enhanced by ClO_2 in P120 and P130 but was mitigated in W20 (Figure 5-8a). The sum of Br-THM formation (TBM + DBCM + DCBM) was enhanced in W20 from 0.50 μM without pre-oxidation to 0.59 μM after 2 mg L^{-1} ClO_2 pre-oxidation (Figure 5-8b). In P130, Br-THM formation was also enhanced from 0.54 μM without pre-oxidation to 0.69 μM after 1.25 mg L^{-1} ClO_2 pre-oxidation. However the Br-THM formation was

reduced to 0.52 µM after 1.25 mg L^{-1} ClO_2 pre-oxidation (although the TBM and DBCM were still enhanced compared to no pre-oxidation) (Figure 5-8b). A similar effect was observed after pre-oxidation of P120, which enhanced the formation of Br-THMs after 1 mg L^{-1} of ClO_2 while mitigating them at higher ClO_2 doses (Figure 5-8b). Again, the most brominated THMs (TBM and DBCM) remained higher than in absence of pre-oxidation.

Finally, the Br-HAN formation was efficiently mitigated, and increasing the ClO_2 dose improved their mitigation (Figure 5-8c). Up to 74, 72 and 69% of the Br-HANs were mitigated in P120, P130 and W20, respectively.

5.4.4 Practical implications

ClO_2 pre-oxidation dose is limited by the formation of the regulated ClO_2^-. However, during disinfection, significant amounts of ClO_2^- can be oxidized to ClO_2 or to ClO_3^-. The HOCl/ClO_2^- reaction could be modeled to accurately predict ClO_2^- residuals for different synthetic waters and HOCl doses. In real waters, the HOCl/ClO_2^- reaction was found to be catalyzed, leading to greater decreases of ClO_2^- concentration than predicted. This resulted in ClO_2^- concentrations below the 0.7 mg L^{-1} guideline for all tested ClO_2 doses (1–2 mg L^{-1}). In real conditions, the contact time between HOCl and ClO_2^- before reaching the tap of the customer may be much lower than the 24 h used in the present study. However, knowing the pH of the water and the chlorine demand, the ClO_2^- abatement, could be predicted by the model and the water deliver safely. Furthermore, pre-treatment with ClO_2 was significantly increasing the chlorine residual (Figure 5-8b). Therefore, in practice, the chlorine dose could be reduced and the DBP formation further mitigated. The lower exposure of ClO_2^- to chlorine, would need to be taken into account, and be predicted by the model.

Concurrently to the decrease of ClO_2^-, ClO_3^- was formed, which is also considered for regulation. In this case, a trade-off between ClO_3^- formation, ClO_2^- residual and DBP mitigation would need to be found (Figure 5-8c). As ~ 70% of the ClO_2^- was oxidized to ClO_3^- in synthetic and real waters (Figure A-5-5 and A-5-8), the sum of oxychloro species ($ClO_2^- + ClO_3^-$) was reduced during chlorination. The molar sum of oxychloro species was decreased by about 19% during chlorination (Figure A-5-9).

By increasing the ClO_2 dose beyond 1 mg L^{-1}, significant improvements in DBP mitigation were obtained. The regulated THMs were hardly reduced in a highly reactive water (DOC = 6.8 mgC L^{-1}, SUVA = 3.5 L mgC^{-1} m^{-1}) but were readily mitigated in a low reactive water (DOC = 3 mgC L^{-1}, SUVA = 2.3 L mgC^{-1} m^{-1}) and increased doses of ClO_2 could reduce THM formation in an intermediate water (DOC = 4.2 mgC L^{-1}, SUVA = 2.5 L mgC^{-1} m^{-1}). Furthermore, the presence of bromide can be problematic as brominated THMs may be enhanced by ClO_2 pretreatment. However, in waters with lower reactivity, increasing the ClO_2 dose can be sufficient to prevent any significant increase in Br-DBPs and efficiently mitigate the Cl-DBPs. Therefore, both the Br^-/DOC and ClO_2/DOC ratios have to be considered. Nevertheless, ClO_2 pre-oxidation is a very efficient strategy to mitigate both chlorinated and brominated HANs (50–81% reduction), which are more significant than the THMs in terms of DBP-induced toxicity (c.f Chapter 6).

5.5 References

1. Rook, J. J., Chlorination reactions of fulvic acids in natural waters. *Environ. Sci. Technol.* **1977,** *11*, (5), 478-482.
2. Richardson, S. D.; Plewa, M. J.; Wagner, E. D.; Schoeny, R.; DeMarini, D. M., Occurrence, genotoxicity, and carcinogenicity of regulated and emerging disinfection by-products in drinking water: A review and roadmap for research. *Mutat. Res-Rev. Mutat.* **2007,** *636*, (1–3), 178-242.
3. Sedlak, D. L.; von Gunten, U., The Chlorine Dilemma. *Science* **2011,** *331*, (6013), 42-43.
4. Yang, X.; Guo, W.; Lee, W., Formation of disinfection byproducts upon chlorine dioxide preoxidation followed by chlorination or chloramination of natural organic matter. *Chemosphere* **2013,** *91*, (11), 1477-1485.
5. Werdehoff, K. S.; Singer, P. C., Chlorine Dioxide Effects on THMFP, TOXFP, and the Formation of Inorganic By-products. *J. Am. Water Works Ass.* **1987,** *79*, (9), 107-113.
6. Holden, G. W., Chlorine Dioxide Preoxidation for DBP Reduction. *J Am Water Works Assoc* **2017,** *109*, (7), 36-43.
7. USEPA, Disinfectants and Disinfection Byproducts final rule. In Federal Register: 1998; Vol. 63, pp 69390-69476.
8. WHO, Guidelines for Drinking-Water Quality. In 4th ed.; WHO, Ed. Geneva, 2017.
9. Commission, E., Proposal for a directive of the european parliament and of the council on the quality of water intended for human consumption. In *2017/0332*, Brussels, 2017.
10. Sorlini, S.; Collivignarelli, C., Chlorite removal with ferrous ions. *Desalination* **2005,** *176*, (1–3), 267-271.
11. Sorlini, S.; Collivignarelli, C., Chlorite removal with granular activated carbon. *Desalination* **2005,** *176*, (1), 255-265.
12. Peintler, G.; Nagypal, I.; Epstein, I. R., Systematic design of chemical oscillators. 60. Kinetics and mechanism of the reaction between chlorite ion and hypochlorous acid. *J. Phys. Chem.***1990,** *94*, (7), 2954-2958.
13. Jia, Z.; Margerum, D. W.; Francisco, J. S., General-Acid-Catalyzed Reactions of Hypochlorous Acid and Acetyl Hypochlorite with Chlorite Ion. *Inorg. Chem.* **2000,** *39*, (12), 2614-2620.
14. Junli, H.; Li, W.; Nenqi, R.; Li, L. X.; Fun, S. R.; Guanle, Y., Disinfection effect of chlorine dioxide on viruses, algae and animal planktons in water. *Water Res.* **1997,** *31*, (3), 455-460.
15. Aieta, E. M.; Roberts, P. V., Kinetics of the reaction between molecular chlorine and chlorite in aqueous solution. *Environ. Sci. Technol.* **1986,** *20*, (1), 50-55.
16. Emmenegger, F.; Gordon, G., The rapid interaction between sodium chlorite and dissolved chlorine. *Inorg. Chem.* **1967,** *6*, (3), 633-635.
17. Gordon, G.; Tachiyashiki, S., Kinetics and mechanism of formation of chlorate ion from the hypochlorous acid/chlorite ion reaction at pH 6-10. *Environ. Sci. Technol.* **1991,** *25*, (3), 468-474.
18. Singer, P. C.; O'Neil, W. K., Technical Note: The Formation of Chlorate From the Reaction of Chlorine and Chlorite in Dilute Aqueous Solution. *J. Am. Water Works Ass.* **1987,** *79*, (11), 75-76.
19. Karpel Vel Leitner, N.; De Laat, J.; Doré, M.; Suty, H., The Use of ClO_2 in Drinking Water Treatment: Formation and Control of Inorganic By-Products (ClO_2^-,

ClO_3^-). In *Disinfection by-Products in Water Treatment: The Chemistry of their Formation and Control*, Roger, A. M.; Amy, G. L., Eds. CRC Press: 1996; pp 393-407.
20. Furman, C. S.; Margerum, D. W., Mechanism of Chlorine Dioxide and Chlorate Ion Formation from the Reaction of Hypobromous Acid and Chlorite Ion. *Inorg. Chem.* **1998,** *37*, (17), 4321-4327.
21. Granstrom, M. L.; Lee, G. F., Generation and Use of Chlorine Dioxide in Water Treatment. *J. Am. Water Works Ass.* **1958,** *50*, (11), 1453-1466.
22. Gates, D. J., *The Chlorine Dioxide Handbook*. American Water Works Association: 1998.
23. Pinkernell, U.; Nowack, B.; Gallard, H.; Von Gunten, U., Methods for the photometric determination of reactive bromine and chlorine species with ABTS. *Water Res.* **2000,** *34*, (18), 4343-4350.
24. USEPA, Method 326.0: Determination of Inorganic Oxyhalide Disinfection By-Products in Drinking Water Using Ion Chromatography Incorporating the Addition of a Suppressor Acidified Postcolumn Reagent for Trace Bromate Analysis. In 2002.
25. Allard, S.; Charrois, J. W. A.; Joll, C. A.; Heitz, A., Simultaneous analysis of 10 trihalomethanes at nanogram per liter levels in water using solid-phase microextraction and gas chromatography mass-spectrometry. *J. Chromatogr. A* **2012,** *1238*, 15-21.
26. Kristiana, I.; Joll, C.; Heitz, A., Analysis of halonitriles in drinking water using solid-phase microextraction and gas chromatography–mass spectrometry. *J. Chromatogr. A* **2012,** *1225*, 45-54.
27. Langsa, M.; Allard, S.; Kristiana, I.; Heitz, A.; Joll, C. A., Halogen-specific total organic halogen analysis: Assessment by recovery of total bromine. *J. Environ. Sci.* **2017,** *58*, 340-348.
28. Wang, L.; Margerum, D. W., Hypohalite Ion Catalysis of the Disproportionation of Chlorine Dioxide. *Inorg. Chem.* **2002,** *41*, (23), 6099-6105.
29. Qualls, R. G.; Johnson, J. D., Kinetics of the short-term consumption of chlorine by fulvic acid. *Environ. Sci. Technol.* **1983,** *17*, (11), 692-698.
30. Zhai, H.; Zhang, X.; Zhu, X.; Liu, J.; Ji, M., Formation of Brominated Disinfection Byproducts during Chloramination of Drinking Water: New Polar Species and Overall Kinetics. *Environ. Sci. Technol.* **2014,** *48*, (5), 2579-2588.
31. I.H.S.S http://humic-substances.org (September 2018),
32. Leenheer, J. A.; Croué, J. P., Characterizing aquatic dissolved organic matter. *Environ. Sci. Technol.* **2003,** *37*, (1), 18A-26A.
33. Rougé, V.; Allard, S.; Croué, J.-P.; von Gunten, U., In Situ Formation of Free Chlorine During ClO_2 Treatment: Implications on the Formation of Disinfection Byproducts. *Environ. Sci. Technol.* **2018,** *52*, (22), 13421-13429.
34. Hoigné, J.; Bader, H., Kinetics of reactions of chlorine dioxide (OClO) in water-I. Rate constants for inorganic and organic compounds. *Water Res.* **1994,** *28*, (1), 45-55.
35. Deborde, M.; von Gunten, U., Reactions of chlorine with inorganic and organic compounds during water treatment–Kinetics and mechanisms: A critical review. *Water Res.* **2008,** *42*, (1–2), 13-51.
36. Korn, C.; Andrews, R. C.; Escobar, M. D., Development of chlorine dioxide-related by-product models for drinking water treatment. *Water Res.* **2002,** *36*, (1), 330-342.

37. Ison, A.; Odeh, I. N.; Margerum, D. W., Kinetics and Mechanisms of Chlorine Dioxide and Chlorite Oxidations of Cysteine and Glutathione. *Inorg. Chem.* **2006,** *45*, (21), 8768-8775.
38. Aieta, E. M.; Berg, J. D., A Review of Chlorine Dioxide in Drinking Water Treatment. *J. Am. Water Works Ass.* **1986,** *78*, (6), 62-72.
39. Allard, S.; Tan, J.; Joll, C. A.; von Gunten, U., Mechanistic Study on the Formation of Cl-/Br-/I-Trihalomethanes during Chlorination/Chloramination Combined with a Theoretical Cytotoxicity Evaluation. *Environ. Sci. Technol.* **2015,** *49*, (18), 11105-11114.
40. Ersan, M. S.; Liu, C.; Amy, G.; Karanfil, T., The interplay between natural organic matter and bromide on bromine substitution. *Sci. Total Environ.* **2019,** *646*, 1172-1181.
41. Hua, G.; Reckhow, D. A., Effect of pre-ozonation on the formation and speciation of DBPs. *Water Res.* **2013,** *47*, (13), 4322-4330.

Every reasonable effort has been made to acknowledge the owners of copyright material. I would be pleased to hear from any copyright owner who has been omitted or incorrectly acknowledged.

Chapter 6. Comparison of the Impact of Ozone, Chlorine Dioxide, Ferrate and Permanganate Pre-oxidation on Disinfection Byproduct Formation during Chlorination

The content of Chapter 6 and Appendix 6 is unable to be reproduced here as they are under embargo due to current consideration for publication in the journal *Water Research*, with the following contributing co-authors: Sébastien Allard, Jean-Philippe Croué and Urs von Gunten.

I, Valentin Rougé, as the primary author, conducted all the experimental work and data analysis, including creating figures and tables, and writing and editing the manuscript.

I, as a Co-Author, endorsed that this level of contribution by the candidate indicated above is appropriate.

Sébastien Allard

Jean-Philippe Croué

Urs von Gunten

6.1 Abstract

Pre-oxidation can be used to reduce the formation of disinfection byproducts during disinfection. A comparative study of the impact of four pre-oxidants, ozone (O_3), chlorine dioxide (ClO_2), permanganate (Mn(VII)) and ferrate (Fe(VI)), on the formation of adsordable organic halogens (AOX), trihalomethanes (THMs) and haloacetonitriles (HANs) in chlorinated synthetic and real waters was conducted. To compare the efficiency of the four oxidants on DBPs mitigation, the pre-oxidant doses were based on their impact on NOM reactivity measured by the electron donating capacity before chlorination. The influence of pH (6.5–8.1) and the presence of bromide (0–500 µg L^{-1}) on the efficiency of the different pre-oxidation strategies was evaluated and a theoretical toxicity assessment was performed based on the formation of THMs and HANs.

All oxidants were found to be efficient in mitigating the formation of AOX and HANs. A significant abatement of THMs was observed for O_3, ClO_2 and Fe(VI) but not for Mn(VII). O_3 was generally more efficient than the other oxidants to decrease the formation of AOX and THMs but all the pre-oxidants were readily reducing the formation of HANs (> 45% reduction at high dose). Decreasing the pH enhanced the efficiency of O_3 on AOX reduction (from 43 to 64%) and THM reduction (from 31 to 52%), the efficiency of Fe(VI) on AOX reduction (from < 2% to 15%) while diminishing the efficiency of Mn(VII) pre-oxidation on the reduction of all DBPs. In presence of bromide, pre-oxidation was mitigating the brominated DBPs less efficiently than the chlorinated DBPs which was illustrated by an increase in bromine substitution factor for all pre-oxidants and all DBPs. The formation of di- and tribrominated DBPs were often enhanced especially with O_3.

Although HANs were formed at low concentration compared to the THMs, they were driving the calculated toxicity, particularly the brominated HANs. The increase of dibromochloroacetonitrile after pre-oxidation was a major factor counteracting the benefit of the overall DBPs mitigation. The doses of ClO_2 and O_3 leading to a good trade-off between chlorinated DBP mitigation and brominated DBP enhancement were 15 µM (medium dose) and 2.2 µM (low dose), respectively. No consistent trend was observed for Fe(VI) and Mn(VII). In comparison to the other oxidants, the use of a practical dose of ClO_2 (15 µM, 1 mg L^{-1}) was a consistently good option for the mitigation of HANs and for the estimated toxicity in the different conditions tested.

6.2 Introduction

Chlorine is the most widely used disinfectant for drinking water treatment. However, the formation of disinfection byproducts (DBPs) has been an on-going issue.[1-3] Pre-oxidation has been successfully used to reduce the formation of DBPs during chlorination.[4-6] Potential pre-oxidants such as O_3, Fe(VI) or Mn(VII) are chlorine-free, and therefore are not able to produce chlorinated DBPs (Cl-DBPs) while degrading their precursors. ClO_2, another pre-oxidant, is not directly able to halogenate NOM but was recently shown to produce *in situ* HOCl, which can in turn form Cl-DBPs (Chapter 4).[7] The formation of halogenated DBPs after ClO_2 treatment is however much lower than from HOCl. Together with the reduction of the water matrix reactivity, the use of pre-oxidation can have complementary benefits such as the degradation of contaminants,[8-10] disinfection[11-15] (except for Mn(VII)),[16, 17] or coagulation aid.[13, 15, 18-20]

DBP reduction has been achieved by pre-oxidizing various water matrices with ClO_2,[6, 21 22] O_3,[4, 23, 24] Fe(VI),[22, 25] and Mn(VII)[26]. However, only a few studies compared the efficiency of different pre-oxidants. ClO_2 and Fe(VI) efficiency on the DBP formation during chlorination of 12 waters has been compared.[22] It was found that 20 mgFe L^{-1} of Fe(VI) was more efficient to mitigate HAN formation and less efficient for THM mitigation compared to 1 mg L^{-1} of ClO_2. In another comparative study, equivalent mass concentrations of Fe(VI) and O_3 gave similar THM and HAN abatement in two real waters.[5]

The reactivity of the water (described by DOC and UVA_{254}), the pH as well as the presence of halides such as bromide or iodide will impact the formation of DBPs, and their mitigation.[27-29] It has been previously shown that ClO_2 and O_3 pre-oxidation impacted the speciation of DBPs in bromide-containing waters,[4, 21, 23, 30] and that O_3 pre-oxidation efficiency was affected by pH.[24] The presence of bromide leads to the formation of brominated DBPs (Br-DBPs) during chlorination,[27, 28] which are generally more toxic than their chlorinated analogues.[31] The pH is also an important parameter affecting the formation and the speciation of DBPs.[27] Typically, increasing the pH will enhance the formation of trihalomethanes (THMs) and lowering the pH will lead to higher haloacetonitriles (HANs) formation.

When pre-oxidation is used, the reactivity of the pre-oxidants toward bromide needs to be considered. For instance O_3 is known to readily react with bromide to form bromine, leading to the formation of organic Br-DBPs and potentially bromate.[32] However, bromide is in competition with some highly reactive NOM moieties for reaction with O_3.[30] Therefore, the formation of Br-DBPs and bromate will be highly dependent on the O_3 dose, the bromide concentration and the NOM characteristics. ClO_2 is unreactive toward bromide but may form HOBr through the *in situ* formation of HOCl,[7] while Fe(VI) was recently found to slowly react with bromide, leading to bromine and bromate in absence of phosphate.[33]

It is challenging to make broad conclusions about the impact of pre-oxidation treatment on the trend in DBPs formation due to variability of experimental conditions across studies. Furthermore, supplementary treatments after pre-oxidation, such as coagulation, (biological) activated carbon filtration, are likely to affect the NOM characteristics and therefore the formation of DBPs during subsequent chlorination.[25, 34-36] In previous studies, the choice of the pre-oxidant doses has usually been based on molar concentration, mass concentration or best practice.[5, 22, 37-40] Recently (Chapter 3), it was proposed to compare the efficiency of pre-oxidants based on their impact on NOM characteristics. The electron donating capacity (EDC) is an electrochemical measurement which is a proxy for activated aromatic,[41, 42] generally decreasing more readily than the UVA_{254} upon oxidative treatments. Furthermore, the EDC is not affected by interferences of inorganic species such as metals or anions absorbing UVA_{254}. Therefore, it is a more accurate surrogate to monitor changes in NOM characteristics.

This study provides a comparative study on the impact of four pre-oxidants, ClO_2, O_3, Fe(VI) and Mn(VII), on the formation of AOX, THMs and HANs during subsequent chlorination, using doses inducing equivalent effects on NOM electrochemical characteristics. The impact of pre-oxidant dose, bromide concentration and pH on the reduction and the speciation of DBPs is evaluated. The benefit of pre-oxidation is also discussed in terms of calculated toxicity based on THM and HAN formation. The work presented here does not aim to reproduce real water treatment conditions since no coagulation or biofiltration step was applied after pre-oxidation but to provide a better mechanistic understanding of the impact of the different oxidants linking NOM properties to further DBP formation.

6.3 Materials and methods

6.3.1 Chemicals and reagents

Sodium chlorite (80%) and a sodium hypochlorite solution (10–15%) were purchased from Sigma-Aldrich. All other chemicals were of analytical grade quality (≥ 98%). Solutions were prepared with ultrapure water (Purelab Ultra, Elga, UK). Suwannee River NOM extract was purchased from the International Humic Substances Society (Cat. No. 2R101N).

6.3.2 Preparation of oxidant solutions

Chlorine stock solutions were prepared from a sodium hypochlorite solution standardized by direct UV measurement at 292 nm ($\varepsilon_{292} = 362\ M^{-1}\ cm^{-1}$).[43] ClO_2 was produced by mixing solutions of sodium persulfate (40 g L^{-1}) and sodium chlorite (80 g L^{-1}) under N_2 bubbling for about 1 h.[44, 45] The ClO_2 produced was retrieved in chilled ultrapure water and standardized by direct UV measurement at 359 nm ($\varepsilon_{359} = 1230\ M^{-1}\ cm^{-1}$).[43] The K_2FeO_4 was prepared by oxidation of ferric nitrate with potassium hypochlorite.[46] The final product purity was 43% and was stable for months. The rest of the solid was potassium hydroxide. The Mn(VII) and Fe(VI) solutions were prepared by dissolution of $KMnO_4$ in ultrapure water for Mn(VII), or of K_2FeO_4 in a phosphate/borate buffer at pH 9.5 (5 mM / 1 mM) for Fe(VI). The stock solutions were then filtered through 0.22 µm (Polyethersulfone, Merck Millipore) and standardized by direct UV measurement at 525 nm ($\varepsilon_{525} = 2430\ M^{-1}\ cm^{-1}$)[47] for Mn(VII) or 510 nm ($\varepsilon_{510} = 1150\ M^{-1}\ cm^{-1}$)[48] for Fe(VI). O_3 stock solution was prepared by bubbling an ozone-oxygen mixture produced by an ozone generator (American Ozone System Inc.) in ultrapure water cooled at < 5°C. The O_3 stock solution was standardized by direct UV measurement at 258 nm ($\varepsilon_{258} = 2900\ M^{-1}\ cm^{-1}$).[49]

6.3.3 Pre-oxidation and chlorination experiments

The synthetic waters were prepared with 3.0 mgC L^{-1} of a Suwannee River NOM extract buffered at pH 6.5 (40 mM phosphate) or pH 8 (40 mM borate) with or without bromide (150 or 500 µg L^{-1}). The synthetic waters (500 mL) were spiked with O_3 (with or without 5 mM of tert-butanol, tBuOH), ClO_2, $KMnO_4$ or K_2FeO_4 (1–104 µM, the doses are given in Table 6-2), kept without headspace (< 10% of total volume) and protected from light until complete depletion of the oxidants. All the sample was

filtered through 0.22 µm (Polyethersulfone, Merck Millipore). Around 200 mL of the samples was used for electron donating capacity (EDC), bromide, AOX, THM and HAN analyses and 200 mL was chlorinated with 85 µM of sodium hypochlorite (6.0 $mgCl_2\ L^{-1}$) for 3 days, without headspace (< 10% of total volume) and protected from light. The chlorine dose was sufficient to ensure an oxidant residual of about 1.5 $mgCl_2\ L^{-1}$ after 3 days at pH 8, without bromide and without pre-treatment. The oxidant residual was quenched by sulfite (10% excess) for AOX, bromide and bromate measurements, or by a large excess of ascorbic acid for THMs and HANs. All experiments with SRNOM were duplicated, except the highest doses of Fe(VI) and Mn(VII).

A similar experiment was conducted on a real water with 155 µM of chlorine (12.4 $mgCl_2\ L^{-1}$). The chlorine doses was chosen based on a preliminary chlorine demand experiment allowing to obtain an oxidant residual of about 1.5 $mgCl_2\ L^{-1}$ after 3 days at pH 6.5.The main characteristics of the real and synthetic waters are given in Table 6-1.

Table 6-1. Main characteristics of the real and synthetic waters.

NOM	pH	DOC ($mgC\ L^{-1}$)	SUVA ($L\ mgC^{-1}\ cm^{-1}$)	Bromide ($\mu g\ L^{-1}$)	Relative EDC
SRNOM	6.5 or 8	3	4.0	0, 150 or 500	1.04
W20	6.5	4.5	3.4	144	2.04

6.3.4 Analytical methods

THMs and HANs were analyzed by headspace GC-MS with a method adapted from previously published methods, of which details are given in Text A-3-1.[50, 51] The AOX was measured by combustion and ion chromatography after adsorbing samples on activated carbon.[52] The chlorine residual was measured by ABTS (2,2'-azino-bis(3-ethylbenzothiazoline-6-sulfonic acid) diammonium salt).[53] Bromide and bromate were measured by ion chromatography using an AS9-HC column with a Na_2CO_3 eluent (9 mM, 1 mL min^{-1}).[54]

The electron donating capacity (EDC), a proxy for antioxidant capacity of NOM,[41, 55] was measured on an Agilent 1100 series system using a size-exclusion chromatography (SEC) (Text A-3-2, Chapter 2).[56, 57] The EDC is presented as

percentage of reduction compared to the untreated sample, or relatively to a 3 mgC L^{-1} unbuffered SRNOM sample.

6.4 Results and discussions

6.4.1 Impact of pre-oxidation treatment

6.4.1.1 SRNOM electrochemical properties

Pre-oxidants were spiked at different doses in 3 mgC L^{-1} of SRNOM. Three doses were applied, low, medium and high, corresponding to an estimated EDC reduction of 20, 50 and 70% at pH 8, respectively (Table 6-2). As shown in Chapter 3 (Figure 3-1), very low doses of Mn(VII) were inducing large EDC reductions. It was therefore difficult to accurately reach low EDC reductions. Therefore, only medium and high dose of Mn(VII) were applied in this study. The EDC reduction after pre-oxidation are shown in Table 6-2.

Table 6-2. Doses applied for the different oxidants, and corresponding EDC reduction at pH 8 and at pH 6.5 (between brackets). The range of data represents triplicate experiments.

	Dose (µM)			% EDC reduction		
Oxidant	**Low**	**Medium**	**High**	**Low**	**Medium**	**High**
ClO_2	3.5	15.1	39.3	27 ± 3 (36 ± 3)	56 ± 2 (64 ± 2)	77 ± 1
O_3-tBuOH	2.2	39.8	104.1	9 ± 2 (13 ± 4)	61 ± 2 (69 ± 2)	74 ± 3
Fe(VI)	2.5	14.7	50	20 ± 2 (17 ± 4)	49 ± 3 (27 ± 1)	68 ± 2
Mn(VII)		1	8.6		36 ± 2 (37 ± 2)	69 ± 1 (75 ± 1)

6.4.1.2 DBP formation

As expected, in absence of bromide, low concentrations of Cl-DBPs were produced only during ClO_2 pre-oxidation, through the *in situ* formation of HOCl (Figure A-6-1a,b). A maximum of 2.1 ± 1.2 µM of AOCl and 10 ± 0.1 nM of trichloromethane (TCM) were formed, consistent with a previous study.[7]

In presence of bromide, O_3-tBuOH and ClO_2 (through the *in situ* formation of HOCl) formed Br-DBPs. As a result, a significant decrease of bromide was observed after

pre-oxidation at high doses of ClO_2 and O_3-tBuOH with 7–22% of decrease (Figure A-6-2). Consequently, up to 1.8 ± 0.3 µM and 1.1 ± 0.05 µM of AOBr was formed after pre-oxidation with high doses of ClO_2 and O_3-tBuOH, respectively (Figure A-6-1a,c). Tribromomethane (TBM) was also formed at high dose of O_3-tBuOH (up to 69 ± 0.7 nM), while all four THMs were produced after ClO_2 pre-oxidation (total THMs < 10 nM) (Figure A-6-1b,d). No decrease of bromide concentration was observed after Fe(VI) and Mn(VII) pre-oxidation (< 5%, Figure A-6-2) and consequently no Br-DBPs were measured. Furthermore, no bromate was detected in O_3-tBuOH and Fe(VI) experiments.

6.4.2 Efficiency of pre-oxidation treatment on DBP mitigation during final chlorination: no bromide

All the results for the experiments conducted at pH 8 are presented in Figure 6-1.

6.4.2.1 Blanks

Without pre-oxidation (blanks) and in absence of bromide, 16.6 ± 0.9 µM of AOCl (Figure 6-1a), 2.8 ± 0.1 µM of THMs (TCM, Figure 6-1d) and 50 ± 1 nM of HANs (about 95% dichloroacetonitrile (DCAN) and 5% trichloroacetonitrile (TCAN), Figure 6-1g) were formed after 72 h of chlorination. These results were consistent with a previous study carried out with the Suwannee River Fulvic Acids extract, which produced 16 µM and 2.5 µM of AOCl and TCM, respectively, after 5 days of chlorination at pH 7.5.[58] In this previous study HANs were not detected probably because of the longer reaction time, promoting HAN hydrolysis.[59]

6.4.2.2 Pre-oxidation

When a pre-oxidation treatment was applied, the formations of AOCl, TCM and HANs were mitigated to various extents (Figure 6-1a,d,g). The mitigation generally increased with increasing pre-oxidant doses. For the highest pre-oxidant dose, AOCl formation was reduced by 30, 53, 21 and 20% for ClO_2, O_3-tBuOH, Fe(VI) and Mn(VII), respectively compared to the blank (no pre-oxidation) (Figure 6-1a). It was previously shown that equivalent EDC reduction were leading to equivalent AOX mitigation for ClO_2, Fe(VI) and Mn(VII) (Chapter 3). The slightly higher AOCl mitigation by ClO_2 compared to Fe(VI) and Mn(VII) could be explained by the slightly higher EDC removal (77% versus 68–69%, Table 6-2). By comparison, O_3-tBuOH was more

efficient than the other pre-oxidants due to a different mode of oxidation leading to aromatic ring cleavage, hence to less halogenation (Figure 6-1a).[60, 61]

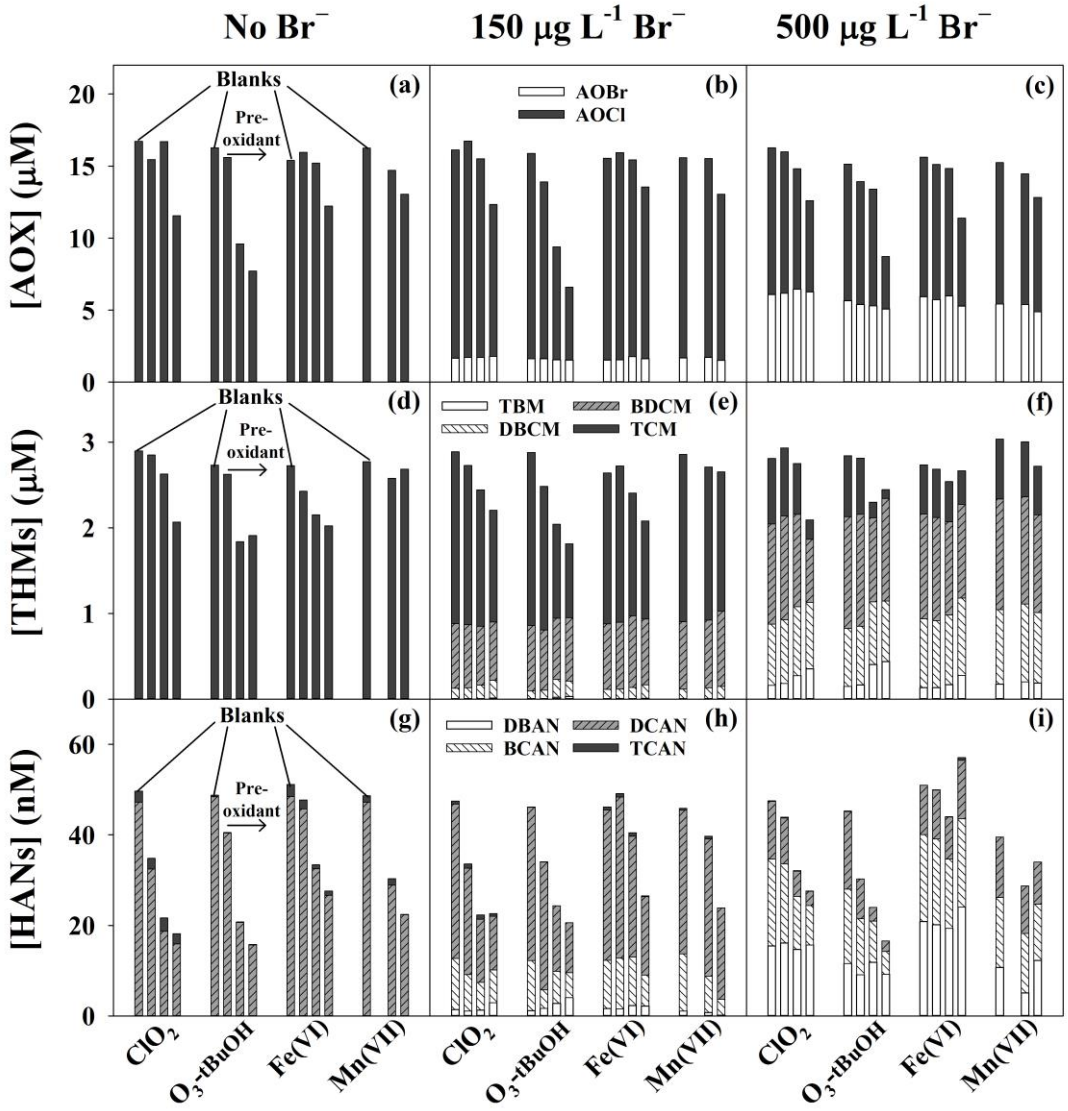

Figure 6-1. Formation of AOX (a–c), THMs (d–f) and HANs (g–i) after chlorination at pH 8, with and without (blank) pre-oxidation. Pre-oxidant doses are given in Table 6-2, [SRNOM] = 3 mgC L^{-1}.

High doses of ClO_2, O_3-tBuOH and Fe(VI) also reduced THM formation by 29, 30% and 26%, respectively (Figure 6-1d). In comparison, Mn(VII) was not efficient to remove THMs (≤ 10%), consistently with previous studies.[26, 35, 62] While the THMs represented 49–54% of the AOX in samples without pre-treatment, this fraction was substantially increased by O_3-tBuOH (up to 74%) and Mn(VII) (up to 62%) while it remained unaffected by ClO_2 (47–55%) and Fe(VI) (42–50%) (Figure A-6-3). Compared to AOX and THMs, the HAN formation was much more efficiently mitigated by all the oxidants with 66, 68, 45 and 53% of reduction at high dose of

ClO_2, O_3-tBuOH, Fe(VI) and Mn(VII), respectively (Figure 6-1g), which may be a major benefit of pre-treatment as HANs are much more toxic than THMs.[63]

6.4.3 Efficiency of pre-oxidation treatment on DBP mitigation during final chlorination: impact of bromide

6.4.3.1 Total DBP

In presence of 150 and 500 µg L^{-1} of bromide and without pre-oxidation, 15.8 ± 1.5 µM and 15.6 ± 1.3 µM of AOX was produced, respectively, which was not significantly different from the AOX formation without bromide (Figure 6-1a–c). Similarly, the total THM (2.8–2.9 ± 0.3 µM) and the total HAN (50–59 ± 8–15 nM) formation in presence of bromide was not significantly different from the sample without bromide (Figure 6-1d–f and Figure 6-1g–i). The AOX and THM formation was consistent with a previous study on a Suwannee River Fulvic Acids extract in presence of 104 µg L^{-1} of bromide.[58]

The pre-oxidation efficiency on the total formation of AOX, THMs and HANs was generally reduced by the presence of bromide (Figure 6-1). For the highest doses of ClO_2, O_3-tBuOH and Mn(VII), the AOX mitigation decreased from 30, 53 and 20% without bromide to 23, 42% and 16%, with 500 µg L^{-1} of bromide, respectively, (Figure 6-1a,c). A similar impact of bromide was observed on the mitigation of THMs and HANs (Figure 6-1d–i) except for Mn(VII) for which THM mitigation efficiency increased with increasing bromide concentration. However, the formation of THMs after Mn(VII) pre-oxidation was still higher than ClO_2 and O_3-tBuOH for 500 µg L^{-1} of bromide (2.7 µM versus 2.1–2.4 µM at high dose, Figure 6-1f).

The results for Fe(VI) with 500 µg L^{-1} bromide at the highest doses showed an increased mitigation of AOX while total THM and HAN concentrations were enhanced. This pattern cannot be explained and might come from an experimental error. However, a pattern similar to the other oxidants was obtained for the medium dose with a decrease of THM and HAN mitigation in presence of bromide.

6.4.3.2 DBP Speciation

Although the total DBPs was not affected by the presence of bromide in samples without pre-oxidation, Br-DBPs were formed. At 150 and 500 µg L^{-1} of bromide, 1.6 ± 0.1 and 5.8 ± 0.3 µM of AOBr were produced, respectively, representing 85–

93 ± 5% of the initial bromide (Figure 6-1b,c). About half of the bromide (49–57%) was recovered in the THMs as TBM, dibromochloromethane (DBCM) and dichlorobromomethane (DCBM) (Figure 6-1e,f) while 0.7–1.2% was found in the HANs as dibromoacetonitrile (DBAN) and bromochloroacetonitrile (BCAN) (Figure 6-1h,i). When bromide was present in the solution, the speciation of all DBPs shifted from Cl-DBPs to Br-DBPs for all oxidants (Figure 6-a–i). As expected, the increase of bromide from 150 to 500 µg L^{-1} led to increasing concentrations of Br-DBPs as well as increasing bromination (di- and tri-bromination) in each class of DBPs (Figure 6-1b,c,e,f,h,i). After pre-oxidation, the AOBr formation was not significantly impacted by any pre-oxidant at 150 or 500 µg L^{-1} of bromide (≤ 10% mitigation, Figure 6-1b,c), while the concentration of brominated THMs and HANs could be enhanced. At 150 µg L^{-1} of bromide, the sum of BDCM and DBCM concentrations was increasing with increasing dose for all the pre-oxidants (Figure 6-1e). For 500 µg L^{-1} of bromide, a similar behavior was observed for DBCM and TBM concentrations, the most brominated THMs (Figure 6-1f). For the HANs, the DCAN was mitigated with increasing dose of pre-oxidants even in presence of bromide while no clear trends were observed for DBAN and BCAN concentrations (Figure 6-1).

Overall, the Cl-DBPs were more efficiently mitigated by the pre-oxidants than the Br-DBPs. This was illustrated by the bromine substitution factor (BSF) (Figure 6-2). The BSF is commonly used to represent the fraction of bromine among the total halogens of a specific group of DBPs,[64] and is calculated by eq 6-1:

$$BSF = \frac{[Br-DBPs]}{[X-DBPs]} \times 100 \qquad \text{eq 6-1}$$

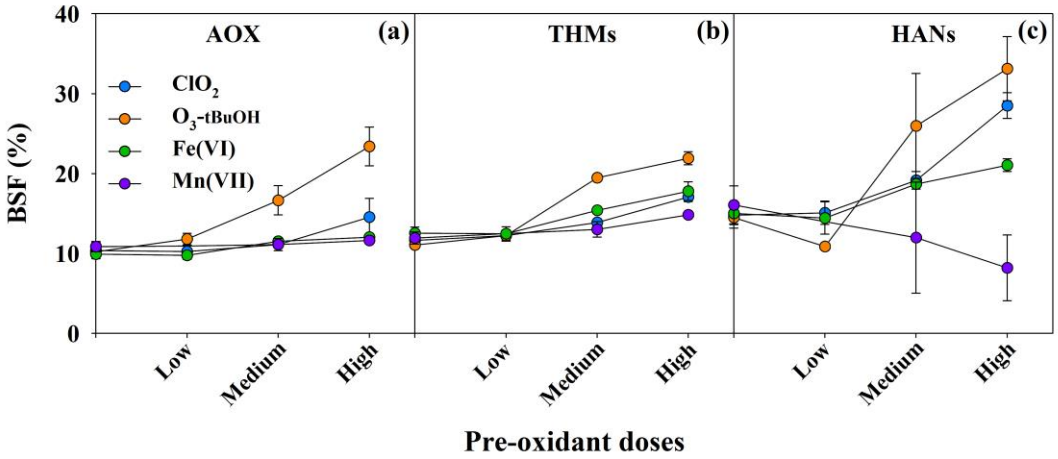

Figure 6-2. Bromine Substitution Factor (BSF) in AOX (a), THMs (b) and HANs (c) after chlorination in presence of 150 µg L^{-1} of bromide, with and without pre-oxidation. Pre-oxidant doses are given in Table 6-2, [SRNOM] = 3 mgC L^{-1}. Error bars represent the range of analytical results for duplicated experiments (except the high dose of Fe(VI) and Mn(VII)).

The addition of 150 µg L^{-1} of bromide led to BSF of 11 ± 1%, 12 ± 0.5% and 13 ± 3% in AOX, THMs and HANs, respectively (Figure 6-2). Increasing the bromide dose to 500 µg L^{-1} increased the BSF in AOX, THMs and HANs to 39 ± 2%, 38 ± 2% and 52 ± 6%, respectively (Figure A-6-4). Interestingly, increasing the bromide concentration had more impact on the HAN BSF than on the AOX or the THM BSF.

Figure 6-2 shows that the BSF was increasing for all the DBPs after pre-oxidation at both 150 and 500 µg L^{-1} of bromide (Figure 6-2and A-6-4). The only exception was the reduction of the BSF by Mn(VII) for the HANs at 150 µg L^{-1} of bromide (Figure 6-2c), although the variations of the data were high. The impact of the pre-oxidants on the increase of BSF generally ranked in the order O_3-tBuOH > ClO_2 > Fe(VI) > Mn(VII).

More specifically, the mitigation efficiency of a class of DBP was decreasing with increasing the number of bromine atoms in the compound. In presence of 500 µg L^{-1} of bromide, TCM and DCBM were mitigated by 19–85% and 8–37%, respectively, while DBCM and TBM were enhanced by 4–12% and 7–195%, respectively (Figure 6-3). Similar patterns were observed for the THMs at 150 µg L^{-1} of bromide (Figure A-6-5) and with HANs (Figure A-6-6).

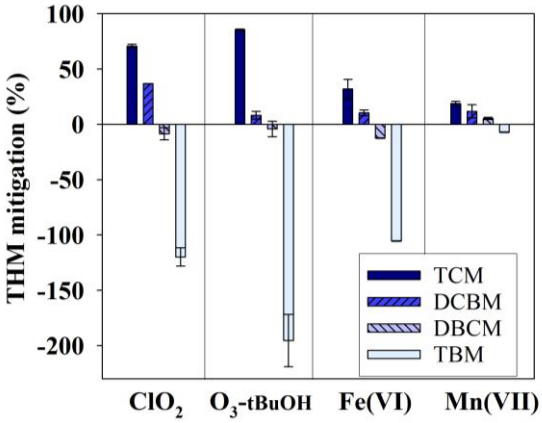

Figure 6-3. Reduction of individual THM by a high dose of pre-oxidants in presence of 500 µg L^{-1} of bromide. [ClO_2] = 39.3 µM, [O_3-tBuOH] = 104.1 µM, [Fe(VI)] = 50 µM, [Mn(VII)] = 8.6 µM, [SRNOM] = 3 mgC L^{-1}, pH 8. Error bars represent the range of analytical results one experiment.

6.4.3.3 Discussion

In presence of chlorine, bromide is rapidly oxidized to bromine, which in turn reacts with NOM 1 to 2 orders of magnitude faster than chlorine.[65] About 20% of the bromine will react through electrophilic aromatic substitutions, i.e. forming AOBr, while the rest will be reduced back to bromide via electron transfers.[66] In excess of chlorine, the remaining bromide will be re-oxidized until all the bromide is incorporated in NOM as AOBr.[28] The pre-oxidation treatment only inhibited a fraction of the reactive sites which were still in excess compared to the available bromine. Furthermore, as HOBr reacts much faster than HOCl, the pre-treatment had no significant impact on AOBr formation. However, the remaining fraction of AOX precursors available to react with the excess of HOCl was reduced, leading to a mitigation of AOCl. Furthermore, it was previously shown that bromine could substitute chlorine already incorporated in NOM.[28] The decrease of reactive sites after pre-oxidation also favored multiple bromination of the same site and formation of di- and tri- Br-DBPs. In comparison, the pre-oxidation was not enhancing multiple chlorination since an excess of chlorine and a long reaction time ensured multiple halogenation of most of DBP precursors with or without pre-oxidation.

6.4.4 Efficiency of pre-oxidation treatment on DBP mitigation during final chlorination: impact of pH

The same experiments were carried out at pH 6.5 (40 mM phosphate) with and without bromide (150 µg L^{-1}). The AOX, THM and HAN formations are given in Figure A-6-7.

6.4.4.1 Blanks

Without pre-oxidation, higher concentrations of AOX and HANs were produced at pH 6.5 (17.6–18.2 µM of AOX 74–87 nM of HANs) (Figure A-6-7a,b,e,f) compared to pH 8 (15.7–16.6 µM of AOX and 45–50 nM of HANs) (Figure 6-1a,b,g,h). However, THM formation was lower at pH 6.5 (1.9–2.1 µM, Figure A-6-7c,d) compared to pH 8 (2.8–2.9 µM, Figure 6-1d,e). Therefore THMs accounted for a much lower AOX fraction compared to pH 8 (32–35% vs 49–54%).

The higher AOX formation at pH 6.5 is explained by the higher reactivity of HOCl with AOX precursors compared to OCl^-.[66, 67] At pH 6.5, 92% of the chlorine was present as HOCl while it represents only 27% of the chlorine at pH 8 (assuming a HOCl/OCl^- pka of 7.56).[68] This led to an increase of the chlorine demand (from 57 ± 1 µM to 61 ± 0.5 µM) and consequently to an increase in AOX. The lower HAN and higher THM formations at higher pH are consistent with their base-catalyzed degradation[59] and formation,[69] respectively.

6.4.4.2 Pre-oxidation

3 mgC L^{-1} of SRNOM buffered at pH 6.5 (40 mM phosphate) was pre-treated with low and medium doses (medium and high for Mn(VII)) of each oxidant, in presence or absence of bromide (150 µg L^{-1}). In order to compare the impact of the pH on the pre-oxidation efficiency, the DBP formation was normalized based on the samples without pre-oxidation (Figure 6-4, Figure A-6-8 to A-6-10). At pH 6.5, medium doses of O_3-tBuOH and Fe(VI) mitigated larger fractions of the AOX, 15% and 60%, respectively, compared to pH 8, < 2% and 40%, respectively (Figure 6-4). For these oxidants, equivalent relative reductions of AOX were obtained at pH 6.5 for doses 3 times lower than at pH 8 (Figure 6-4). Higher relative reductions of THMs were also obtained at pH 6.5 after O_3-tBuOH pre-oxidation (Figure A-6-9). Conversely,

lowering the pH decrease the relative reduction of AOX, THMs and HANs by Mn(VII) (Figure A-6-8 to A-6-10).

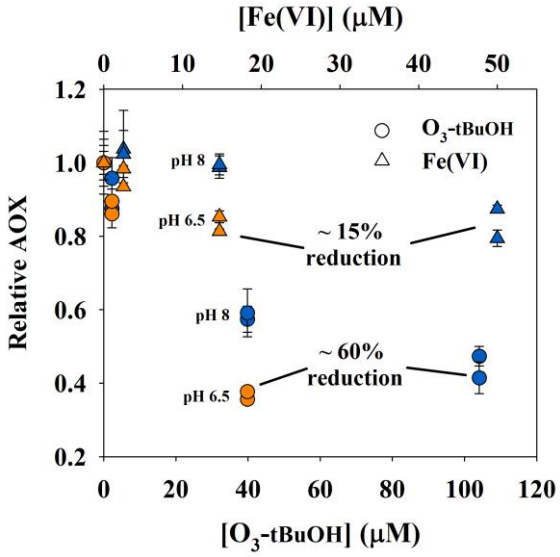

Figure 6-4. Relative AOX formation after O_3-tBuOH and Fe(VI) pre-oxidation at pH 6.5 (orange) and 8 (blue). [SRNOM] = 3 mgC L^{-1}, [Br^-] = 0–150 µg L^{-1}. Error bars represent the range of analytical results for one experiment.

6.4.4.3 Discussion

Based on the relative values, the benefit of decreasing the pH during pre-oxidation was globally ranking in the order O_3-tBuOH > Fe(VI) > ClO_2 > Mn(VII). The increase of O_3-tBuOH efficiency with decreasing pH can be attributed to an increase in O_3-tBuOH stability[70] leading to higher aromatic ring cleavage.[71, 72] In comparison to O_3-tBuOH, ClO_2 self-decay is too slow to impact on its oxidative efficiency.[73, 74] In contrast to O_3-tBuOH, Fe(VI) stability decreases with decreasing pH.[75] However, Fe(VI) reactivity toward a large range of compounds is also increasing with decreasing pH.[76, 77] For example, the apparent rate constant of Fe(VI) with phenol and 4-methylphenol increases by about 2 and 4 times, respectively, whereas it decreases by about 30 times for O_3-tBuOH and ClO_2.[78, 79] The improved mitigation of AOX at lower pH suggests that the higher reactivity of Fe(VI) toward AOX precursors at lower pH counterbalanced its enhanced decomposition. The lower efficiency of Mn(VII) at pH 6.5 could not be explained. These results are presented as relative abatement, since a higher formation of AOX at pH 6.5 compared to pH 8 was observed in samples without pre-oxidation, no definitive conclusion could be drawn on the impact of pH. However, using a low pH for the pre-treatment to enhance the degradation of DBP precursors and a higher pH for disinfection to lower the formation of DBPs seems to

be more efficient. Therefore, raising the pH after pre-oxidation might be an interesting strategy.

6.4.5 Efficiency of pre-oxidation treatment on DBP mitigation during final chlorination: calculated toxicity.

6.4.5.1 Blank

The calculated toxicity was estimated by dividing the concentration of each DBP (C) by its cytotoxicity (C_{50}), represented by the concentration of a specific DBP resulting in a 50% reduction of Chinese hamster ovary cells density.[63] Figure 6-5 shows the calculated toxicity (C/C_{50}) of THMs and HANs (bars) compared to the sum of THM and HAN concentrations (triangles), with and without bromide (150 µg L^{-1}). The results for 500 µg L^{-1} of bromide and for pH 6.5 are presented in Figure A-6-12 and Figure A-6-13, respectively.

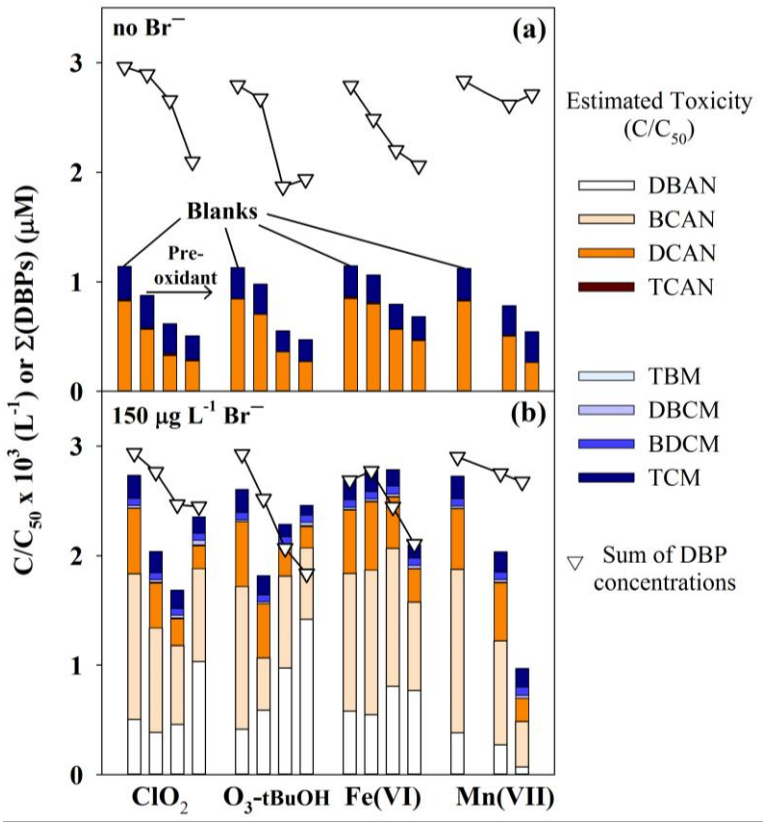

Figure 6-5. Calculated toxicity (bars) compared to DBP formation (triangles) after chlorination without bromide (a) and with 150 µg L^{-1} of bromide (b). [ClO_2] = 3.5–39.3 µM, [O_3-tBuOH] = 2.2–104.1 µM, [Fe(VI)] = 2.5–50 µM, [Mn(VII)] = 1–8.6 µM, [SRNOM] = 3 mgC L^{-1}, pH 8.

Although the HAN levels were much lower compared to the THMs, they are more potent compounds (C_{50} = 10^{-3}–10^{-2} vs 10^{-6}–10^{-4} M).[63] At pH 8, THMs represented

≥ 98% of the sum of THMs and HANs, but was accounting for only ≤ 25% of the calculated toxicity without bromide (Figure 6-5a). The weight of THMs on toxicity was even lower in presence of bromide (≤ 11% and ≤ 5% in presence of 150 and 500 µg L^{-1} of bromide, respectively) (Figure 6-5b, Figure A-6-12). The significant impact of HANs on calculated toxicity is consistent with a previous study.[80]

Since Br-DBPs are more toxic than the chlorinated ones, the cumulative calculated toxicity was increasing with increasing bromide dose. In presence of 150 and 500 µg L^{-1} of bromide and at pH 8, the calculated toxicity was multiplied by 2.4 and 8.8, respectively, compared to samples without bromide, while the sum of the THMs and HANs was constant (2.8 ± 0.1 µM, Figure 6-5 and Figure A-6-12).

In comparison to pH 8, more HANs and less THMs were formed at pH 6.5 (Figure 6-1d,e,g,h and Figure A-6-7c–f). As HANs are more toxic, the calculated toxicity in absence of bromide and without pre-oxidation was 50% higher at pH 6.5 (Figure 6-5a, Figure A-6-13a). In presence of 150 µg L^{-1} of bromide, it was previously discussed that the brominated HANs were not increasing with decreasing pH (Figure 6-1h and Figure A-6-7f). As they accounted for a significant fraction of the calculated toxicity, no significant difference was observed between pH 6.5 and 8 in presence of 150 µg L^{-1} of bromide and without pre-oxidation (5%, Figure 6-5b, Figure A-6-13b).

6.4.5.2 Pre-oxidation

In absence of bromide and at pH 6.5 and 8, both TCM and DCAN were mitigated by pre-oxidation (Figure 6-1d,g and Figure A-6-7c,e). Therefore, the cumulated calculated toxicity was also decreasing (Figure 6-5a and Figure A-6-13a). In presence of 150 µg L^{-1} of bromide and at pH 8, DCAN, BCAN and TCM formation was mitigated while TBM, DBCM and DBAN concentrations were enhanced (Figure 6-1e,h). Although DBAN levels were very low (< 2 nM without pre-oxidation), its increase can overcome the benefit of DCAN and BCAN mitigation in terms of calculated toxicity (Figure 6-5b, the impact of THMs was negligible). The detrimental effect of pre-oxidation treatment on the cumulative calculated toxicity was particularly obvious for O_3-tBuOH. A low dose of O_3-tBuOH significantly decreased BCAN and DCAN while a small increase in DBAN was observed, resulting in a calculated toxicity reduced by 31% (Figure 6-5b). Increasing the dose of O_3-tBuOH

further decreased the DCAN, but didn't affect significantly the BCAN while significantly enhancing DBAN formation. This resulted in an increase in estimated toxicity compared to the low O_3-tBuOH pre-oxidation dose (only 6% reduction at high dose), whereas a continuous decrease of total DBPs was observed (Figure 6-5b). Similar effects were observed at pH 6.5 for O_3-tBuOH and both pH 6.5 and 8 with the other oxidants (Figure 6-5b, Figure A-6-13b). Nevertheless, a medium dose of ClO_2 reduced DCAN and BCAN formation without enhancing DBAN formation at both pH 6.5 and 8 (Figure 6-1h, Figure A-6-7f), leading to an efficient reduction in cumulative calculated toxicity (38–47%, Figure 6-5b, Figure A-6-13b).

6.4.5.3 Correlations

To further evaluate the impact of the different DBPs on the calculated toxicity, the concentrations of the different class or group of DBPs at both pH 6.5 and 8 were plotted against the cumulative calculated toxicity and are presented in Figure A-6-14. In absence of bromide, no correlation was observed between the sum of THMs and HANs and the cumulative calculated toxicity ($r^2 < 0.1$, Figure A-6-14a). When only HANs were considered, a good correlation was obtained ($r^2 = 0.907$, Figure A-6-14a). However, when the experiments with bromide were added, the sum of HANs was not well correlated to the calculated toxicity ($r^2 = 0.287$, Figure A-6-14b). The correlation greatly improved when only brominated HANs were considered ($r^2 = 0.967$, Figure A-6-14b). Overall these correlations suggest that (i) THMs have a limited significance in terms of toxicity, and that they are not necessarily a good surrogate for the mitigation of more potent DBPs and (ii) that in presence of bromide, the formation of brominated HANs need to be considered. Other compounds such as the regulated HAAs or non-regulated but very potent halonitromethanes or haloacetamides may significantly impact the correlations presented in Figure A-6-14. It was estimated in a recent study that the impact of HAAs on calculated toxicity would be higher than the impact of THMs, but much lower than the impact of HANs.[80]

6.4.6 Impact of pre-oxidation on DBP mitigation in real groundwater

The different pre-oxidants were tested in real groundwater, W20, (main characteristics are given in Table 6-1). O_3 was also tested without tBuOH to mimic a more practical application. The doses of pre-oxidants were chosen based on a 50% reduction of the EDC for W20 and are shown in Table 6-3.

Table 6-3. Pre-oxidant doses and EDC reduction in W20.

Oxidant	Dose (µM)	%EDC reduction
ClO_2	10	50
O_3-tBuOH	30	59
O_3	30	50
Fe(VI)	24	50
Mn(VII)	10	42

All the results for W20 are presented in Figure 6-6. Without pre-oxidation, the chlorination of W20 produced 23.8 ± 0.9 µM of AOX, 2.4 ± 0.1 µM of THMs and 143 ± 16 nM of HANs. Similarly to SRNOM at pH 6.5 (Figure A-6-7b,d), THMs represented 30% of the AOX (Figure 6-6a,b). The presence of 145 µg L^{-1} of bromide led to the formation of Br-DBPs. Similarly to SRNOM at pH 6.5, 94%, 33% and 1% of the bromide was recovered in the AOX, THMs and HANs, respectively (Figure 6-6).

The AOX and the HAN formation was reduced by pre-oxidation while THM formation was enhanced by all pre-oxidants. AOX mitigation efficiency ranked in the order O_3-tBuOH (33%) > Fe(VI) (25%) > O_3 (14%) > Mn(VII) (7%) > ClO_2 (5%) (Figure 6-6a). A similar ranking was observed for HAN reduction, Fe(VI) (72%) > O_3-tBuOH (60%) > O_3 (56%) > Mn(VII) (46%) > ClO_2 (41%) (Figure 6-6c). The enhancing effect of pre-oxidants on THM formation ranked in the order O_3-tBuOH (7%) < ClO_2 (13%) < Fe(VI) (15%) < Mn(VII) (16%) < O_3 (22%) (Figure 6-6b).

The AOBr formation was not significantly affected by pre-oxidation (≤ 10% reduction, Figure 6-6a). The brominated and chlorinated THM formation was enhanced to a similar extent by ClO_2, Fe(VI) and Mn(VII) while O_3 (with and without tBuOH) was enhancing the brominated THM to a higher extent compared to the chlorinated THMs (Figure 6-6b). This was illustrated by the increase of the BSF from 9% to 15% and 13% after pre-oxidation by O_3-tBuOH and O_3, respectively (Figure 6-6b). The sum of

brominated HANs was efficiently mitigated by ClO_2 and Fe(VI) (38–43%) while O_3-tBuOH, O_3 and Mn(VII) had little impact (7–12%) (Figure 6-6c). Furthermore, O_3-tBuOH and O_3 were strongly enhancing the formation of DBAN (+ 333–362%, Figure 6-6c). Overall, ClO_2 was the only oxidant that mitigate the formation of chlorinated and brominated HANs to a similar extent while O_3-tBuOH, O_3, Fe(VI) and Mn(VII) increased the BSF from 7% to 21%, 19%, 16% and 12%, respectively (Figure 6-6c).

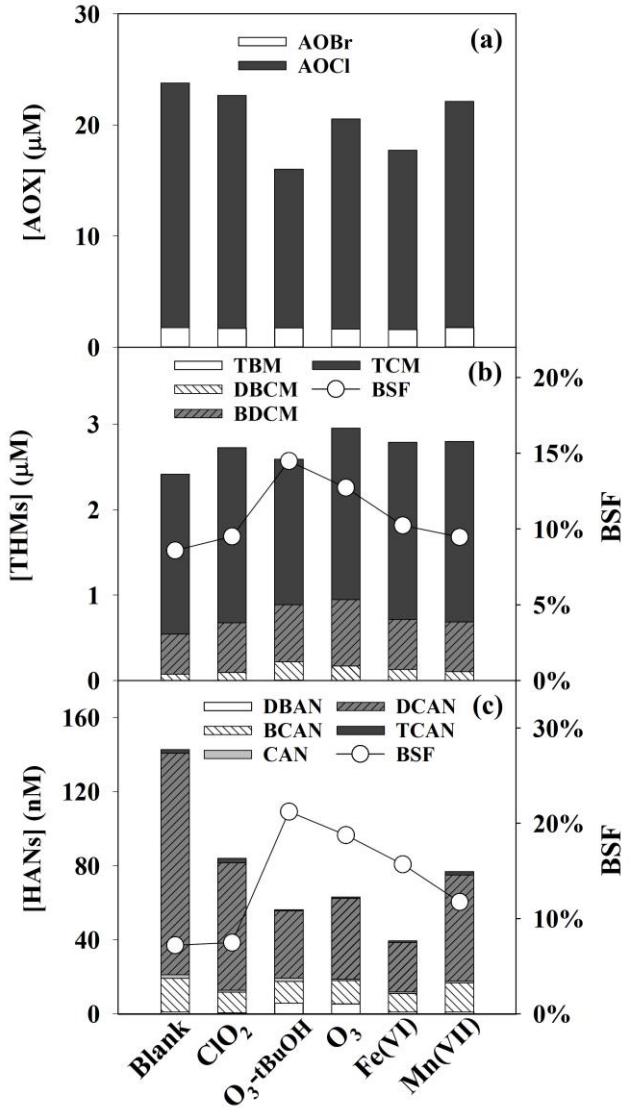

Figure 6-6. Formation of AOX (a), THMs (b) and HANs (c) in a real water with and without pre-oxidation. BSF are also shown for THMs and HANs. The water characteristics and the pre-oxidant doses are given in Table 6-1 and Table 6-3, respectively.

In comparison to O_3 alone, the presence of tBuOH was improving the mitigation of AOX and HANs and limited the increase of THMs (Figure 6-6). Together with the

higher EDC abatement in presence of tBuOH (Table 6-3), this confirms that in absence of tBuOH the O_3 exposure is reduced due to auto-decomposition catalyzed by $^{\bullet}OH$. Interestingly, the concentrations of brominated THMs and HANs were similar after ozonation with and without tBuOH in THMs and HANs, respectively.

Finally, the efficiency of pre-oxidation on the reduction of cumulative estimated toxicity ranked in the order Fe(VI) (54%) > ClO_2 (39%) > Mn(VII) (29%) > O_3-tBuOH (11%) > O_3 (9%) (Figure A-6-15).

The pre-oxidation doses tested on W20 were not beneficial in terms of regulated THM control, as all the pre-oxidants were enhancing their formation. The pre-oxidation was nevertheless an interesting option because of an efficient mitigation of HAN, which is more relevant for DBP-induced toxicity. However, the enhancement of DBAN formation, especially with O_3-tBuOH, could be largely counter-productive.

6.5 Conclusion

- Pre-oxidation is an efficient way to reduce DBP formation from chlorination. The doses of O_3 (2.2–104 µM, 0.1–5 mg L^{-1}), Fe(VI) (2.5–50 µM, 0.1–2.8 mgFe L^{-1}) and Mn(VI) (1–8.6 µM, 0.05–0.5 mgMn L^{-1}) were within the range of concentrations typically used in drinking water treatment, although Fe(VI) and Mn(VI) doses can be significantly higher.[26, 81, 82] In practice, ClO_2 dose is limited at about 15 µM (1 mg L^{-1}), which is lower than the highest dose used in this study (39 µM, 2.8 mg L^{-1}), because of the formation of the regulated chlorite.
- In synthetic waters, O_3 and Fe(VI) proved to be efficient in reducing the formation of THMs, AOX and HANs. ClO_2 and Mn(VII) were less efficient in reducing THM concentrations (considering a maximum dose of 15 µM for ClO_2) but all oxidants were greatly mitigating HANs (> 45% at high dose).
- Decreasing the pH was significantly improving the normalized AOX mitigation by O_3-tBuOH and Fe(VI) pre-oxidation and the THM mitigation by O_3-tBuOH pre-oxidation. A lower pH was, however, decreasing the normalized HAN mitigation by Fe(VI) and Mn(VII), and the THM and AOX mitigation by Mn(VII).
- Cl-DBPs were efficiently mitigated. However, increasing the pre-oxidant dose was generally enhancing the formation of the more toxic Br-DBPs whenever bromide was present in solution. O_3-tBuOH had generally the highest detrimental effect on the formation of Br-DBPs, especially at high dose. Conversely, the use of ClO_2 at practical doses (≤ 15 µM, 1 mg L^{-1}) was efficient in reducing HAN formation, without promoting or even efficiently mitigating brominated HANs.
- The same chlorine dose was used with and without pre-oxidation. This led to chlorine residuals much higher than 1.5 mgCl_2 L^{-1} in pre-oxidized samples (Figure A-6-16). In practice, the chlorine dose could therefore be optimized, which will reduce the overall formation of DBPs. Furthermore, the aim of the present work was to compare the impact of oxidative treatments on DBP precursors. However, in practice supplementary treatments are likely to be applied between pre-oxidation and disinfection such as coagulation-sedimentation-filtration or the use of biofiltration to remove the assimilable

organic carbon that may arise from pre-oxidation, notably from O_3, Fe(VI) and Mn(VII) treatment.[47]

- The assessment of toxicity based on theoretical cytotoxicity of THMs and HANs suggest that regulated THMs are not significantly affecting the DBP-induced toxicity, especially in presence of bromide. Furthermore, their reduction during pre-treatment is not representative of the reduction of other more potent DBPs such as HANs, and may not be a good surrogate for toxicity. The impact of pre-oxidation on HAN formation was therefore an important factor for toxicity assessment. The enhancement of DBAN was a major factor counteracting the efficiency of pre-oxidation for all oxidants in terms of estimated toxicity. Lower pre-oxidant doses, particularly of O_3-tBuOH, were more efficient in controlling the ratio between Cl^- and more toxic Br-DBPs. In comparison to the other oxidants, ≤ 15 µM of ClO_2 was a consistently good option for the mitigation of HANs and for the estimated toxicity in the different conditions tested.
- The formation of other DBPs such as the widespread HAAs or other very potent DBPs such as haloacetamide, haloketones, halonitromethanes and iodinated DBPs, might heavily impact the calculated toxicity and their formation may be impacted very differently upon pre-oxidation. Furthermore, calculated toxicity is merely illustrative of the weight of various compounds on DBP-induced toxicity, based on individual measurements, and the effects may not necessarily be simply cumulative in complex matrices.[83] Therefore, toxicity assays should be performed to evaluate the efficiency of the different pre-oxidation strategies.

6.6 References

1. Rook, J. J., Chlorination reactions of fulvic acids in natural waters. *Environ. Sci. Technol.* **1977,** *11*, (5), 478-482.
2. Richardson, S. D.; Plewa, M. J.; Wagner, E. D.; Schoeny, R.; DeMarini, D. M., Occurrence, genotoxicity, and carcinogenicity of regulated and emerging disinfection by-products in drinking water: A review and roadmap for research. *Mutat. Res-Rev. Mutat.* **2007,** *636*, (1–3), 178-242.
3. Sedlak, D. L.; von Gunten, U., The Chlorine Dilemma. *Science* **2011,** *331*, (6013), 42-43.
4. Hua, G.; Reckhow, D. A., Effect of pre-ozonation on the formation and speciation of DBPs. *Water Res.* **2013,** *47*, (13), 4322-4330.
5. Jiang, Y.; Goodwill, J. E.; Tobiason, J. E.; Reckhow, D. A., Comparison of the Effects of Ferrate, Ozone, and Permanganate Pre-oxidation on Disinfection Byproduct Formation from Chlorination. In *Ferrites and Ferrates: Chemistry and Applications in Sustainable Energy and Environmental Remediation*, American Chemical Society: 2016; Vol. 1238, pp 421-437.
6. Werdehoff, K. S.; Singer, P. C., Chlorine Dioxide Effects on THMFP, TOXFP, and the Formation of Inorganic By-products. *J. Am. Water Works Ass.* **1987,** *79*, (9), 107-113.
7. Rougé, V.; Allard, S.; Croué, J.-P.; von Gunten, U., In Situ Formation of Free Chlorine During ClO2 Treatment: Implications on the Formation of Disinfection Byproducts. *Environ. Sci. Technol.* **2018,** *52*, (22), 13421-13429.
8. Lee, Y.; von Gunten, U., Oxidative transformation of micropollutants during municipal wastewater treatment: Comparison of kinetic aspects of selective (chlorine, chlorine dioxide, ferrateVI, and ozone) and non-selective oxidants (hydroxyl radical). *Water Res.* **2010,** *44*, (2), 555-566.
9. Rodríguez, E.; Majado, M. E.; Meriluoto, J.; Acero, J. L., Oxidation of microcystins by permanganate: Reaction kinetics and implications for water treatment. *Water Res.* **2007,** *41*, (1), 102-110.
10. Jiang, J.; Pang, S.-Y.; Ma, J.; Liu, H., Oxidation of Phenolic Endocrine Disrupting Chemicals by Potassium Permanganate in Synthetic and Real Waters. *Environ. Sci. Technol.* **2012,** *46*, (3), 1774-1781.
11. von Gunten, U., Ozonation of drinking water: Part II. Disinfection and by-product formation in presence of bromide, iodide or chlorine. *Water Res.* **2003,** *37*, (7), 1469-1487.
12. Junli, H.; Li, W.; Nenqi, R.; Li, L. X.; Fun, S. R.; Guanle, Y., Disinfection effect of chlorine dioxide on viruses, algae and animal planktons in water. *Water Res.* **1997,** *31*, (3), 455-460.
13. Jiang, J.-Q.; Wang, S.; Panagoulopoulos, A., The exploration of potassium ferrate(VI) as a disinfectant/coagulant in water and wastewater treatment. *Chemosphere* **2006,** *63*, (2), 212-219.
14. Korich, D. G.; Mead, J. R.; Madore, M. S.; Sinclair, N. A.; Sterling, C. R., Effects of ozone, chlorine dioxide, chlorine, and monochloramine on Cryptosporidium parvum oocyst viability. *Appl. Environ. Microb.* **1990,** *56*, (5), 1423.
15. Jiang, J. Q.; Lloyd, B.; Grigore, L., Preparation and evaluation of potassium ferrate as an oxidant and coagulant for potable water treatment. *Environ. Eng. Sci.* **2001,** *18*, (5), 323-328.
16. Singer Philip, C., Control of Disinfection By-Products in Drinking Water. *J. Environ. Eng.* **1994,** *120*, (4), 727-744.

17. Anderson, W. B.; Mayfield, C. I.; Dixon, D. G.; Huck, P. M., Endotoxin inactivation by selected drinking water treatment oxidants. *Water Res.* **2003,** *37*, (19), 4553-4560.
18. Chen, J.-J.; Yeh, H.-H.; Tseng, I. C., Effect of ozone and permanganate on algae coagulation removal – Pilot and bench scale tests. *Chemosphere* **2009,** *74*, (6), 840-846.
19. Ma, J.; Li, G., Laboratory and Full-Scale Plant Studies of Permanganate Oxidation as an Aid in Coagulation. *Water Sci. Technol.* **1993,** *27*, (11), 47-54.
20. Zhang, L.; Ma, J.; Li, X.; Wang, S., Enhanced removal of organics by permanganate preoxidation using tannic acid as a model compound – Role of in situ formed manganese dioxide. *J. Environ. Sci.* **2009,** *21*, (7), 872-876.
21. Yang, X.; Guo, W.; Lee, W., Formation of disinfection byproducts upon chlorine dioxide preoxidation followed by chlorination or chloramination of natural organic matter. *Chemosphere* **2013,** *91*, (11), 1477-1485.
22. Yang, X.; Guo, W.; Zhang, X.; Chen, F.; Ye, T.; Liu, W., Formation of disinfection by-products after pre-oxidation with chlorine dioxide or ferrate. *Water Res.* **2013,** *47*, (15), 5856-5864.
23. Wert, E. C.; Rosario-Ortiz, F. L., Effect of Ozonation on Trihalomethane and Haloacetic Acid Formation and Speciation in a Full-Scale Distribution System. *Ozone: Science & Engineering* **2011,** *33*, (1), 14-22.
24. De Vera, G. A.; Stalter, D.; Gernjak, W.; Weinberg, H. S.; Keller, J.; Farré, M. J., Towards reducing DBP formation potential of drinking water by favouring direct ozone over hydroxyl radical reactions during ozonation. *Water Res.* **2015,** *87*, 49-58.
25. Jiang, Y.; Goodwill, J. E.; Tobiason, J. E.; Reckhow, D. A., Impacts of ferrate oxidation on natural organic matter and disinfection byproduct precursors. *Water Res.* **2016,** *96*, 114-125.
26. Singer, P. C.; Borchardt, J. H.; Colthurst, J. M., The Effects of Permanganate Pretreatment on Trihalomethane Formation in Drinking Water. *J. Am. Water Works Ass.* **1980,** *72*, (10), 573-578.
27. Hua, G.; Reckhow, D. A., Evaluation of bromine substitution factors of DBPs during chlorination and chloramination. *Water Res.* **2012,** *46*, (13), 4208-4216.
28. Langsa, M.; Heitz, A.; Joll, C. A.; von Gunten, U.; Allard, S., Mechanistic Aspects of the Formation of Adsorbable Organic Bromine during Chlorination of Bromide-containing Synthetic Waters. *Environ. Sci. Technol.* **2017,** *51*, (9), 5146-5155.
29. Allard, S.; Tan, J.; Joll, C. A.; von Gunten, U., Mechanistic Study on the Formation of Cl-/Br-/I-Trihalomethanes during Chlorination/Chloramination Combined with a Theoretical Cytotoxicity Evaluation. *Environ. Sci. Technol.* **2015,** *49*, (18), 11105-11114.
30. Allard, S.; Nottle, C. E.; Chan, A.; Joll, C.; von Gunten, U., Ozonation of iodide-containing waters: Selective oxidation of iodide to iodate with simultaneous minimization of bromate and I-THMs. *Water Res.* **2013,** *47*, (6), 1953-1960.
31. Wagner, E. D.; Plewa, M. J., CHO cell cytotoxicity and genotoxicity analyses of disinfection by-products: An updated review. *J. Environ. Sci.* **2017,** *58*, 64-76.
32. Von Gunten, U.; Hoigne, J., Bromate formation during ozonation of bromide-containing waters: Interaction of ozone and hydroxyl radical reactions. *Environ. Sci. Technol.* **1994,** *28*, (7), 1234-1242.
33. Jiang, Y.; Goodwill, J. E.; Tobiason, J. E.; Reckhow, D. A., Bromide oxidation by ferrate(VI): The formation of active bromine and bromate. *Water Res.* **2016,** *96*, 188-197.

34. Stuart, W. K.; William, A. M.; Paul, W.; Aaron, D., Formation and control of emerging C- and N-DBPs in drinking water. *J. Am. Water Works Ass.* **2012,** *104*, (11), E582-E595.
35. Hu, J.; Chu, W.; Sui, M.; Xu, B.; Gao, N.; Ding, S., Comparison of drinking water treatment processes combinations for the minimization of subsequent disinfection by-products formation during chlorination and chloramination. *Chem. Eng. J.* **2018,** *335*, 352-361.
36. de Vera, G. A.; Keller, J.; Gernjak, W.; Weinberg, H.; Farré, M. J., Biodegradability of DBP precursors after drinking water ozonation. *Water Res.* **2016,** *106*, 550-561.
37. Xie, P.; Ma, J.; Fang, J.; Guan, Y.; Yue, S.; Li, X.; Chen, L., Comparison of Permanganate Preoxidation and Preozonation on Algae Containing Water: Cell Integrity, Characteristics, and Chlorinated Disinfection Byproduct Formation. *Environ. Sci. Technol.* **2013,** *47*, (24), 14051-14061.
38. Lee, C.; Schmidt, C.; Yoon, J.; Von Gunten, U., Oxidation of N-nitrosodimethylamine (NDMA) precursors with ozone and chlorine dioxide: Kinetics and effect on NDMA formation potential. *Environ. Sci. Technol.* **2007,** *41*, (6), 2056-2063.
39. Selbes, M.; Kim, D.; Karanfil, T., The effect of pre-oxidation on NDMA formation and the influence of pH. *Water Res.* **2014,** *66*, 169-179.
40. Chen, Z.; Valentine, R. L., The influence of the pre-oxidation of natural organic matter on the formation of N-nitrosodimethylamine (NDMA). *Environ. Sci. Technol.* **2008,** *42*, (14), 5062-5067.
41. Aeschbacher, M.; Graf, C.; Schwarzenbach, R. P.; Sander, M., Antioxidant properties of humic substances. *Environ. Sci. Technol.* **2012,** *46*, (9), 4916-4925.
42. Walpen, N.; Schroth, M. H.; Sander, M., Quantification of Phenolic Antioxidant Moieties in Dissolved Organic Matter by Flow-Injection Analysis with Electrochemical Detection. *Environ. Sci. Technol.* **2016,** *50*, (12), 6423-6432.
43. Furman, C. S.; Margerum, D. W., Mechanism of Chlorine Dioxide and Chlorate Ion Formation from the Reaction of Hypobromous Acid and Chlorite Ion. *Inorg. Chem.* **1998,** *37*, (17), 4321-4327.
44. Granstrom, M. L.; Lee, G. F., Generation and Use of Chlorine Dioxide in Water Treatment. *J. Am. Water Works Ass.* **1958,** *50*, (11), 1453-1466.
45. Gates, D. J., *The Chlorine Dioxide Handbook*. American Water Works Association: 1998.
46. Li, C.; Li, X. Z.; Graham, N., A study of the preparation and reactivity of potassium ferrate. *Chemosphere* **2005,** *61*, (4), 537-543.
47. Ramseier, M. K.; Peter, A.; Traber, J.; von Gunten, U., Formation of assimilable organic carbon during oxidation of natural waters with ozone, chlorine dioxide, chlorine, permanganate, and ferrate. *Water Res.* **2011,** *45*, (5), 2002-2010.
48. Lee, Y.; Yoon, J.; Von Gunten, U., Spectrophotometric determination of ferrate (Fe(VI)) in water by ABTS. *Water Res.* **2005,** *39*, (10), 1946-1953.
49. Hoigné, J.; Bader, H., The role of hydroxyl radical reactions in ozonation processes in aqueous solutions. *Water Res.* **1976,** *10*, (5), 377-386.
50. Allard, S.; Charrois, J. W. A.; Joll, C. A.; Heitz, A., Simultaneous analysis of 10 trihalomethanes at nanogram per liter levels in water using solid-phase microextraction and gas chromatography mass-spectrometry. *J. Chromatogr. A* **2012,** *1238*, 15-21.

51. Kristiana, I.; Joll, C.; Heitz, A., Analysis of halonitriles in drinking water using solid-phase microextraction and gas chromatography–mass spectrometry. *J. Chromatogr. A* **2012,** *1225*, 45-54.
52. Langsa, M.; Allard, S.; Kristiana, I.; Heitz, A.; Joll, C. A., Halogen-specific total organic halogen analysis: Assessment by recovery of total bromine. *J. Environ. Sci.* **2017,** *58*, 340-348.
53. Pinkernell, U.; Nowack, B.; Gallard, H.; Von Gunten, U., Methods for the photometric determination of reactive bromine and chlorine species with ABTS. *Water Res.* **2000,** *34*, (18), 4343-4350.
54. USEPA, Method 326.0: Determination of Inorganic Oxyhalide Disinfection By-Products in Drinking Water Using Ion Chromatography Incorporating the Addition of a Suppressor Acidified Postcolumn Reagent for Trace Bromate Analysis. In 2002.
55. Wenk, J.; Aeschbacher, M.; Salhi, E.; Canonica, S.; Von Gunten, U.; Sander, M., Chemical oxidation of dissolved organic matter by chlorine dioxide, chlorine, and ozone: Effects on its optical and antioxidant properties. *Environ. Sci. Technol.* **2013,** *47*, (19), 11147-11156.
56. Chon, K.; Salhi, E.; von Gunten, U., Combination of UV absorbance and electron donating capacity to assess degradation of micropollutants and formation of bromate during ozonation of wastewater effluents. *Water Res.* **2015,** *81*, 388-397.
57. Önnby, L.; Walpen, N.; Salhi, E.; Sander, M.; Von Gunten, U., Two analytical approached to quantify the oxidation of dissolved organic matter by chlorine and ozone. *Water Res.* **2018**.
58. Zhang, X.; Echigo, S.; Minear, R. A.; Plewa, M. J., Characterization and Comparison of Disinfection By-Products of Four Major Disinfectants. In *Natural Organic Matter and Disinfection By-Products*, American Chemical Society: 2000; Vol. 761, pp 299-314.
59. Yu, Y.; Reckhow, D. A., Kinetic Analysis of Haloacetonitrile Stability in Drinking Waters. *Environ. Sci. Technol.* **2015,** *49*, (18), 11028-11036.
60. Dickenson, E. R. V.; Summers, R. S.; Croué, J.-P.; Gallard, H., Haloacetic acid and Trihalomethane Formation from the Chlorination and Bromination of Aliphatic β-Dicarbonyl Acid Model Compounds. *Environ. Sci. Technol.* **2008,** *42*, (9), 3226-3233.
61. Bond, T.; Henriet, O.; Goslan, E. H.; Parsons, S. A.; Jefferson, B., Disinfection Byproduct Formation and Fractionation Behavior of Natural Organic Matter Surrogates. *Environ. Sci. Technol.* **2009,** *43*, (15), 5982-5989.
62. Hidayah, E. N.; Yeh, H. H., Effect of Permanganate Preoxidation to Natural Organic Matter and Disinfection by-Products Formation Potential Removal. *J. Phys. Conf. Ser.* **2018,** *953*, (1), 012218.
63. Plewa, M. J.; Wagner, E. D.; Muellner, M. G.; Hsu, K.-M.; Richardson, S. D., Comparative Mammalian Cell Toxicity of N-DBPs and C-DBPs. In *Disinfection By-Products in Drinking Water*, American Chemical Society: 2008; Vol. 995, pp 36-50.
64. Hua, G.; Reckhow, D. A.; Kim, J., Effect of Bromide and Iodide Ions on the Formation and Speciation of Disinfection Byproducts during Chlorination. *Environ. Sci. Technol.* **2006,** *40*, (9), 3050-3056.
65. Westerhoff, P.; Chao, P.; Mash, H., Reactivity of natural organic matter with aqueous chlorine and bromine. *Water Res.* **2004,** *38*, (6), 1502-1513.
66. Criquet, J.; Rodriguez, E. M.; Allard, S.; Wellauer, S.; Salhi, E.; Joll, C. A.; von Gunten, U., Reaction of bromine and chlorine with phenolic compounds and natural organic matter extracts - Electrophilic aromatic substitution and oxidation. *Water Res.* **2015,** *85*, 476-486.

67. Boyce, S. D.; Hornig, J. F., Reaction pathways of trihalomethane formation from the halogenation of dihydroxyaromatic model compounds for humic acid. *Environ. Sci. Technol.* **1983,** *17*, (4), 202-211.
68. Morris, J. C., The Acid Ionization Constant of HOCl from 5 to 35°. *J. Phys. Chem.* **1966,** *70*, (12), 3798-3805.
69. Peters, C. J.; Young, R. J.; Perry, R., Factors influencing the formation of haloforms in the chlorination of humic materials. *Environ. Sci. Technol.* **1980,** *14*, (11), 1391-1395.
70. Staehelin, J.; Hoigne, J., Decomposition of ozone in water: rate of initiation by hydroxide ions and hydrogen peroxide. *Environ. Sci. Technol.* **1982,** *16*, (10), 676-681.
71. Mvula, E.; von Sonntag, C., Ozonolysis of Phenols in Aqueous Solution. *Org. Biomol. Chem.* **2003,** *1*, 1749-1756.
72. Önnby, L.; Salhi, E.; McKay, G.; Rosario-Ortiz, F. L.; von Gunten, U., Ozone and chlorine reactions with dissolved organic matter - Assessment of oxidant-reactive moieties by optical measurements and the electron donating capacities. *Water Res.* **2018,** *144*, 64-75.
73. von Heijne, G.; Teder, A., Kinetics of the Decomposition of Aqueous Chlorine Dioxide Solutions. *Acta Chem. Scand.* **1973,** *27*, 4018-4029.
74. Odeh, I. N.; Francisco, J. S.; Margerum, D. W., New Pathways for Chlorine Dioxide Decomposition in Basic Solution. *Inorg. Chem.* **2002,** *41*, (24), 6500-6506.
75. Lee, Y.; Kissner, R.; Von Gunten, U., Reaction of ferrate(VI) with ABTS and self-decay of ferrate(VI): Kinetics and mechanisms. *Environ. Sci. Technol.* **2014,** *48*, (9), 5154-5162.
76. Lee, Y.; Yoon, J.; von Gunten, U., Kinetics of the Oxidation of Phenols and Phenolic Endocrine Disruptors during Water Treatment with Ferrate (Fe(VI)). *Environ. Sci. Technol.* **2005,** *39*, (22), 8978-8984.
77. Lee, Y.; Zimmermann, S. G.; Kieu, A. T.; von Gunten, U., Ferrate (Fe(VI)) Application for Municipal Wastewater Treatment: A Novel Process for Simultaneous Micropollutant Oxidation and Phosphate Removal. *Environ. Sci. Technol.* **2009,** *43*, (10), 3831-3838.
78. Hoigné, J.; Bader, H., Rate constants of reactions of ozone with organic and inorganic compounds in water–II. *Water Res.* **1983,** *17*, (2), 185-194.
79. Hoigné, J.; Bader, H., Kinetics of reactions of chlorine dioxide (OClO) in water-I. Rate constants for inorganic and organic compounds. *Water Res.* **1994,** *28*, (1), 45-55.
80. Ersan, M. S.; Liu, C.; Amy, G.; Karanfil, T., The interplay between natural organic matter and bromide on bromine substitution. *Sci. Total Environ.* **2019,** *646*, 1172-1181.
81. Jacangelo, J. G.; Patania, N. L.; Reagan, K. M.; Aieta, E. M.; Krasner, S. W.; McGuire, M. J., Ozonation: Assessing Its Role in the Formation and Control of Disinfection By-products. *J. Am. Water Works Ass.* **1989,** *81*, (8), 74-84.
82. Jiang, J.-Q.; Lloyd, B., Progress in the development and use of ferrate(VI) salt as an oxidant and coagulant for water and wastewater treatment. *Water Res.* **2002,** *36*, (6), 1397-1408.
83. Tang, J. Y. M.; McCarty, S.; Glenn, E.; Neale, P. A.; Warne, M. S. J.; Escher, B. I., Mixture effects of organic micropollutants present in water: Towards the development of effect-based water quality trigger values for baseline toxicity. *Water Res.* **2013,** *47*, (10), 3300-3314.

Every reasonable effort has been made to acknowledge the owners of copyright material. I would be pleased to hear from any copyright owner who has been omitted or incorrectly acknowledged.

Chapter 7. Conclusions and Perspectives

This Thesis provides an advanced knowledge and new insights on the chemistry and application of ClO_2 during drinking water treatment as well as a comparison with O_3, Fe(VI) and Mn(VII) for the mitigation of DBPs.

The developed SEC system could successfully be used to measure the EDC and UVA_{254} of water samples with detection limits corresponding to 0.09 and 0.02 mgC L^{-1} of SRNOM, respectively. The standard deviation of triplicated analyses was $\leq 15\%$ for SRNOM concentrations < 1 mgC L^{-1} and $\leq 5\%$ for SRNOM concentrations > 1 mgC L^{-1}. An internal calibration of the EDC using trolox was carried out and the accuracy of the analytical method validated by comparing the quantified EDC of 8 NOM standards with their respective values quantified by two other methods found in the literature.

The use of EDC showed that ClO_2, O_3-tBuOH, Fe(VI) and Mn(VII) exhibit different reactivity toward NOM (on a molar concentration basis). However, the concomitant use of EDC and UVA_{254} revealed that the overall impact of ClO_2, Fe(VI) and Mn(VII) on NOM characteristics was similar, suggesting analogous reaction pathways, i.e. formation of quinone-type moieties at low dose and aromatic ring cleavage at high dose, while O_3 reacted via distinct mechanisms involving more aromatic ring cleavage. The distinctive impact of O_3-tBuOH on NOM compared to the other investigated pre-oxidants was confirmed by the lowest formation of AOX. ClO_2, Fe(VI) and Mn(VII) led to similar mitigation of AOX formation for an equivalent EDC reduction, while O_3-tBuOH led to lower concentrations of AOX. However, the EDC was poorly correlated to the formation of THMs. In this case, UVA_{254} was a better surrogate. Interestingly, while UVA_{254} was a useful surrogate for AOX and THM formation, it was not representative of HAN formation whereas EDC showed an oxidant-independent correlation. The capacity of EDC and UVA_{254} to be representative of the formation of other DBPs remains to be explored.

It was demonstrated that FAC was formed as a secondary oxidant during ClO_2 treatment (up to 25% of the ClO_2 with NOM extracts). The addition of FAC as a degradation product of ClO_2 allows to complete the mass balance on chlorinated inorganic species (i.e. ClO_2^-, ClO_3^-), explains the formation of halogenated DBPs and suggests that the oxidation capacity of ClO_2 is higher than one electron in water treatment conditions. Therefore, the presence of FAC has to be considered whenever ClO_2 is employed.

The primary ClO_2 product, the regulated ClO_2^-, is a limiting factor for ClO_2 application. However, when ClO_2 is used as pre-oxidant, the formed ClO_2^- can be oxidized by FAC during subsequent chlorination. Neutral pH is preferable to enhance FAC/ClO_2^- reaction and regenerate ClO_2. The kinetic model developed allow to predict the concentration of ClO_2^-, ClO_3^- and FAC in synthetic waters. However, the presence of (in)organic acids in real waters may catalyze the reaction and lead to lower concentrations of ClO_2^- than predicted by the model. The impact of real water matrices on the FAC/ClO_2^- reaction needs further investigations. The reaction of ClO_2^- with FAC was found to yield to ~ 70% of ClO_3^-, and the remaining 30% was suggested to be recovered as FAC via the reaction of the *in situ* regenerated ClO_2 with NOM. Therefore, the sum of oxychloro species (ClO_2^- + ClO_3^-) could be reduced during chlorination which is of interest as ClO_3^- is considered for regulation as well. Modelling the FAC/ClO_2^- reaction helps optimizing the ClO_2 pre-oxidation dose depending on the water reactivity, the pH and the contact time. This can significantly reduce the dose of FAC needed for disinfection and improve DBP mitigation, in particular the very potent HANs.

Similarly to ClO_2, O_3-tBuOH, Fe(VI) and Mn(VII) pre-oxidation were efficient pretreatments to reduce the formation of AOX, THMs and, particularly, HANs. One exception was the poor mitigating effect of Mn(VII) on THM formation. Considering the characteristics of the water, such as the pH and the bromide concentration is important when choosing the type and dose of pre-oxidant. For example, a pre-oxidation with O_3 or Fe(VI) at slightly acidic pH followed by an increase of pH before disinfection could be highly efficient in mitigating AOX formation. In presence of bromide, lower oxidant doses may be more beneficial to prevent the enhancement of more toxic brominated DBPs, especially when O_3 is used. Overall, ClO_2 was found to be the most appropriate option for the mitigation of HANs in presence of bromide. In comparison, Fe(VI) and Mn(VII) efficiencies on HAN mitigation were highly affected by pH while O_3-tBuOH greatly enhanced the very potent DBAN. The calculated toxicity based on THM and HAN formation suggests that the mitigation of HANs should be prioritized.

The investigations presented in this Thesis highlighted the following research prospects:

(i) Fundamental mechanistic studies on the reactivity of oxidants with organic compounds, and the products arising from their reaction are needed. Studies with model compounds will help apprehending the impact of oxidation on NOM characteristics and DBP mitigation. There are in particular significant knowledge gaps on the reaction pathways and kinetics of Mn(VII) and, to some extent, Fe(VI) with model compounds in conditions relevant to water treatment.

(ii) A systematic assessment of the impact of pre-oxidation on NOM characteristics (physicochemical and electrochemical) is necessary to compare results across studies. Using such parameters will allow to compare different oxidants (reacting through different mechanisms) and different water matrix (ratio of oxidant concentrations to NOM reactivity).

(iii) Further investigations on the combined capacity of surrogates (UVA, fluorescence, EDC) to characterize DBP precursors are essential to demonstrate their applicability in water treatment plants.

(iv) The impact of pre-oxidation on the type and amount of DBPs formed still warrant further investigation. Specifically, pre-oxidation will oxidize NOM shifting the molecular distribution from high molecular weight compounds to lower molecular weight compounds. Furthermore, the incorporation of the more toxic bromine and iodine can be enhanced after pre-oxidation. Even though the total DBP formation may be reduced after pre-oxidation, the toxicity might be driven by the possible additional formation of low molecular weight halogenated DBPs which are largely unidentified. Therefore, toxicity testing should be performed to validate the benefit of pre-oxidation during water treatment.

Appendix Chapter 2

Table A-2-1. Standard NOM extracts.

NOM extract	Abbreviation	Cat. No.
Pony Lake Fulvic Acid	PLFA	1R109F
Suwannee River Fulvic Acid	SRFA	2S101F
Nordic Lake Fulvic Acid	NLFA	1R105F
Suwannee River Humic Acid	SRHA	2S101H
Leornadite Humic Acid	LHA	1S104H
Upper Mississippi River RO	UMRNOM	1R110N
Suwannee River RO I	SRNOM I	1R101N
Suwannee River RO II	SRNOM II	2R101N

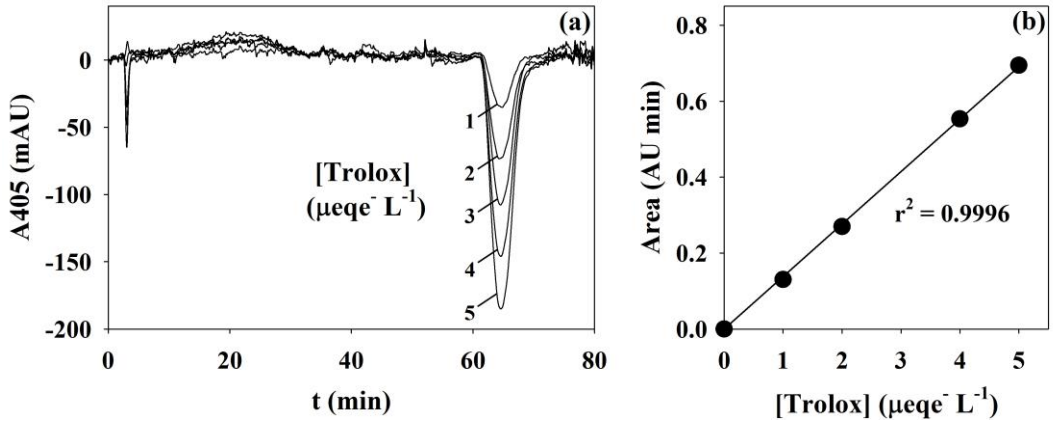

Figure A-2-1. EDC spectra of increasing doses of trolox (a) and the corresponding calibration (b). The trolox spectra were obtained by subtracting the spectra of a blank injection (ultrapure water).

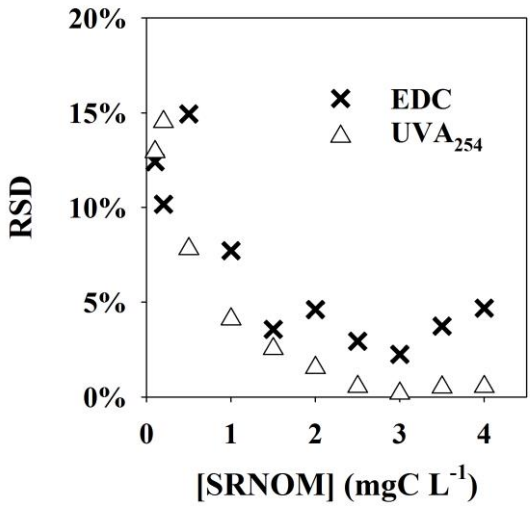

Figure A-2-2. Relative standard deviations of EDC and UVA_{254} for triplicated samples.

Appendix Chapter 3

Text A-3-1. Analytical method for THMs and HANs

The THMs and HANs were analyzed by headspace GC-MS with a method adapted from previously published methods.[1, 2] 3.60 g of sodium sulfate and 0.13 g of a quenching mixture (24 mg ascorbic acid, 1.2 g Na_2HPO_4, 19.8 g KH_2PO_4) were added to 10 mL of a sample previously spiked with an internal standard (5 µg L^{-1} of 1,2-dibromopropane) in a 20 mL screw top amber vial. Within 24 h, samples were shaken in an agitator for 15 min at 50°C, extracted on a DVB-CAR-PDMS fiber for 15 min at 50°C, and desorbed for 5 min in the GC-MS inlet at 220°C. The oven programming was as follows: 40°C hold for 5 min, 3°C min^{-1} to 54°C, 5°C min^{-1} to 150°C and 25°C min^{-1} to 300°C for a total analytical time of 39.9 min. SIM mode was used and the m/z ions used for quantification were similar to the published methods.[1, 2] The limits of detection were ranging from 0.1 to 0.3 nM for THMs and HANs except for mono halogenated HANs which had limits of detection ranging from 2 to 5 nM.

Text A-3-2. EDC and UVA measurements

The method was adapted from previous studies.[3, 4] A borate buffer (50 mM, pH 7.8) was pumped by a Agilent 1100 series system at 0.2 mL min^{-1} through a Toyopearl HW-50S column (8 x 300 mm, 30 µm) followed by a first UV detector at 254 nm. The sample was then mixed through a mixing tee with the post-column reagent, added by a post-column delivery system pressurized by helium at 0.05 mL min^{-1}. The mixing tee was followed by a 750 µL reaction coil and a second UV detector at 405 nm. The post-column reagent was prepared by mixing 6 mM of ABTS with 2 mM of sodium persulfate for 16 h to ensure complete reaction. The expected $ABTS^{+\bullet}$ concentration (4 mM) was then reached and remained stable for a week at room temperature (< 10% of decrease). The resulting solution was then diluted 100-fold in 20 µM H_2SO_4 to obtain the final concentrations: 40 µM $ABTS^{+\bullet}$ and 20 µM ABTS.

Text A-3-3. The reactivity and self-decay of Mn(VII) and Fe(VI) and their intermediates.

Mn(VI) and Mn(V), are highly reactive,[5, 6] but unstable species.[6, 7] At pH 8, Mn(VI) second order self-decay constant is 10^4 M^{-1} s^{-1}, while Mn(V) was too fast to be measurable.[7] However, the degradation of Mn(VI) and Mn(V) involves the regeneration of Mn(VII) and Mn(VI), respectively, which would slow down the overall self-decay of manganate species. Little literature exists on the reactivity of these species at near neutral pH that could be compared to their self-decay. A previous study showed that Mn(VII) was able to exchange 3 electrons with ABTS at near neutral pH,[8] which, together with the much higher EDC removal compared to ClO_2 (Figure 3-1a), suggests that the high reactivity of Mn(VI) and Mn(V) and/or the partial regeneration of Mn(VII) and Mn(VI) during auto-decomposition processes was substantially increasing Mn(VII) reactivity.

Similarly to Mn(VII), Fe(VI) intermediate products are unstable compounds, and Fe(VI) itself decomposes in water.[9, 10] At pH 8, Fe(V) exhibits a fast auto-decomposition (10^7 M^{-1} s^{-1} at pH 8)[9] compared to its reactivity toward phenol (10^2 M^{-1} s^{-1} at pH 7 and 9)[11, 12] or amino acids (10^5 M^{-1} s^{-1} at pH 8.8).[13] Unlike Mn(VI), the decomposition of Fe(V) doesn't regenerate its parent compound but produces the quite unreactive Fe(III).[9, 10] Furthermore, the presence of H_2O_2, notably formed during Fe(VI) decomposition, can enhance the decomposition of Fe(VI) and its intermediates.[10, 14] Contrary to Mn(VII)[8] and similarly to ClO_2,[15] Fe(VI) was shown to exchange only 1 electron with ABTS.[12] This suggests, together with our observed similar EDC abatement between the two oxidants (Figure 3-1a), that the auto-decomposition of Fe(VI) intermediates and, to some extent, Fe(VI) self-decay, are significantly reducing Fe(VI) oxidation capacity, as previously suggested.[10]

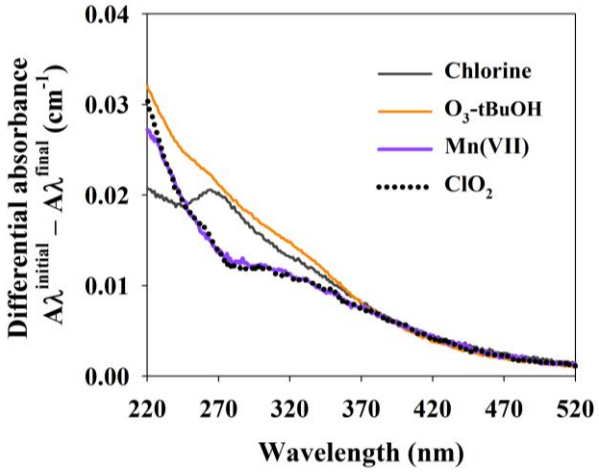

Figure A-3-1. Differential UV spectra after treatment of SRNOM with chlorine, O_3, Mn(VII) and ClO_2. [SRNOM] = 3 mgC L^{-1}, 40 mM borate (pH 8).

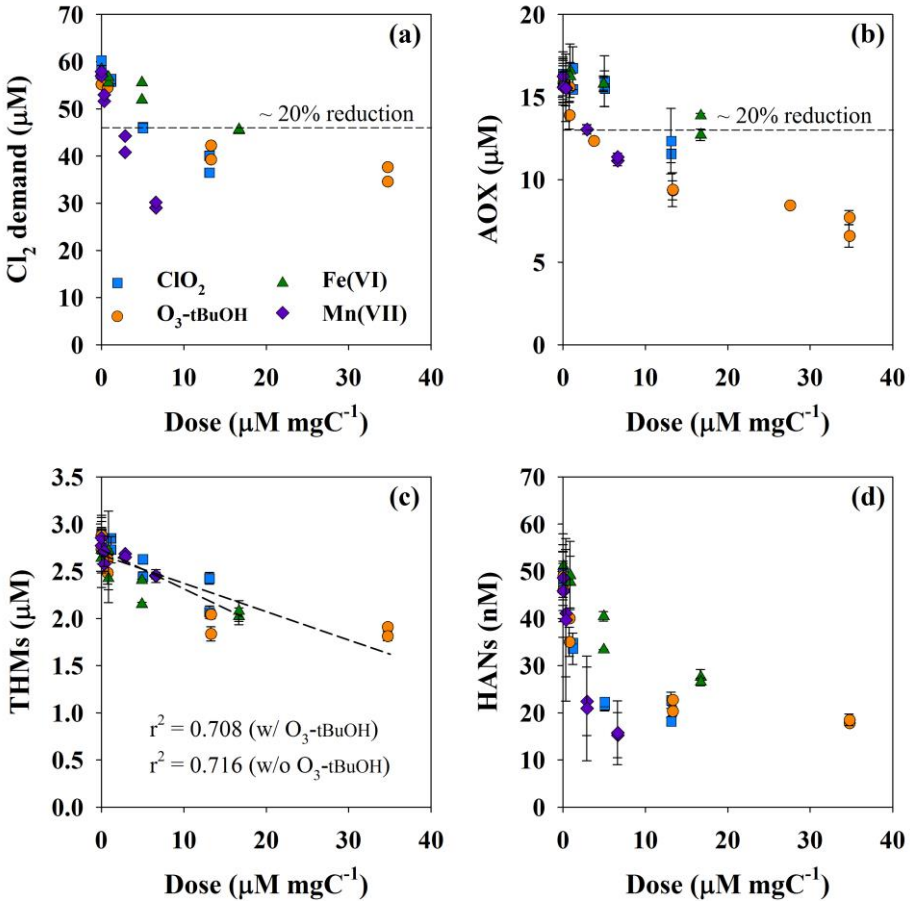

Figure A-3-2. Chlorine demand (a), AOX (b), THMs (c) and HANs (d) compared to the dose of pre-oxidant. [ClO_2] = 3.5 – 39 μM, [O_3-tBuOH] = 2.2 – 104 μM, [Fe(VI)] = 2.5 – 50 μM, [Mn(VII)] = 1 – 20 μM, [SRNOM] = 3 mgC L^{-1}, [Br^-] = 0 or 150 μg L^{-1}, 40 mM borate (pH 8). Error bars represent the range of analytical results for duplicated experiments (the two highest doses of Fe(VI) and Mn(VII) were not duplicated experiments), and chlorine demand was not duplicated.

References

1. Allard, S.; Charrois, J. W. A.; Joll, C. A.; Heitz, A., Simultaneous analysis of 10 trihalomethanes at nanogram per liter levels in water using solid-phase microextraction and gas chromatography mass-spectrometry. *J. Chromatogr. A* **2012,** *1238*, 15-21.
2. Kristiana, I.; Joll, C.; Heitz, A., Analysis of halonitriles in drinking water using solid-phase microextraction and gas chromatography–mass spectrometry. *J. Chromatogr. A* **2012,** *1225*, 45-54.
3. Chon, K.; Salhi, E.; von Gunten, U., Combination of UV absorbance and electron donating capacity to assess degradation of micropollutants and formation of bromate during ozonation of wastewater effluents. *Water Res.* **2015,** *81*, 388-397.
4. Önnby, L.; Walpen, N.; Salhi, E.; Sander, M.; von Gunten, U., Two analytical approaches quantifying the electron donating capacities of dissolved organic matter to monitor its oxidation during chlorination and ozonation. *Water Res.* **2018,** *144*, 677-689.
5. Záhonyi-Budó, É.; Simándi, L., Oxidation of propane-1,2-diol by acidic manganese(V) and manganese(VI). *Inorg. Chim. Acta* **1996,** *248*, (1), 81-84.
6. Simándi, L.; Záhonyi-Budó, É., Relative reactivities of hydroxy compounds with short-lived manganese(V). *Inorg. Chim. Acta* **1998,** *281*, (2), 235-238.
7. Simandi, L. I.; Jaky, M.; Savage, C. R.; Schelly, Z. A., Kinetics and mechanism of the permanganate ion oxidation of sulfite in alkaline solutions. The nature of short-lived intermediates. *J. Am. Chem. Soc.* **1985,** *107*, (14), 4220-4224.
8. Song, Y.; Jiang, J.; Ma, J.; Pang, S.-Y.; Liu, Y.-z.; Yang, Y.; Luo, C.-w.; Zhang, J.-q.; Gu, J.; Qin, W., ABTS as an Electron Shuttle to Enhance the Oxidation Kinetics of Substituted Phenols by Aqueous Permanganate. *Environm. Sci. Technol.* **2015,** *49*, (19), 11764-11771.
9. Rush, J. D.; Bielski, B. H. J., Kinetics of ferrate(V) decay in aqueous solution. A pulse-radiolysis study. *Inorganic Chemistry* **1989,** *28*, (21), 3947-3951.
10. Lee, Y.; Kissner, R.; Von Gunten, U., Reaction of ferrate(VI) with ABTS and self-decay of ferrate(VI): Kinetics and mechanisms. *Environm. Sci. Technol.***2014,** *48*, (9), 5154-5162.
11. Rush, J. D.; Cyr, J. E.; Zhao, Z.; Bielski, B. H. J., The Oxidation of Phenol by Ferrate(VI) Andferrate(V). A Pulse Radiolysis and Stopped-Flow Study. *Free Radical Res.* **1995,** *22*, (4), 349-360.
12. Lee, Y.; Yoon, J.; Von Gunten, U., Spectrophotometric determination of ferrate (Fe(VI)) in water by ABTS. *Water Res.* **2005,** *39*, (10), 1946-1953.
13. Rush, J. D.; Bielski, B. H. J., The Oxidation of Amino Acids By Ferrate(V). A Pre-Mix Pulse Radiolysis Study. *Free Radical Res.* **1995,** *22*, (6), 571-579.
14. Rush, J. D.; Zhao, Z.; Bielski, B. H. J., Reaction of Ferrate (VI)/Ferrate (V) with Hydrogen Peroxide and Superoxide Anion - a Stopped-Flow and Premix Pulse Radiolysis Study. *Free Radical Res.* **1996,** *24*, (3), 187-198.
15. Pinkernell, U.; Nowack, B.; Gallard, H.; Von Gunten, U., Methods for the photometric determination of reactive bromine and chlorine species with ABTS. *Water Res.* **2000,** *34*, (18), 4343-4350.

Appendix Chapter 4

Text A-4-1. Quenching procedure

For experiments with ClO_2 concentrations < 50 μM, no ClO_2 residual remained after 24 h. For experiments with ClO_2 concentrations ≥ 50 μM, samples were quenched with an excess of sulfite to avoid any interferences from chlorite ion (ClO_2^-). A 10 times molar excess relative to the ClO_2^- concentration was used to quench the ClO_2^- and prevent interferences in adsorbable organic chlorine (AOCl) measurements. It was verified that the sulfite was not degrading any AOCl under our experimental conditions. The other oxidant residuals were quenched with ascorbic acid (10% molar excess). Trihalomethanes (THMs) and haloacetonitriles (HANs) samples were quenched separately (Text A-3-1).

Text A-4-2. Direct UV measurement of benzoquinone

Direct UV at 244 nm was used to quantify benzoquinone. At 244 nm, the absorption coefficients of benzoquinone and phenol are respectively: $\varepsilon_{Benzoquinone}$ =19204 M^{-1} cm^{-1} and ε_{Phenol} < 1000 M^{-1} cm^{-1}.[3] Even if all the initial phenol was still present in solution at concentrations equimolar to the final benzoquinone, the interference in UV at 244 nm would be < 10%. As phenol degrades, the benzoquinone concomitantly increases and the interference is expected to be << 10%. The large difference in absorbance between phenol and benzoquinone at 244 nm can be observed in Figure A-4-1a.

Text A-4-3. ABTS measurements[4]

Up to 4 mL of sample was added to 0.5 mL phosphate buffer (500 mM, pH 6.1) and 0.2 mL ABTS (2,2'-azino-bis(3-ethylbenzothiazoline-6-sulfonic acid) diammonium salt) (1.9 mM, 1 g L^{-1}) in a 5 mL volumetric flask. For the total oxidant, 40 μL of potassium iodide (1 mM, 166 mg L^{-1}) was added. Iodide catalyzes the reaction between FAC (or NH_2Cl) and ABTS. For the ClO_2 measurement, 60 μL of glycine

(533 mM, 40 g L^{-1}) and 60 µL of mercury(II) chloride (11 mM, 3 g L^{-1}) were also added. Glycine quenched FAC and NH_2Cl doesn't react with ABTS in absence of iodide. Mercury(II) chloride complexed any potential iodide trace to avoid any catalytic reaction between chlorine, monochloramine or *N*-chloroglycine and ABTS. The volume was topped up to 5 mL with ultrapure water and the absorbance at 405 nm (ε_{405} = 28500 M^{-1} cm^{-1})[1] was measured after about 8 min reaction time. The concentration of FAC (or NH_2Cl) was calculated as the difference between total oxidant and ClO_2.

Text A-4-4. Impact of chloride ions on free available chlorine (FAC) speciation

The NaOCl solution used to spike FAC also contains chloride ions (1.9 µM of Cl^- per 1 µM of FAC, Table A-4-1). Spiking 15 µM of FAC (highest dose used) would also add 28 µM of Cl^-. At pH 8 (used for the experiments comparing ClO_2 and dosed FAC), this would lead to a HOCl to Cl_2 ratio of 2 x 10^9. From a previous study,[7] the apparent second order rate constants for the reactions of Cl_2 and HOCl with phenol would be 2.7 x 10^7 M^{-1} s^{-1} and 2.2 x 10^2 M^{-1} s^{-1}, respectively, under these conditions. The ratio of these rate constants (1.2 x 10^5) is much smaller than the HOCl to Cl_2 ratio (2 x 10^9), meaning that the Cl_2 reaction with phenol, and likely other precursors, is negligible under these conditions.

Table A-4-1. Chlorinated impurities measured in NaOCl and $NaClO_2$ stocks.

	Impurity (Mimpurity/Mstock)	
	Cl^-	**ClO_3^-**
NaOCl	1.9	0.22
$NaClO_2$	0.3	<0.01

Table A-4-2. Water quality parameters.

	DOC (mgC L^{-1})	SUVA (L mgC^{-1} m^{-1})	Relative UVA[b]	Relative EDC[b]	Br^- (µg L^{-1})	pH
NOM extract Cat. No.						
PLFA 1R109F	3.0	3.0[a]	0.83	0.78	0	8.1
UMRNOM 1R110N	3.0	3.2[a]	1.08	0.86	0	8.1
SRNOM 2R101N	3.0	3.4[a]	1.18	1.08	0	8.1
NLFA 1R105F	3.0	4.8[a]	1.41	2.06	0	8.1
Real waters						
P105	2.6	1.6	0.44	0.47	295	7.4
P65	4.2	2.8	1.10	1.38	226	7.2
P100	9.2	3.6	2.69	4.36	185	6.5

[a]Values taken from Walpen et al. (2016). [b]The relative EDC or UVA of the untreated waters were calculated as the EDC or UVA signal of the samples divided by the EDC or UVA signal of an unbuffered 3.0 mgC L^{-1} SRNOM solution.

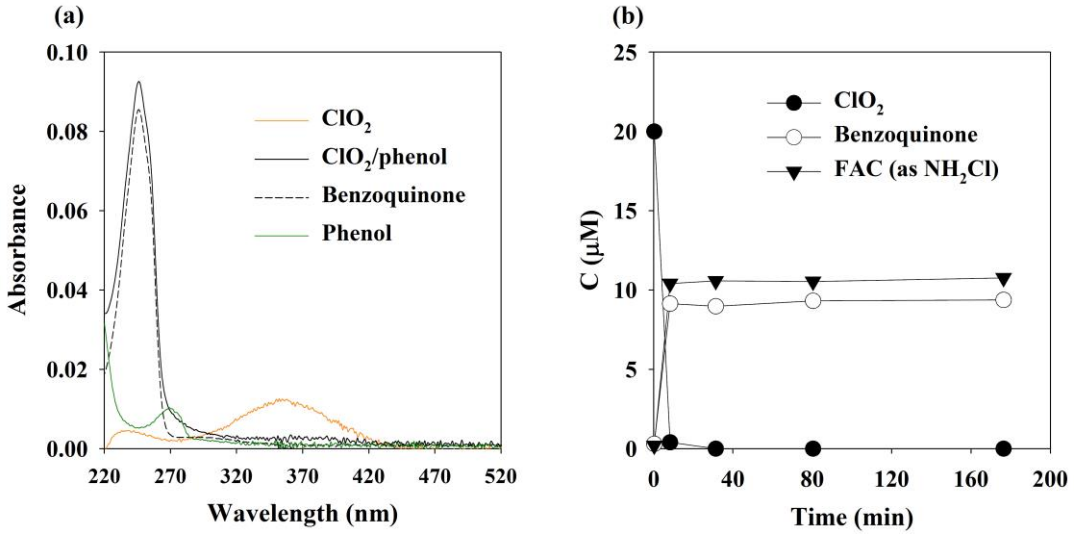

Figure A-4-1. Reaction of ClO_2 with phenol. (a) Spectra of ClO_2 (orange line) and phenol (green line) before and after 10 min (black line) compared to the spectrum of benzoquinone (black dashed line). (b) Kinetics of ClO_2 decrease and formation of FAC (as NH_2Cl) and benzoquinone.

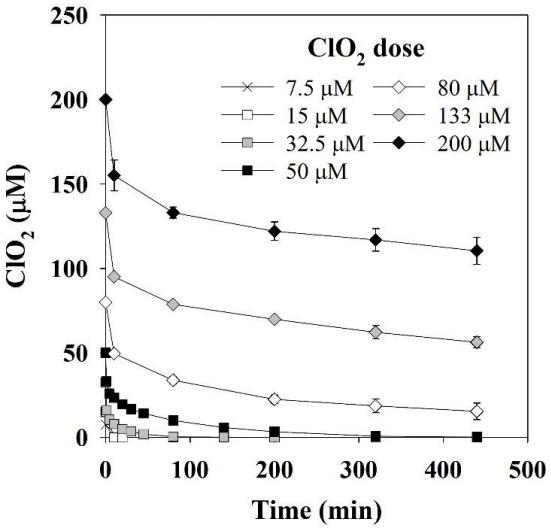

Figure A-4-2. Kinetics of ClO_2 consumption by 3.0 mgC L^{-1} of SRNOM. $[ClO_2]$ = 7.5–200 µM, $[NH_4^+]$ = 150 µM, pH 8.1, 10 mM phosphate. Error bars represent the range of results of duplicate experiments.

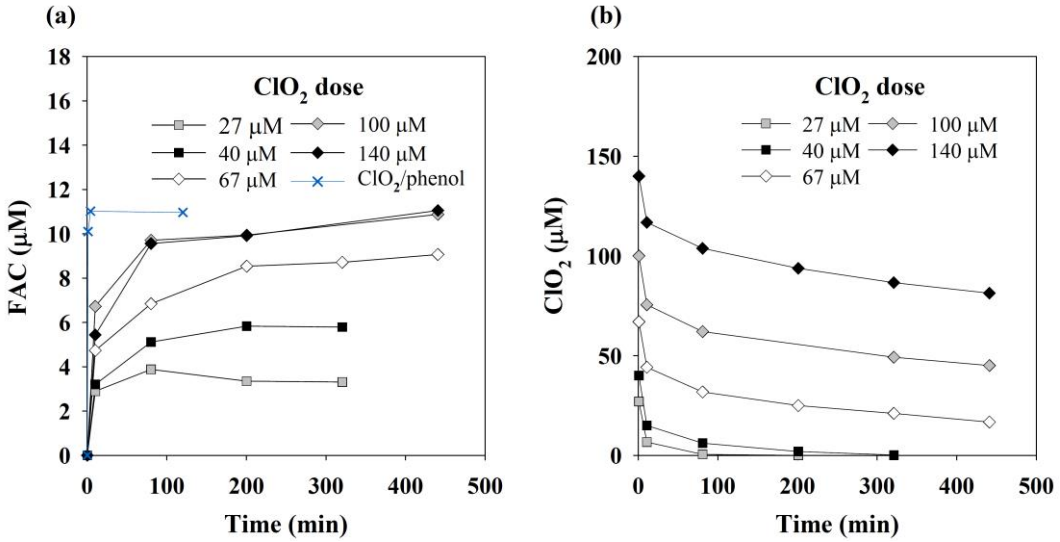

Figure A-4-3. Kinetics of (a) *in situ* FAC formation and (b) ClO_2 decrease from the reaction of ClO_2 with UMRNOM (3.0 mgC L^{-1}). The blue crosses represent the FAC formation from the reaction between ClO_2 and phenol (20/10 µM). $[ClO_2]$ = 27 – 140 µM, $[NH_4^+]$ = 150 µM, pH 8.1, 10 mM phosphate.

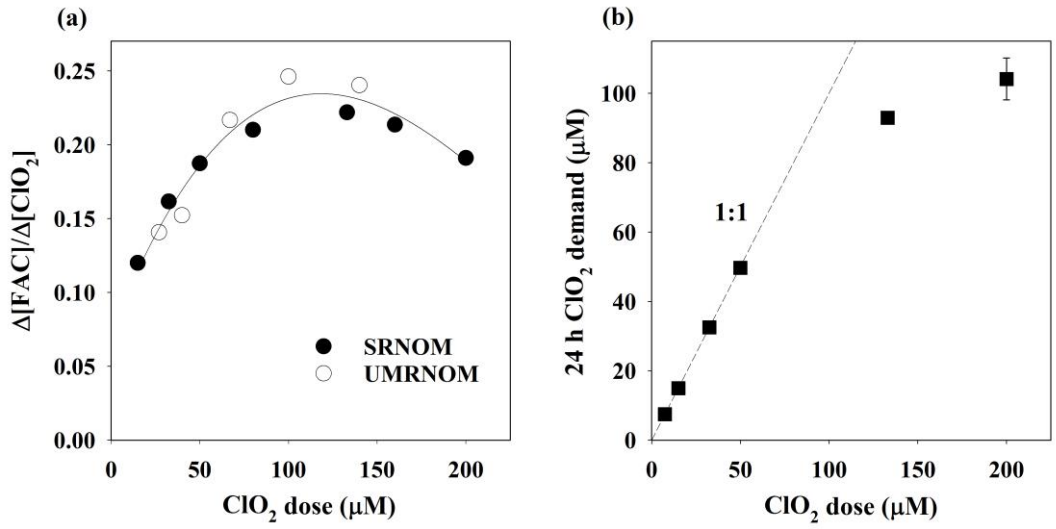

Figure A-4-4. (a) *In situ* FAC formation yield ($\Delta FAC/\Delta ClO_2$) at 400 min from the oxidation of SRNOM and UMRNOM with ClO_2. The curve represents a quadratic fitting on the combined SRNOM and UMRNOM data ($r^2 = 0.934$). (b) ClO_2 demand at 24 h in a SRNOM-containing solution. The dashed line represents a complete consumption of ClO_2. [ClO_2] = 7.5 – 200 μM, [NOM] = 3.0 mgC L^{-1}, pH 8.1, 10 mM phosphate.

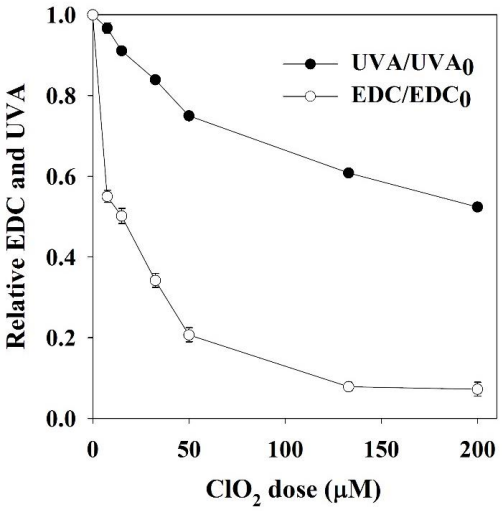

Figure A-4-5. Relative EDC and UVA response for the reaction of ClO_2 with SRNOM. The relative response was calculated as the ratio between the treated samples and the untreated sample. The interference of ClO_2^- on UVA was removed by subtracting the corresponding absorbance resulting from the same ClO_2^- concentration. [ClO_2] = 7.5–200 μM, [SRNOM] = 3.0 mgC L^{-1}, pH 8.1, 10 mM phosphate, 24 h reaction time. Error bars represent the range of results of duplicate experiments.

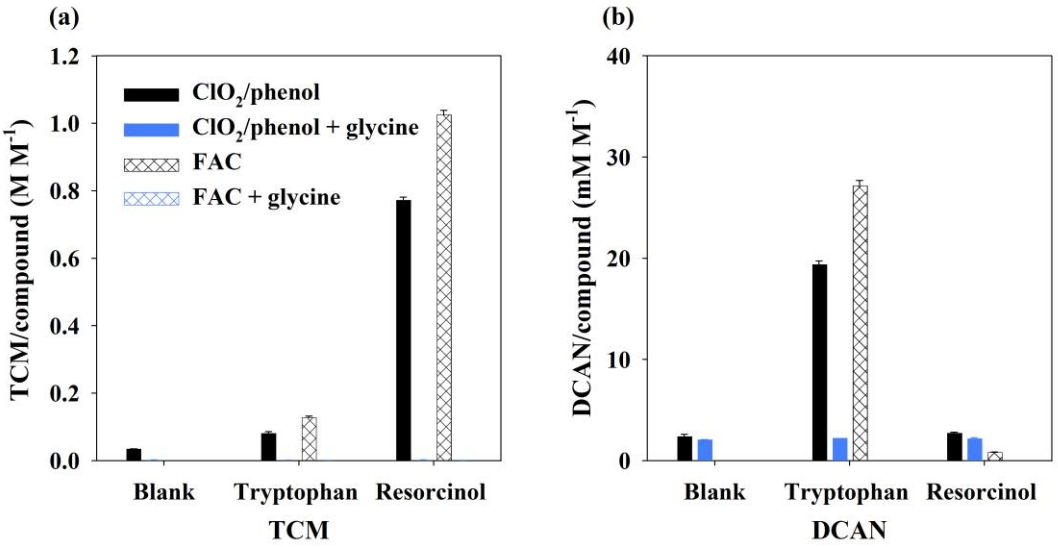

Figure A-4-6. Formation of (a) TCM and (b) DCAN from the reaction between pre-formed FAC (by ClO_2/phenol reaction) or dosed FAC and tryptophan/resorcinol. Solid bars represent the chlorination with pre-formed FAC and patterned bars with dosed FAC. Black and blue bars represent experiments without and with glycine, respectively. [ClO_2] = 80 µM, [phenol] = 40 µM, [FAC] = 40 µM, [glycine] = 0.4 mM, [model compound] = 2 µM, pH 7.5, 25 mM phosphate. Error bars represent the range of results of duplicate analyses.

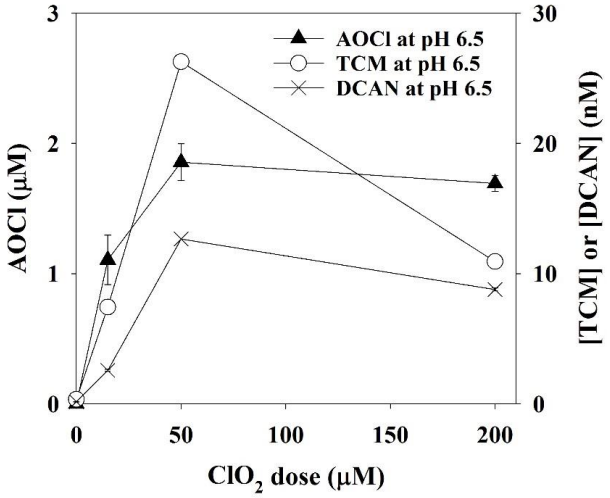

Figure A-4-7. Disinfection by-products formation from the reaction of ClO_2 with SRNOM for varying ClO_2 doses. [ClO_2] = 7.5–200 µM, [SRNOM] = 3.0 mgC L^{-1}, pH 6.5, 10 mM phosphate, 24 h reaction time. Error bars represent the range of results of duplicate analyses.

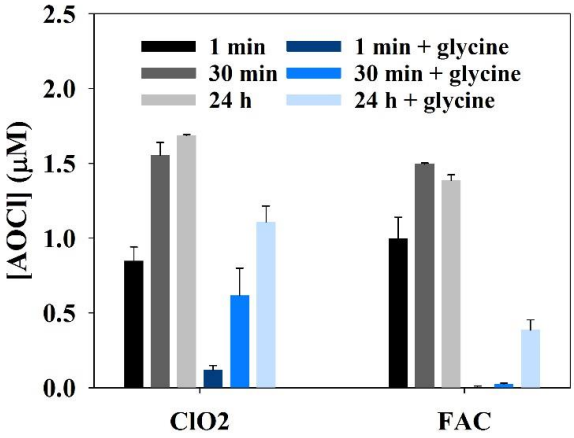

Figure A-4-8. AOCl formation from the reaction of SRNOM with 32.5 μM ClO_2 or 5.3 μM of dosed FAC. Gray and blue bars represent experiments without and with glycine, respectively. DBPs were analyzed after 1 min, 30 min and 24 h. [SRNOM] = 3.0 mgC L^{-1}, pH 8.1, 10 mM phosphate. Error bars represent the range of results of duplicate analyses.

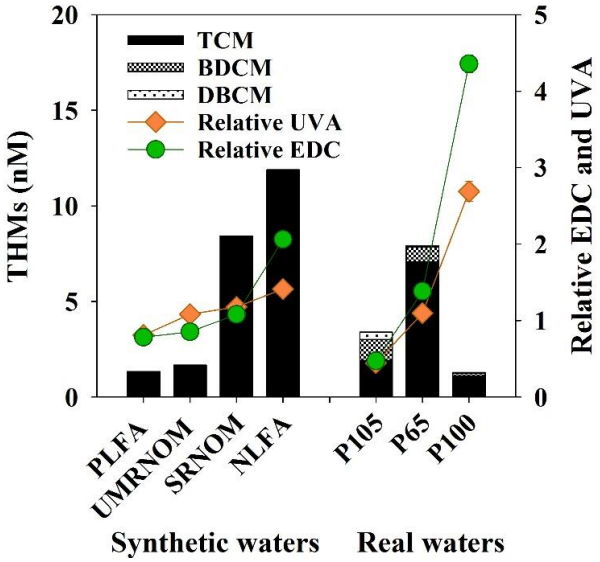

Figure A-4-9. THMs formed from the reactions of ClO_2 with synthetic (PLFA, UMRNOM, SRNOM, NLFA) and real waters (P105, P65, P100) compared to the relative EDC and UVA of the untreated sample. TCM: chloroform, BDCM: bromodichloromethane, DBCM: dibromochloromethane. The relative EDC and UVA were calculated as the EDC or UVA signal of the samples divided by the EDC or UVA signal of an unbuffered 3.0 mgC L^{-1} SRNOM solution, respectively. [ClO_2] = 15 μM, 24 h reaction time, NOM characteristics and characteristic of the real water samples are given in Table A-4-2. No Br^- was spiked into synthetic waters while real waters contained 135–235 μg L^{-1}. Error bars represent the range of results of duplicate analyses.

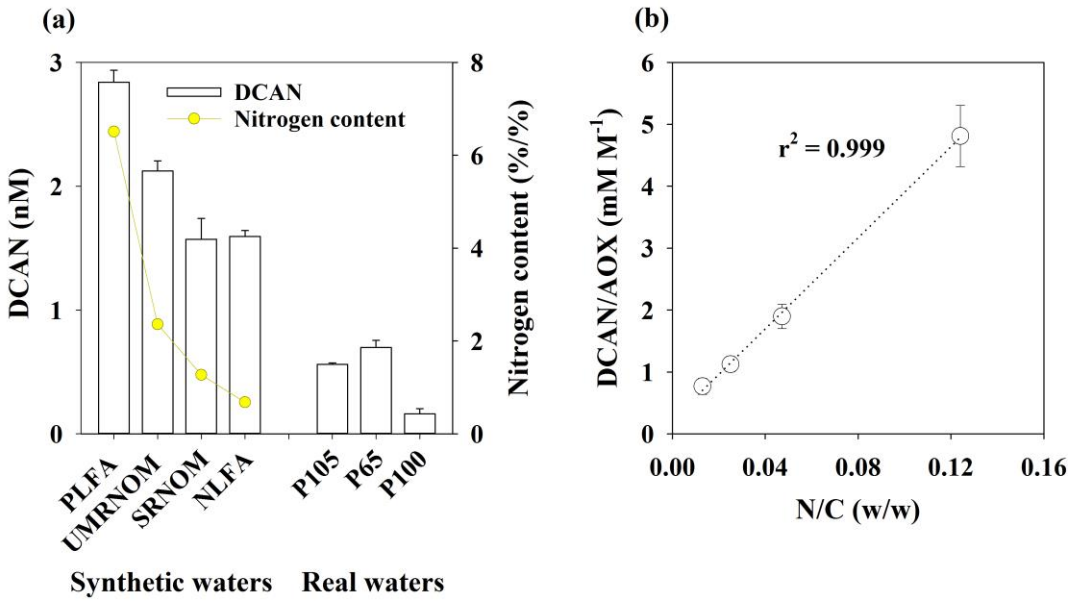

Figure A-4-10. (a) DCAN formed from the reaction of ClO_2 with synthetic (PLFA, UMRNOM, SRNOM, NLFA) and real waters (P105, P65, P100) compared to the nitrogen content[8] and (b) correlation between DCAN/AOX and N/C ratios for synthetic waters. [ClO_2] = 15 µM, 24 h reaction time, NOM characteristics are given in Table A-4-2. Error bars represent the range of results of duplicate analyses.

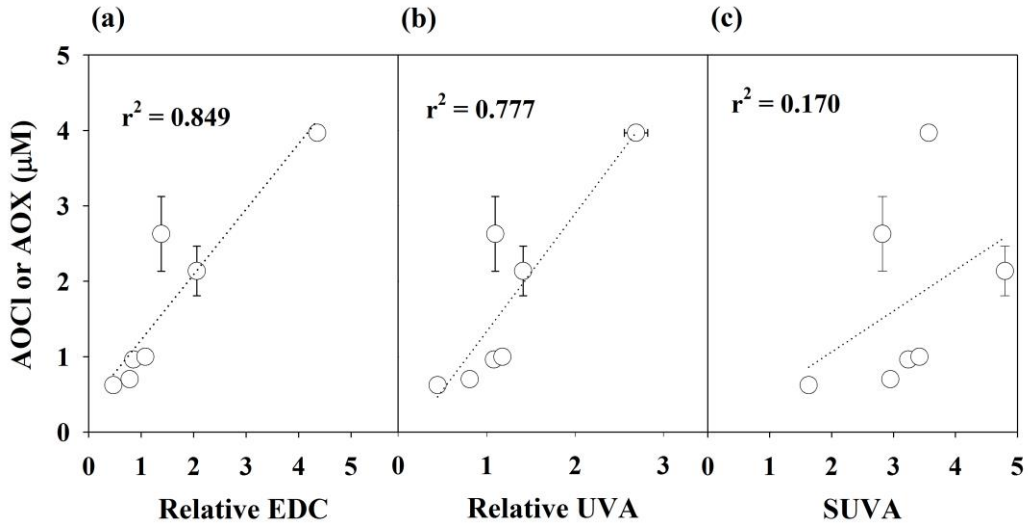

Figure A-4-11. AOX versus the relative EDC (a), the relative UVA (b) and the SUVA (c) for synthetic (PLFA, UMRNOM, SRNOM, NLFA) and real waters (P105, P65, P100). The relative EDC and UVA were calculated as the EDC or UVA signal of the samples divided by the EDC or UVA signal of an unbuffered 3.0 mgC L^{-1} SRNOM solution, respectively. [ClO_2] = 15 µM, 24 h reaction time, NOM characteristics are given in Table A-4-2. Error bars represent the range of results of duplicate analyses.

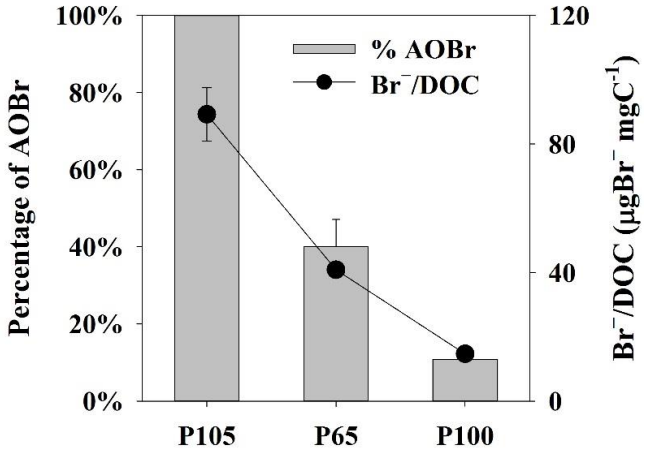

Figure A-4-12. Percentage of AOBr in AOX (bars) compared with Br^-/DOC ratio (symbols) for real water samples. [ClO_2] = 15 µM, 24 h reaction time, water quality parameters of the real water samples are given in Table A-4-2. Error bars represent the range of results of duplicate analyses.

References

1. Allard, S.; Charrois, J. W. A.; Joll, C. A.; Heitz, A., Simultaneous analysis of 10 trihalomethanes at nanogram per liter levels in water using solid-phase microextraction and gas chromatography mass-spectrometry. *J. Chromatogr. A* **2012,** *1238*, 15-21.
2. Kristiana, I.; Joll, C.; Heitz, A., Analysis of halonitriles in drinking water using solid-phase microextraction and gas chromatography–mass spectrometry. *J. Chromatogr. A* **2012,** *1225*, 45-54.
3. Wilke, T.; Schneider, M.; Kleinermanns, K., 1,4-Hydroquinone is a Hydrogen Reservoir for Fuel Cells and Recyclable via Photocatalytic Water Splitting. *Open J. Phys. Chem.* **2013,** *3*, 97-102.
4. Pinkernell, U.; Nowack, B.; Gallard, H.; Von Gunten, U., Methods for the photometric determination of reactive bromine and chlorine species with ABTS. *Water Res.* **2000,** *34*, (18), 4343-4350.
5. Chon, K.; Salhi, E.; von Gunten, U., Combination of UV absorbance and electron donating capacity to assess degradation of micropollutants and formation of bromate during ozonation of wastewater effluents. *Water Res.* **2015,** *81*, 388-397.
6. Önnby, L.; Walpen, N.; Salhi, E.; Sander, M.; von Gunten, U., Two analytical approaches quantifying the electron donating capacities of dissolved organic matter to monitor its oxidation during chlorination and ozonation. *Water Res.* **2018**, *144*, 677-689.
7. Lau, S. S.; Abraham, S. M.; Roberts, A. L., Chlorination Revisited: Does Cl– Serve as a Catalyst in the Chlorination of Phenols? *Environ. Sci. Technol.* **2016,** *50*, (24), 13291-13298.
8. I.H.S.S http://humic-substances.org

Appendix Chapter 5

Table A-5-1. Real waters characteristics.

Water	DOC ($mgC\ L^{-1}$)	SUVA ($L\ mgC^{-1}\ m^{-1}$)	Br^- ($\mu g\ L^{-1}$)	pH
P120	3	2.3	190	6.5
P130	4.2	2.5	260	7.2
W20	6.8	3.5	219	6.6

Table A-5-2. Model for ClO_2 disproportionation catalyzed by OCl^- provided by Wang et al.[1]

Equations	Rate constant
$ClO_2 + OCl^- \rightarrow ClO_2^- + ClO$	$9.1 \times 10^{-1}\ M^{-1}s^{-1}$
$ClO_2^- + ClO \rightarrow ClO_2 + OCl^-$	$3.6 \times 10^{9}\ M^{-1}s^{-1}$
$ClO_2 + ClO \rightarrow OCl^- + ClO_3^-$	$7.0 \times 10^{9}\ M^{-1}s^{-1}$

Table A-5-3. Equations and rate constants for the equilibrium between Cl_2, HOCl and Cl^- provided by Peintler et al.[2]

Equations	Rate constant
$Cl_2 + H_2O \rightarrow HOCl + Cl^- + H^+$	$11\ s^{-1}$
$HOCl + Cl^- + H^+ \rightarrow Cl_2 + H_2O$	$1.8 \times 10^{4}\ M^{-2}s^{-1}$

Table A-5-4. Individually fitted rate constants for Model 1, 2 and 3.

	Fitted constant (M^{-2} s^{-1})
Model 1	k1 = 4.59 x 10^5
Model 2	k6a = 4.74 x 10^5 k6b = 4.90 x 10^1
Model 3	k9 = 2.28 x 10^8

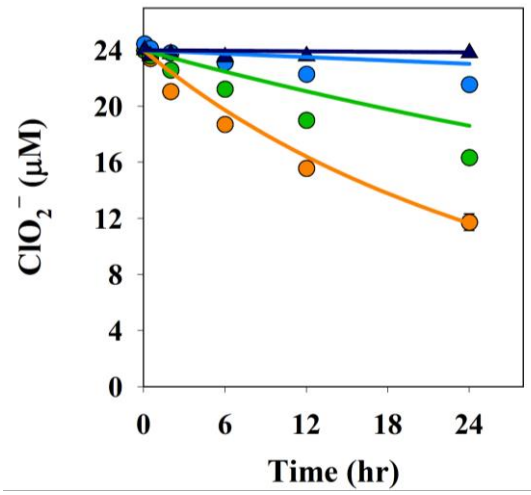

Figure A-5-1. Comparison between the Model 2, with k6b fitted, (lines) and experimental data (circles) of the decrease of ClO_2^- overtime. The fitted constant was k6b and is provided in Table A-5-4. [ClO_2^-]i = 23.7 μM, [HOCl]i = 65 μM, pH 6.6–8.1 (10 mM phosphate). Error bars represent duplicated experiments.

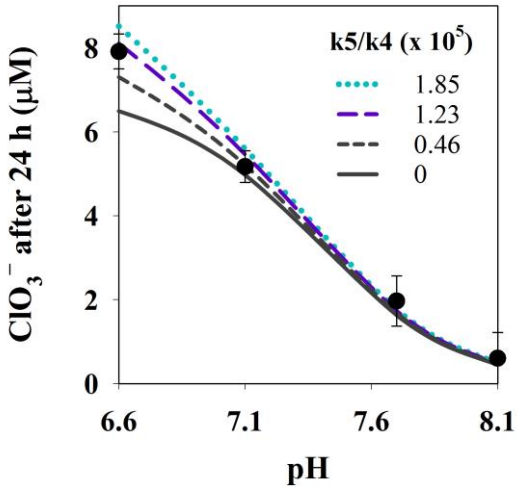

Figure A-5-2. Fitting of k5/k4 based on ClO_3^- formation after 24 h. The blue line represents the model after fitting of k1 (2.25 x 10^5 M^{-2} s^{-1}) and k3 (1.43 x 10^3 M^{-2} s^{-1}) (Figure 5-2) while the purple line represents the selected model. [ClO_2^-]i = 23.7 μM, [HOCl]i = 65 μM, pH 6.6–8.1 (10 mM phosphate).

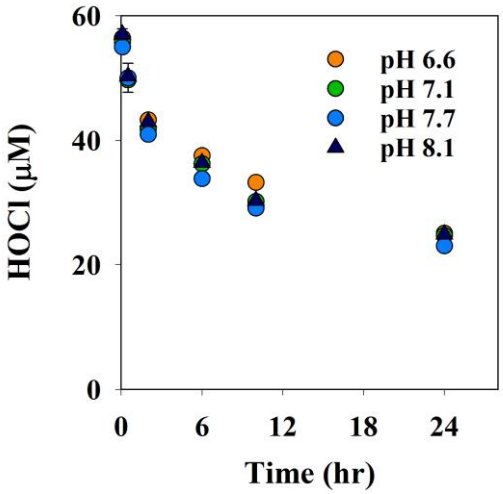

Figure A-5-3. HOCl decay in 3 mgC L^{-1} of UMRNOM at different pHs. [HOCl]i = 65 μM, 10 mM phosphate.

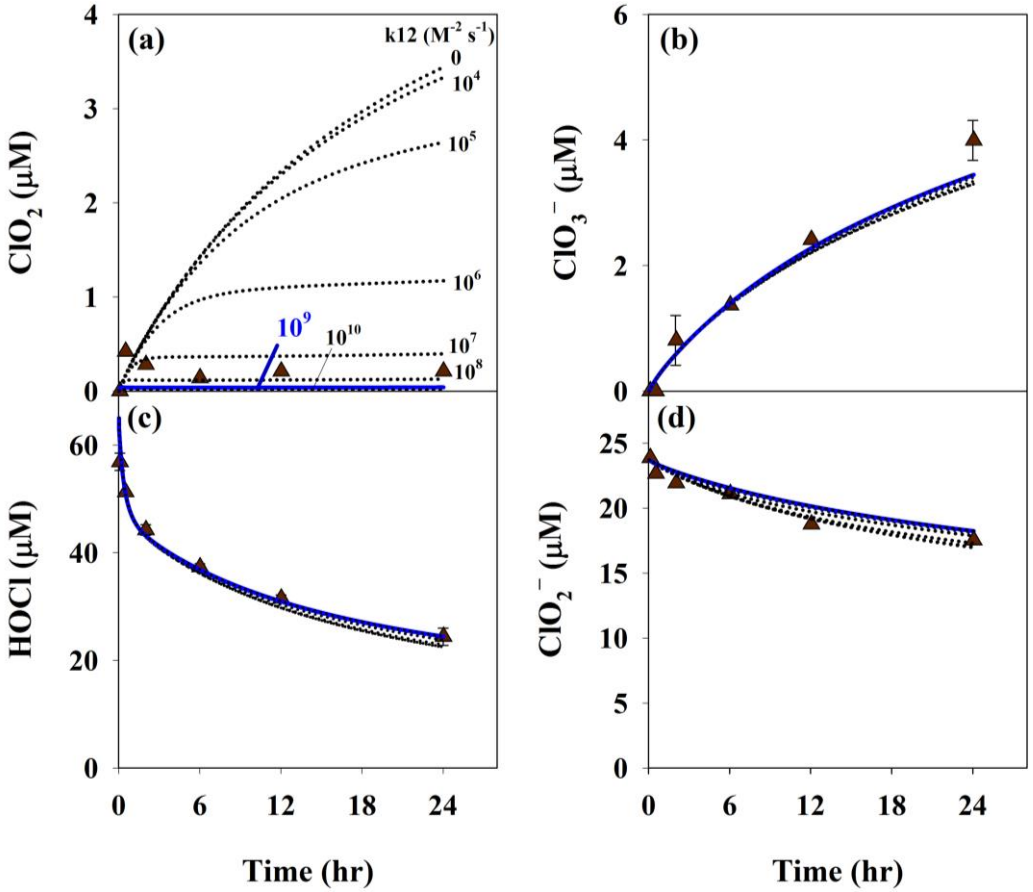

Figure A-5-4. Sensitivity analysis of k12 (0–10^{10} M^{-2} s^{-1}) on ClO_2 formation in presence of NOM (a). The impact on ClO_3^- formation (b) and HOCl (c) and ClO_2^- (d) decay is also shown. [ClO_2^-]i = 23.7 μM, [HOCl]i = 65 μM, [UMRNOM] = 3 mgC L^{-1}, pH 6.5.

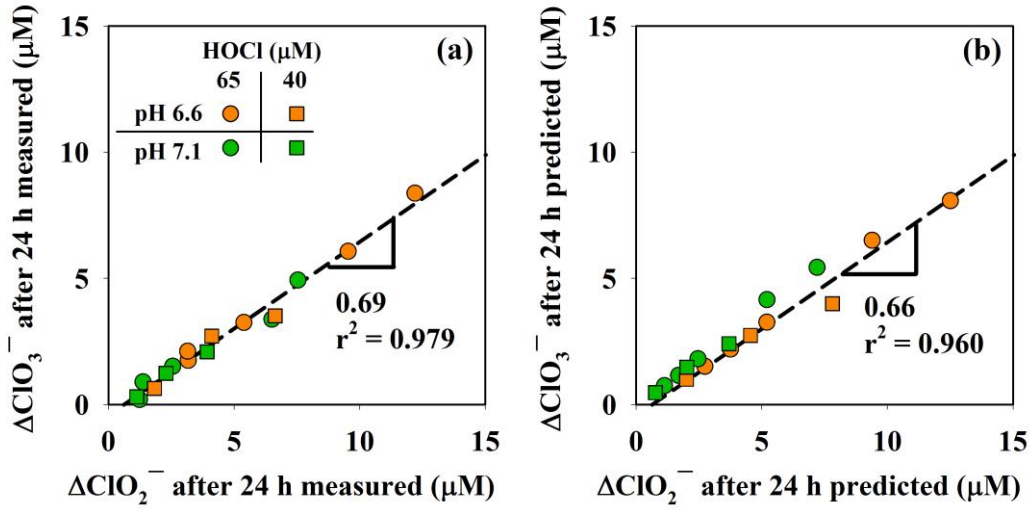

Figure A-5-5. Formation of ClO_3^- compared to the loss of ClO_2^- at various conditions. The comparison is made for measured (a) and predicted (b) data. [ClO_2^-]i = 23.7 μM, [HOCl]i = 40–65 μM, [UMRNOM] = 1–5 mgC L^{-1}, [NLFA] = 3 mgC L^{-1}, pH 6.6–7.1 (10 mM phosphate).

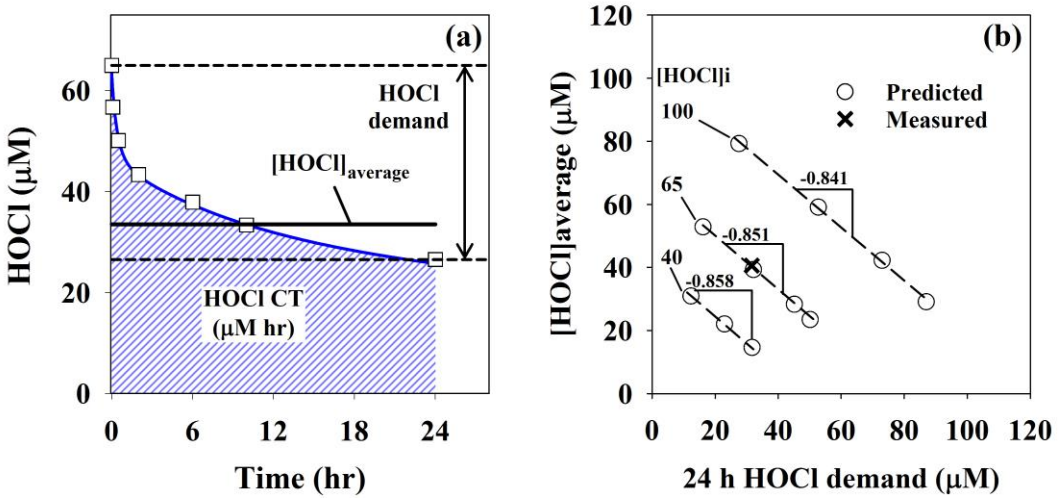

Figure A-5-6. (a) Example of HOCl exposure (CT), average HOCl and HOCl demand. (b) Correlation between the predicted average HOCl concentration and the predicted HOCl demand at various conditions. The experimental data corresponding to the HOCl decays observed in Figure A-5-3 is also shown. [HOCl]i = 40–100 μM, [aromatic carbon] = 15–120 μM, 24 h.

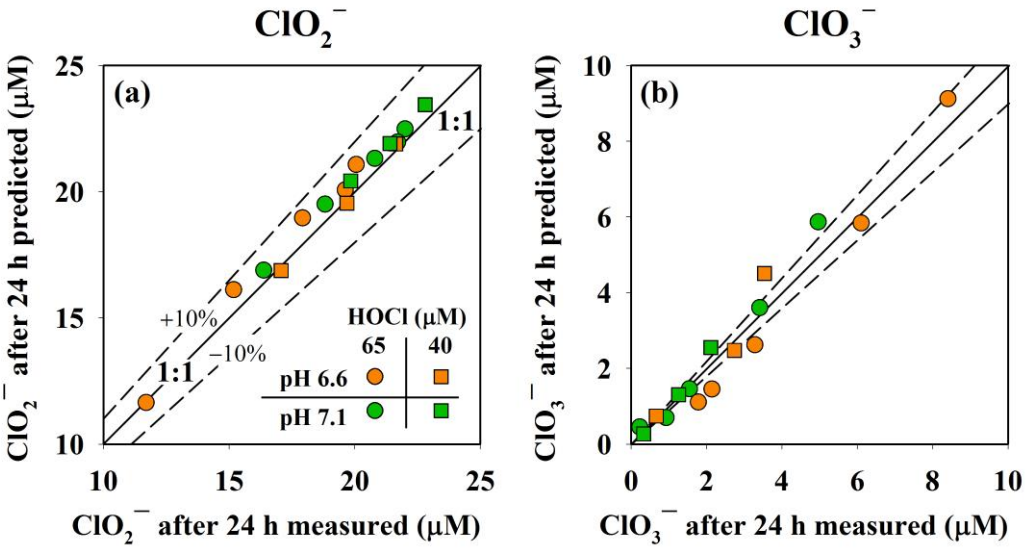

Figure A-5-7. Predicted versus measured ClO_2^- (a) and ClO_3^- (b) after 24 h. The values were predicted by using a fixed HOCl calculated from eq 5-13. $[ClO_2^-]i$ = 23.7 μM, [HOCl]i = 40–65 μM, [UMRNOM] = 1–5 mgC L^{-1}, [NLFA] = 3 mgC L^{-1}, pH 6.6–7.1 (10 mM phosphate).

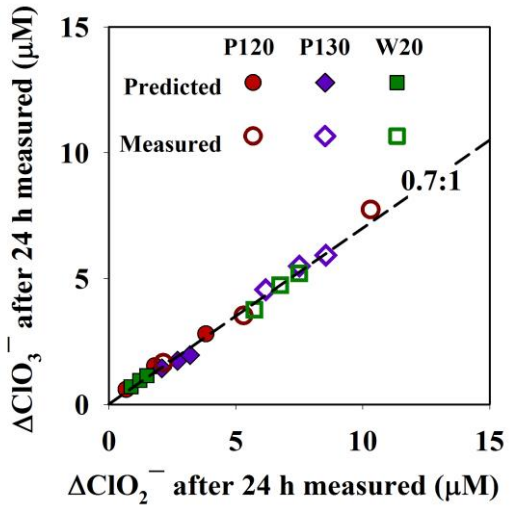

Figure A-5-8. Formation of ClO_3^- compared to the loss of ClO_2^- during chlorination in real waters. Predicted and measured data are shown in closed and open symbols, respectively. $[ClO_2]$ = 15–30 μM (1–2 mg L^{-1}), [HOCl] = 52–124 μM (3.7–8.8 mgCl_2 L^{-1}), 24 h reaction time. Characteristics of the real water samples are given in Table A-5-1 and ClO_2^- concentrations before chlorination are shown in Figure 5-7.

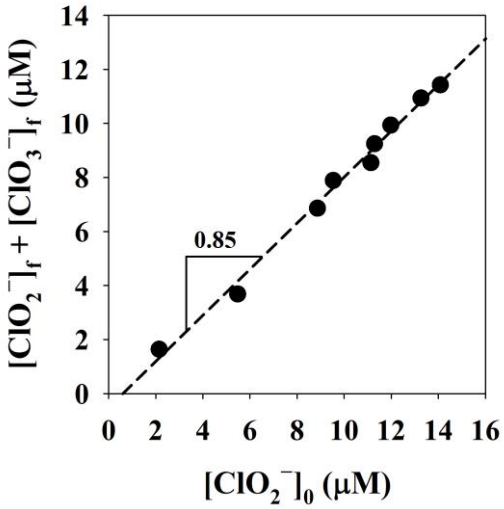

Figure A-5-9. Sum of ClO_2^- and ClO_3^- concentrations after chlorination compared to ClO_2^- concentration before chlorination in real waters. [HOCl] = 52–124 μM (3.7–8.8 mgCl_2 L^{-1}), 24 h reaction time. Characteristics of the real water samples are given in Table A-5-1 and ClO_2^- concentrations before chlorination are shown in Figure 5-7.

References

1. Wang, L.; Margerum, D. W., Hypohalite Ion Catalysis of the Disproportionation of Chlorine Dioxide. *Inorg. Chem.* **2002,** *41*, (23), 6099-6105.
2. Peintler, G.; Nagypal, I.; Epstein, I. R., Systematic design of chemical oscillators. 60. Kinetics and mechanism of the reaction between chlorite ion and hypochlorous acid. *J. Phys. Chem.* **1990,** *94*, (7), 2954-2958.

Appendix Chapter 6

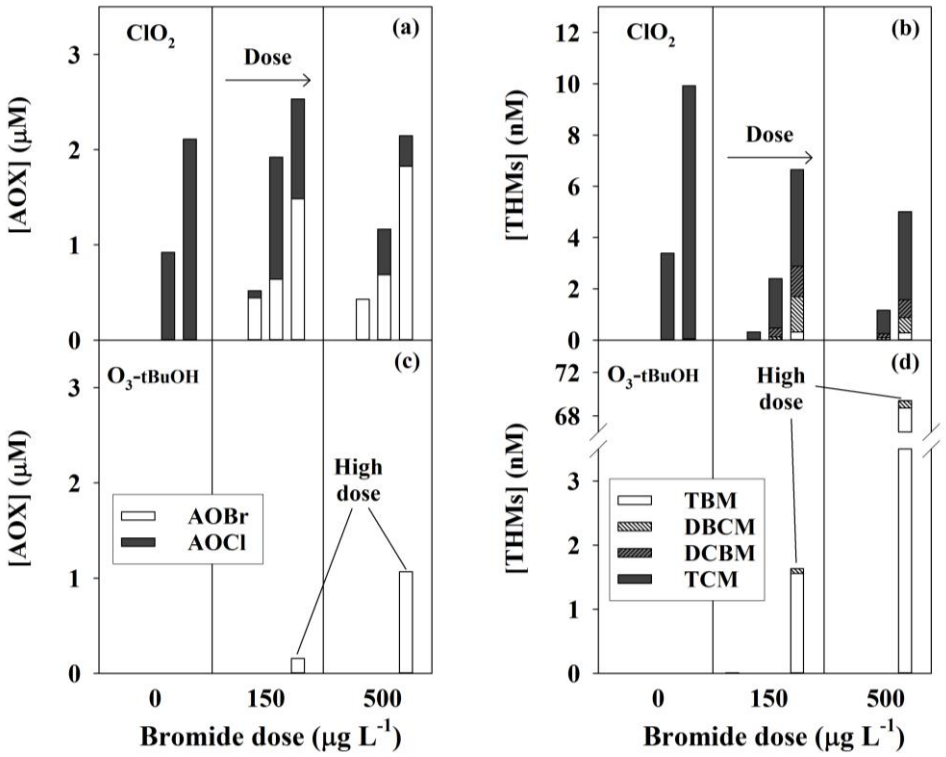

Figure A-6-1. Formation of AOX (a,c) and THMs (b,d) after ClO_2 and O_3-tBuOH pre-oxidation. [ClO_2] = 3.5–39.3 µM, [O_3-tBuOH] = 2.2–104.1 µM, [SRNOM] = 3 mgC L^{-1}, pH 8 (40 mM borate), [Br^-] = 0–500 µg L^{-1}.

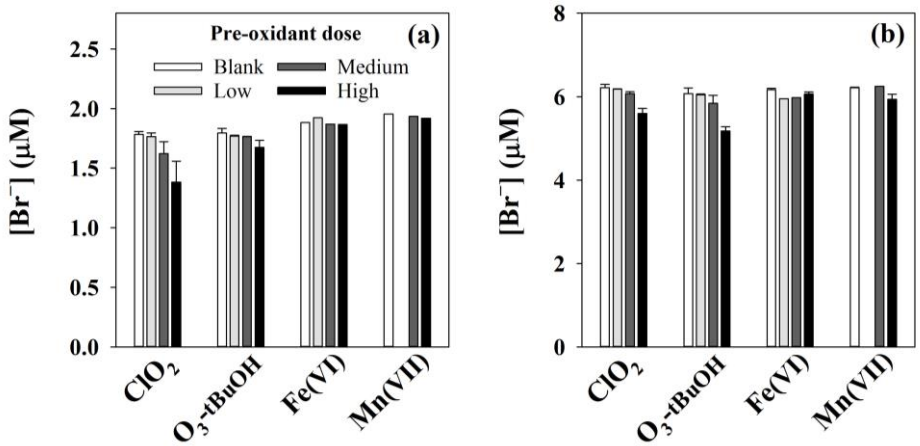

Figure A-6-2. Bromide concentration after pre-oxidation at pH 8. [ClO_2] = 3.5–39.3 µM, [O_3-tBuOH] = 2.2–104.1 µM, [Fe(VI)] = 2.5–50 µM, [Mn(VII)] = 1–8.6 µM, [SRNOM] = 3 mgC L^{-1}, pH 8 (40 mM borate), [Br^-] = 150–500 µg L^{-1}.

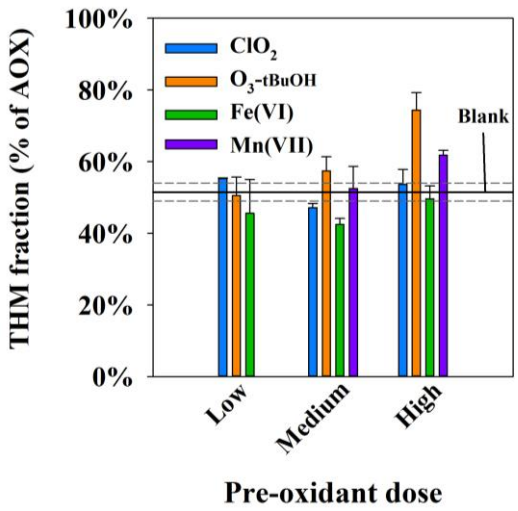

Figure A-6-3. Impact of pre-oxidation on THM fraction. The dashed bars represent the upper and lower limits of the THM fraction in the different blanks. [ClO_2] = 3.5–39.3 µM, [O_3-tBuOH] = 2.2–104.1 µM, [Fe(VI)] = 2.5–50 µM, [Mn(VII)] = 1–8.6 µM, [SRNOM] = 3 mgC L^{-1}, pH 8 (40 mM borate), no bromide. Error bars represent the range of analytical results for duplicated experiments (except the high dose of Fe(VI) and Mn(VII)).

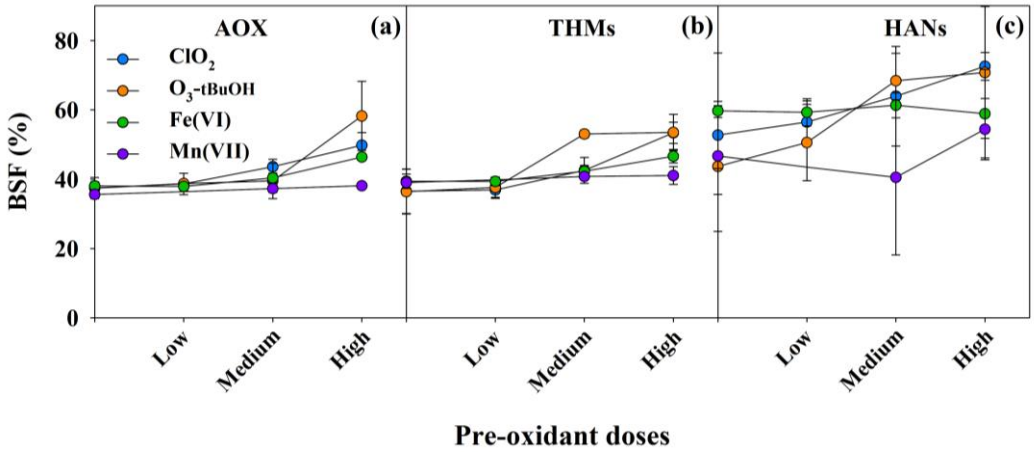

Figure A-6-4. Bromine Substitution Factor (BSF) in AOX (a), THMs (b) and HANs (c) after chlorination in presence of 500 µg L^{-1} of bromide, with and without pre-oxidation. [ClO_2] = 3.5–39.3 µM, [O_3-tBuOH] = 2.2–104.1 µM, [Fe(VI)] = 2.5–50 µM, [Mn(VII)] = 1–8.6 µM, [SRNOM] = 3 mgC L^{-1}, pH 8 (40 mM borate). Error bars represent the range of analytical results for duplicated experiments (except the high dose of Fe(VI) and Mn(VII)).

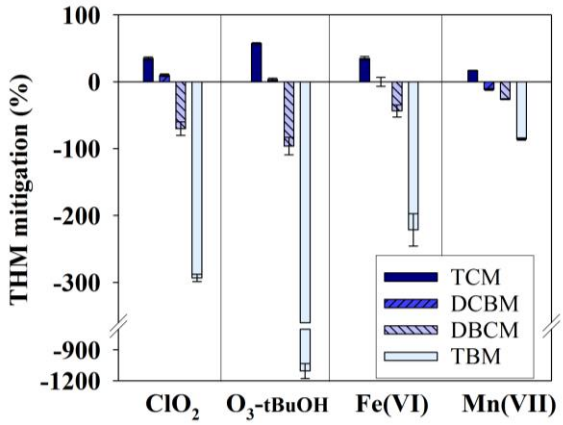

Figure A-6-5. Reduction of individual THMs by a high dose of pre-oxidants in presence of 150 µg L^{-1} of bromide. [ClO_2] = 39.3 µM, [O_3-tBuOH] = 104.1 µM, [Fe(VI)] = 50 µM, [Mn(VII)] = 8.6 µM, [SRNOM] = 3 mgC L^{-1}, pH 8 (40 mM borate). Error bars represent the range of analytical results one experiment.

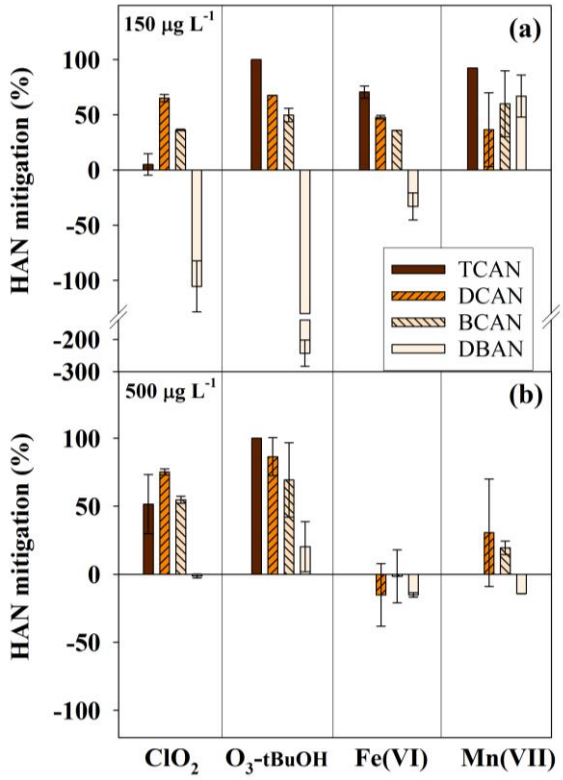

Figure A-6-6. Reduction of individual HANs by a high dose of pre-oxidants in presence of 150 µg L^{-1} (a) or 500 µg L^{-1} (b) of bromide. [ClO_2] = 39.3 µM, [O_3-tBuOH] = 104.1 µM, [Fe(VI)] = 50 µM, [Mn(VII)] = 8.6 µM, [SRNOM] = 3 mgC L^{-1}, pH 8 (40 mM borate). Error bars represent the range of analytical results for one experiment.

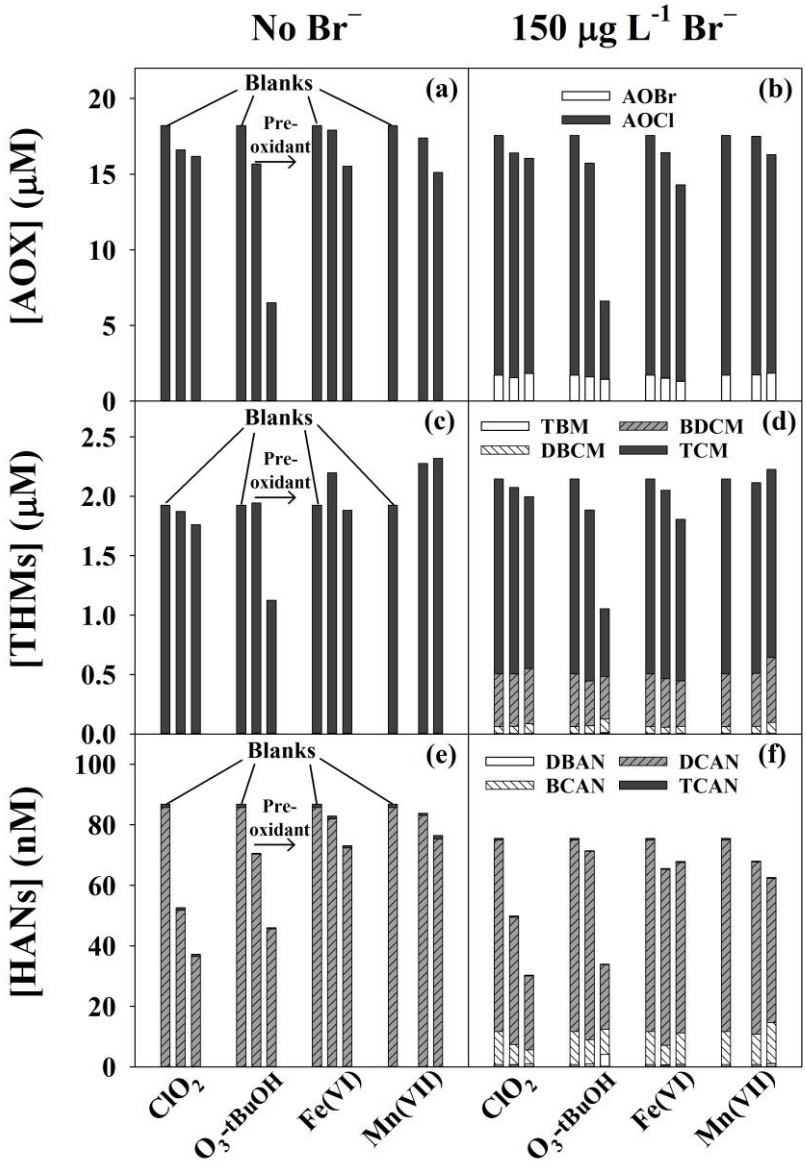

Figure A-6-7. Formation of AOX (a–b), THMs (c–d) and HANs (e–f) after chlorination at pH 6.5, with and without (blank) pre-oxidation. [ClO_2] = 3.5–15.1 µM, [O_3-tBuOH] = 2.2–39.8 µM, [Fe(VI)] = 2.5–14.7 µM, [Mn(VII)] = 1–8.6 µM, [SRNOM] = 3 mgC L^{-1}, pH 6.5 (40 mM phosphate), [Br^-] = 0–150 µg L^{-1}.

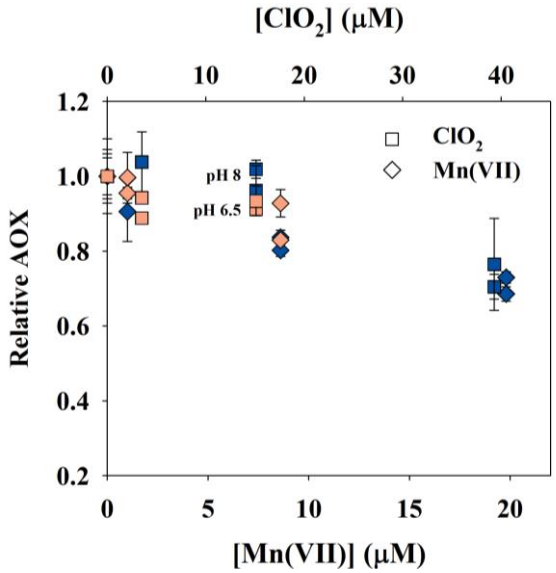

Figure A-6-8. Relative AOX formation after ClO_2 and Mn(VII) pre-oxidation at pH 6.5 (orange) and 8 (blue). [SRNOM] = 3 mgC L^{-1}, [Br^-] = 0–150 µg L^{-1}. Error bars represent the range of analytical results for one experiment.

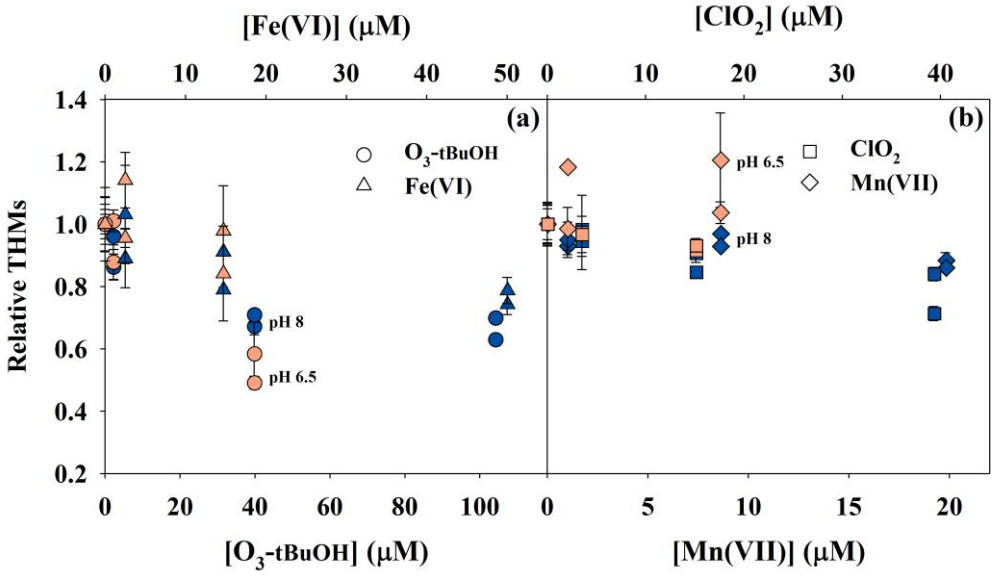

Figure A-6-9. Relative THM formation after O_3-tBuOH, Fe(VI), ClO_2 and Mn(VII) pre-oxidation at pH 6.5 (orange) and 8 (blue). [SRNOM] = 3 mgC L^{-1}, [Br^-] = 0–150 µg L^{-1}. Error bars represent the range of analytical results for one experiment.

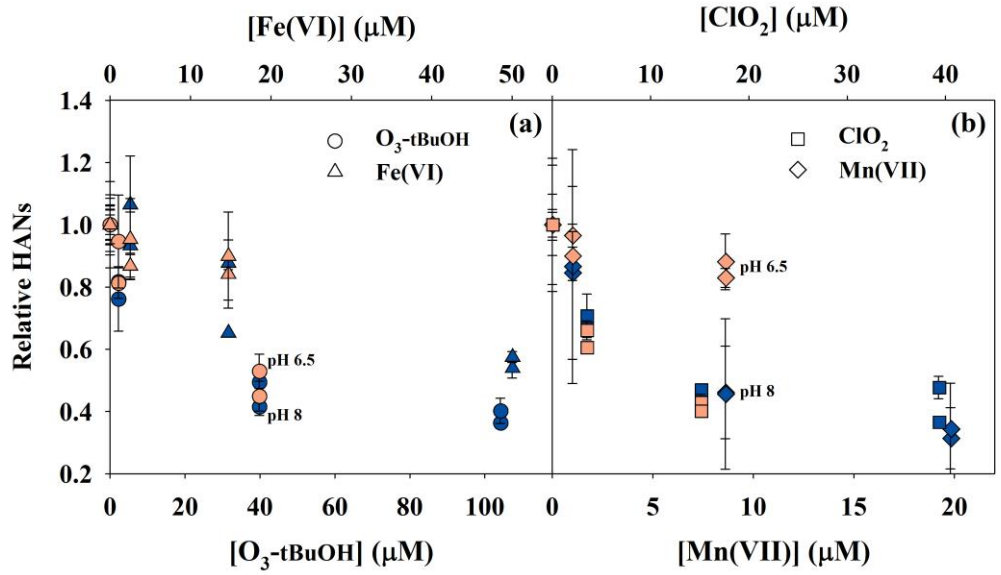

Figure A-6-10. Relative HAN formation after O_3-tBuOH, Fe(VI), ClO_2 and Mn(VII) pre-oxidation at pH 6.5 (orange) and 8 (blue). [SRNOM] = 3 mgC L^{-1}, [Br^-] = 0–150 μg L^{-1}. Error bars represent the range of analytical results for one experiment.

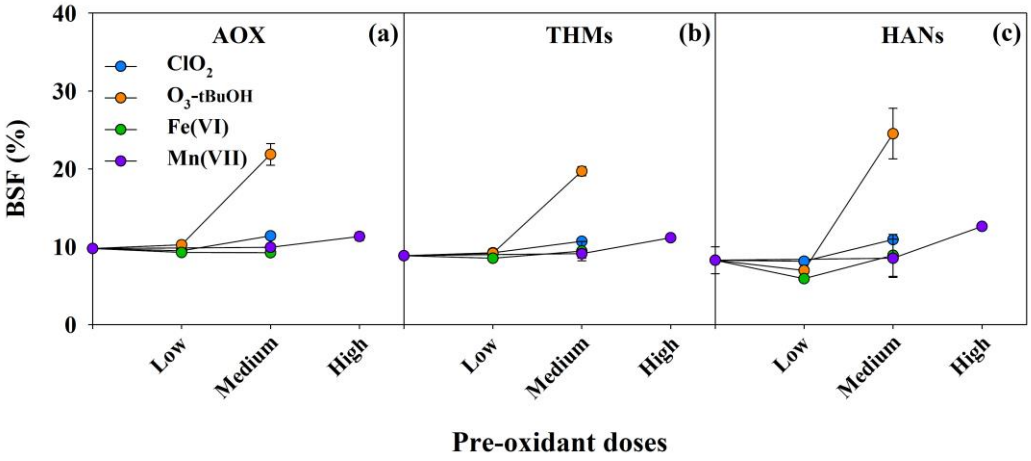

Figure A-6-11. Bromine Substitution Factor (BSF) in AOX (a), THMs (b) and HANs (c) after chlorination in presence of 150 μg L^{-1} of bromide at pH 6.5, with and without pre-oxidation. [ClO_2] = 3.5–39.3 μM, [O_3-tBuOH] = 2.2–104.1 μM, [Fe(VI)] = 2.5–50 μM, [Mn(VII)] = 1–8.6 μM, [SRNOM] = 3 mgC L^{-1}, pH 6.5 (40 mM phosphate). Error bars represent the range of analytical results for duplicated experiments (except the high dose of Fe(VI) and Mn(VII)).

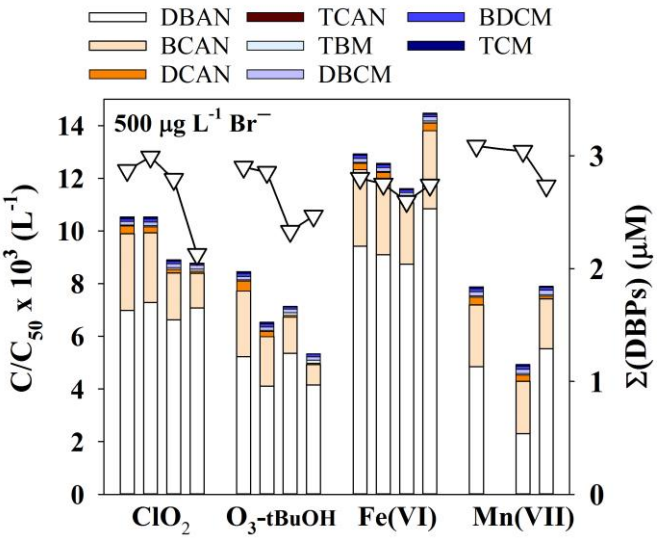

Figure A-6-12. Calculated toxicity (bars) compared to DBP formation (triangles) after chlorination in presence of 500 µg L^{-1} of bromide. [ClO_2] = 3.5–39.3 µM, [O_3-tBuOH] = 2.2–104.1 µM, [Fe(VI)] = 2.5–50 µM, [Mn(VII)] = 1–8.6 µM, [SRNOM] = 3 mgC L^{-1}, pH 8.

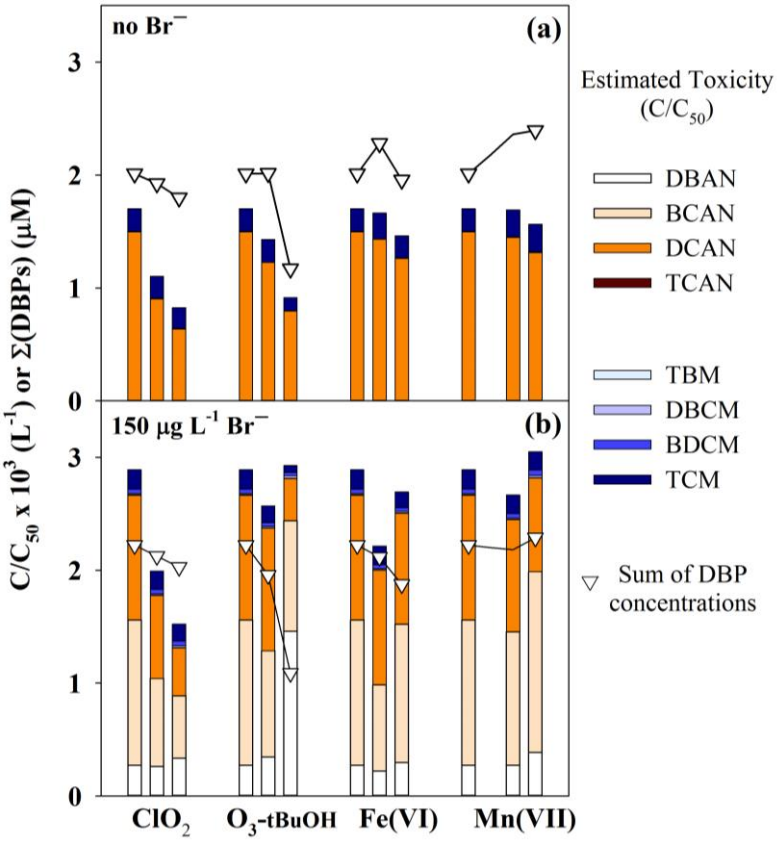

Figure A-6-13. Calculated toxicity (bars) compared to DBP formation (triangles) after chlorination without bromide (a) and with 150 µg L^{-1} of bromide (b). [ClO_2] = 3.5–15.1 µM, [O_3-tBuOH] = 2.2–39.8 µM, [Fe(VI)] = 2.5–14.7 µM, [Mn(VII)] = 1–8.6 µM, [SRNOM] = 3 mgC L^{-1}, pH 6.5.

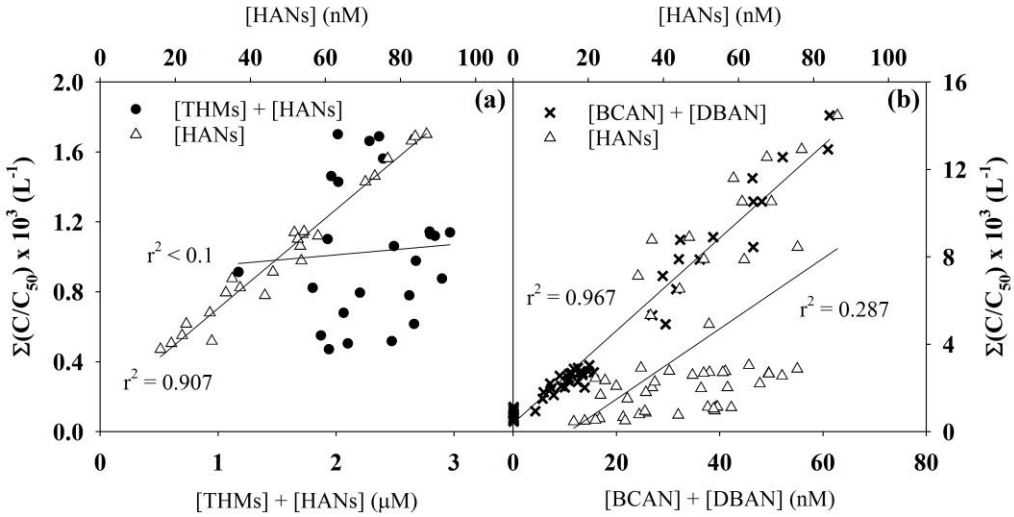

Figure A-6-14. Correlation between the estimated cumulative toxicity and DBP concentration for samples without bromide (a) and all the samples (b). [ClO_2] = 3.5–39.3 µM, [O_3-tBuOH] = 2.2–104.1 µM, [Fe(VI)] = 2.5–50 µM, [Mn(VII)] = 1–8.6 µM, [SRNOM] = 3 mgC L^{-1}, pH 6.5 (40 mM phosphate) or 8 (40 mM borate), [Br^-] = 0–500 µg L^{-1}.

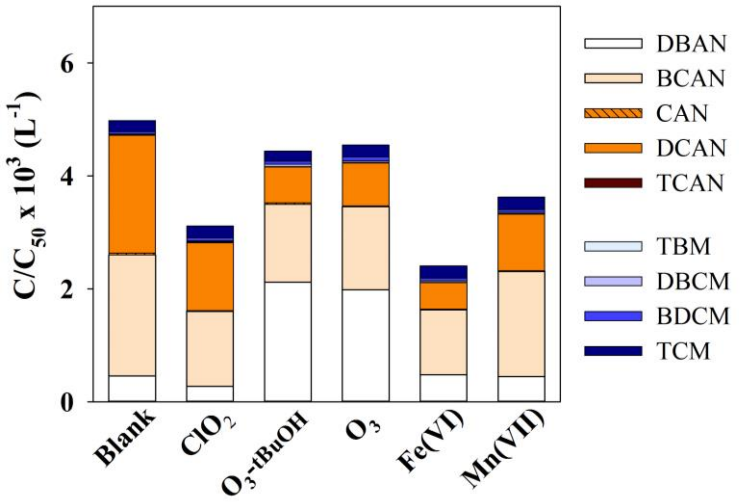

Figure A-6-15. Calculated toxicity after chlorination of a real water, with and without (blank) pre-oxidation. [ClO_2] = 10 µM, [O_3-tBuOH] = [O_3] = 30 µM, [Fe(VI)] = 24 µM, [Mn(VII)] = 10 µM. The water characteristics are given in Table A-6-1.

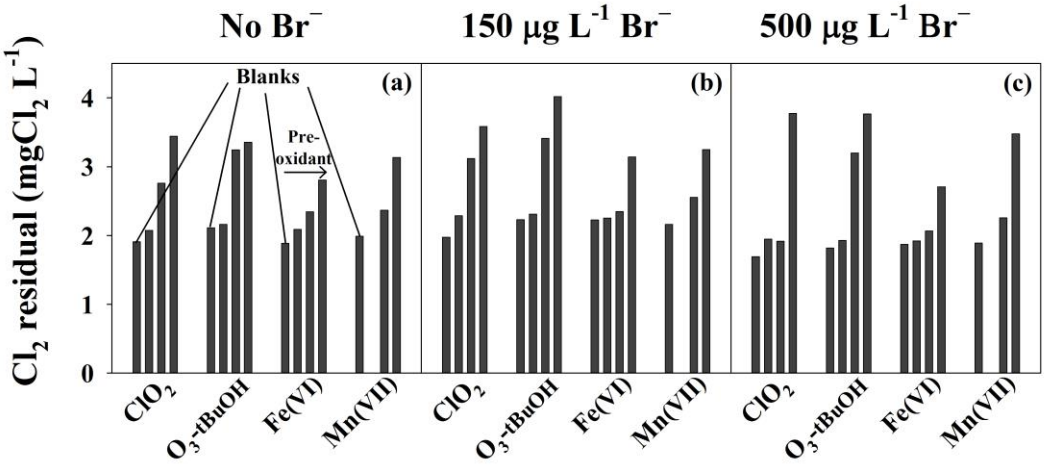

Figure A-6-16. Impact of pre-oxidation on chlorine residual without bromide (a) and with 150 µg L^{-1} (b) and 500 µg L^{-1} (c) of bromide. [ClO_2] = 3.5–39.3 µM, [O_3-tBuOH] = 2.2–104.1 µM, [Fe(VI)] = 2.5–50 µM, [Mn(VII)] = 1–8.6 µM, [SRNOM] = 3 mgC L^{-1}, pH 8 (40 mM borate), [Br^-] = 0–500 µg L^{-1}.

Permission Statement

Home | Create Account | Help

Title:	In Situ Formation of Free Chlorine During ClO2 Treatment: Implications on the Formation of Disinfection Byproducts
Author:	Valentin Rougé, Sébastien Allard, Jean-Philippe Croué, et al
Publication:	Environmental Science & Technology
Publisher:	American Chemical Society
Date:	Nov 1, 2018

Copyright © 2018, American Chemical Society

LOGIN

If you're a copyright.com user, you can login to RightsLink using your copyright.com credentials.

Already **a RightsLink user** or want to learn more?

PERMISSION/LICENSE IS GRANTED FOR YOUR ORDER AT NO CHARGE

This type of permission/license, instead of the standard Terms & Conditions, is sent to you because no fee is being charged for your order. Please note the following:

- Permission is granted for your request in both print and electronic formats, and translations.
- If figures and/or tables were requested, they may be adapted or used in part.
- Please print this page for your records and send a copy of it to your publisher/graduate school.
- Appropriate credit for the requested material should be given as follows: "Reprinted (adapted) with permission from (COMPLETE REFERENCE CITATION). Copyright (YEAR) American Chemical Society." Insert appropriate information in place of the capitalized words.
- One-time permission is granted only for the use specified in your request. No additional uses are granted (such as derivative works or other editions). For any other uses, please submit a new request.

BACK | CLOSE WINDOW

Copyright © 2018 Copyright Clearance Center, Inc. All Rights Reserved. Privacy statement. Terms and Conditions.
Comments? We would like to hear from you. E-mail us at customercare@copyright.com